AN ABSTRACT OF THE DISSERTATION OF

Vanessa E. Holfeltz for the degree of Doctor of Philosophy in
Radiation Health Physics presented on January 5, 2018.
Title: Investigation of f-Element Extraction and Ligand Association in the ALSEP Extraction System for Used Nuclear Fuel Reprocessing.

Abstract approved: _____

Alena Paulenova

Effective separation of lanthanides (Ln) from the minor actinides (MA) is a crucial technical challenge to closing the nuclear fuel cycle. This separation is a necessary prerequisite to transmute long-lived isotopes of Am and Cm, which will allow a reduction of the repository volume, thermal load, and radiological toxicity of nuclear wastes. The US Department of Energy (USDOE) Fuel Cycle Research and Development initiative is investigating the Actinide Lanthanide Separation (ALSEP) solvent extraction process to perform the Ln/MA separation from dissolved used nuclear fuel. ALSEP has achieved substantial improvements upon currently available separations, but further development of ALSEP requires an enhanced understanding of the fundamental aspects of this complicated multicomponent system. The focus of this research has been to determine the coordination environment in the organic phase, particularly, of the ligands and of the extracted lanthanides and minor actinides.

The ALSEP process combines the neutral extractant *N,N,N′,N′*-tetra-2-ethylhexyl diglycolamide (T2EHDGA) with HEH[EHP] in an aliphatic diluent. The ALSEP feed is a nitric acid-based post-PUREX raffinate with uranium, plutonium, and neptunium removed. Trivalent actinides and lanthanides are co-extracted by the ALSEP solvent, and Ln/An separation is achieved by subsequent selective stripping stages using buffered polyaminocarboxylic acid solutions. Little knowledge exists regarding the functionality of HEH[EHP] during metal extraction in the combined T2EHDGA -HEH[EHP] sol-

vent system. In this work, the role of HEH[EHP] in the metal extraction step is investigated as a function of aqueous phase acidity. The ALSEP system is found to exhibit synergistic metal extraction toward trivalent Eu and Am, and this synergism is found to be dependent on aqueous phase acid concentration. Spectroscopic (IR and UV-vis) evidence is consistent with the participation of HEH[EHP] in the extracted organic phase metal complex. NMR spectroscopy indicates adduct formation between the ligands T2EHDGA and HEH[EHP] in organic phases before contact with any aqueous phase. Adduct formation is substantiated by diffusion ordered spectroscopy (DOSY) NMR, which further indicates the presence of HEH[EHP] in the extracted metal complexes, consistent with the UV-vis and IR spectroscopic results.

Investigation of f-Element Extraction and Ligand Association in the ALSEP Extraction System for Used Nuclear Fuel Reprocessing

by

Vanessa E. Holfeltz

A DISSERTATION

submitted to

Oregon State University

in partial fulfillment of
the requirements for the
degree of

Doctor of Philosophy

Presented January 5, 2018
Commencement June 2018

Doctor of Philosophy dissertation of Vanessa E. Holfeltz presented on January 5, 2018.

APPROVED:

Major Professor, representing Radiation Health Physics

Head of the Department of Nuclear Engineering and Radiation Health Physics

---

Dean of the Graduate School

I understand that my dissertation will become part of the permanent collection of Oregon State University libraries. My signature below authorizes release of my dissertation to any reader upon request.

Vanessa E. Holfeltz, Author

ACKNOWLEDGMENTS

My advisor, Alena Paulenova, and Tatiana Levitskaia, my mentor at PNNL, have not only guided this work, but have consistently pushed me to become a better scientist and have provided the means for many new doors to be opened: thank you.

Many thanks are due to Gregg Lumetta, in particular, for supporting my work on this project.

Throughout this project, I have had the support of my research groups, first at Oregon State University and now at Pacific Northwest National Laboratory: thank you. In particular, Emily Campbell, Gabriel Hall, and Joseph Lapka have contributed immeasurable support, guidance, and insightful discussions: thank you.

The experiments performed at national user facilities during the course of this project would not have been successful without the excellent support and assistance of many beamline scientists and spectroscopists: thank you, Sungsik Lee, Ben Reinhart, Soenke Seifert, Changwoo Do, Nancy Washton, Robert Young, and Ying Chen. Robert and Ying, thank you for going above and beyond at every step.

A portion of this research was performed using EMSL, a DOE Office of Science User Facility sponsored by the Office of Biological and Environmental Research.

This work was supported by U.S. Department of Energy, Office of Nuclear Energy, through the Fuel Cycle Research and Development Program, and through the Nuclear Energy University Program (NEUP), award number DE-NE0000720.

Financial support for the author was also provided by the Henry W. and Janice C. Schuette Fellowship.

Pacific Northwest National Laboratory is operated by Battelle Memorial Institute for the U.S. Department of Energy under contract DE-AC05-76RL01830.

TABLE OF CONTENTS

TABLE OF CONTENTS (Continued)

Page

TABLE OF CONTENTS (Continued)

Page

TABLE OF CONTENTS (Continued)

Page

LIST OF FIGURES

LIST OF FIGURES (Continued)

LIST OF FIGURES (Continued)

LIST OF TABLES

LIST OF TABLES (Continued)

ABBREVIATIONS AND SYMBOLS

[X]	concentration of species X (mol L^{-1} unless otherwise noted)
ALSEP	Actinide Lanthanide Separation
An	actinide
CMPO	octyl(phenyl)-N,N-diisobutylcarbamoylmethylphosphine oxide
D	Diffusion coefficient (in chapter 7 only)
D	Distribution ratio
D_M	Distribution ratio of metal M
DEH[EHP]	di(2-ethylhexyl)2-ethylhexyl phosphonate
1,4-DIPB	1,4-diisopropylbenzene
DGA	diglycolamide (e.g., TODGA or T2EHDGA)
DOSY	diffusion ordered spectroscopy
EHPA	2-ethylhexylphosphonic acid
ESI-MS	electrospray ionization mass spectrometry
FP	fission products
FTIR	Fourier transform infrared (spectroscopy)
GC/MS	gas chromatography mass spectrometry
HDEHP	bis(2-ethylhexyl)phosphoric acid
HEH[EHP]	mono 2-ethylhexyl phosphonic acid
HNO_3	nitric acid
L	ligand (generically, as in an equation)
Ln	lanthanide
K	equilibrium constant
M	metal (generically, as in an equation)
MA	minor actinide
NMR	nuclear magnetic resonance
PFG	pulsed field gradient
PUREX	Plutonium Uranium Reduction Extraction
P&T	Partitioning & Transmutation
TALSPEAK	Trivalent Actinide Lanthanide Separation by Phosphorus-reagent Extraction from Aqueous Complexes
T2EHDGA	N,N,N',N'-tetra-2-ethylhexyl diglycolamide
TEDGA	N,N,N',N'-tetraethyl diglycolamide
TBP	tri-*n*-butylphosphate
TODGA	N,N,N',N'-tetraoctyl diglycolamide
UNF	used nuclear fuel

1 Introduction

Nuclear energy is a clean, carbon-neutral energy source that can mitigate the effects of climate change in the coming decades by replacing fossil fuel energy sources. Political and societal acceptance of nuclear power hinges, in part, on tractable solutions for the final disposition of used nuclear fuel (UNF). The increased demand for nuclear as a carbon-neutral power source requires a responsible and proliferation-resistant disposal method. Closing the nuclear fuel cycle is necessary to meet these goals, and will be achieved only through advancements in reprocessing methods.

To safely and responsibly manage UNF, it should be isolated from the biosphere (e.g., in a repository) until the radiological toxicity reaches a low level (i.e., that of natural uranium ore). Reprocessing offers a means to optimize used fuel disposal and reduce the volume and radioactivity of used nuclear fuel. "Advanced reprocessing" refers to the separation of the minor actinides (Np, Am, and Cm, collectively, MA) from used nuclear fuel, which presents one option to closing the nuclear fuel cycle. Advanced reprocessing can optimize permanent repository storage, as it provides the greatest reduction in radioactive waste inventory and greatest reduction in long-term hazard. In tandem with the partitioning and transmutation (P&T) strategy, advanced reprocessing offers an optimized route for UNF disposal and closure of the fuel cycle. In the P&T strategy, the MA, which are the main contributors to repository radiation dose, heat, and radiotoxicity in the first 10,000 years, are first partitioned from the other elements present in UNF and then transmuted via fission or neutron capture. This significantly reduces their half-lives, long-term radiotoxicity and thermal burden to a waste repository.[1]

A key technical challenge and crucial step in advanced reprocessing is separation of the MA from the trivalent lanthanides (Ln), which to date remains challenging. The Actinide Lanthanide SEParation (ALSEP) concept is a solvent extraction method which has been proposed for MA/Ln separation, and is currently studied by the United States Department of Energy (USDOE) to advance the current state of knowledge of

fuel reprocessing to support waste reduction goals. ALSEP offers a simple and streamlined engineering level process compared to alternative Ln/MA separation methods.[2] But at the molecular level, ALSEP is one of the most complex UNF reprocessing schemes.

The objective of the work presented in this dissertation has been to close some of the knowledge gaps in the ALSEP concept identified above, and in so doing, to advance the understanding of MA/Ln separations used in advanced reprocessing, pursuant to closing the nuclear fuel cycle. This dissertation contains material from one accepted, peer-reviewed article (Chapter 3), as well as material in preparation for publication in peer-reviewed journals. The dissertation is divided into eight chapters, which are outlined below.

Chapter 2 provides background information on the nuclear fuel cycle, the composition of used nuclear fuel, and the motivation for reprocessing and for the MA/Ln separation. This is followed by a brief review of the chemistry of the *f*-elements, as pertaining to reprocessing. A review of solvent extraction systems used for reprocessing and for MA/Ln separations is presented, leading to the discussion of the ALSEP concept.

In Chapter 3, the role of impurities in the phosphonic acid, HEH[EHP], on Am(III) stripping of the ALSEP system is explored in detail. Major impurities present in commercially available HEH[EHP] are identified, the efficacy of existing purification methods is determined, and a new purification method is presented. The ALSEP system is used as a case study to determine impurities in HEH[EHP] which are problematic toward the process application of this system (i.e., impurities which cause retention of Am(III) in the organic phase). The content of this chapter has been published in the peer-reviewed journal *Solvent Extraction and Ion Exchange*.

Chapter 4 presents the extraction behavior of Am(III) and Eu(III) in the ALSEP system from HNO_3 solutions of varying acid concentration. The extraction dependence of each ligand, acting independently, is also determined. The concentration of the acidic extractant, HEH[EHP], is varied in solutions containing constant concentration

of T2EHDGA to determine its role in metal extraction in the mixed-ligand system. The effect of diluent on metal extraction is determined, for Am(III) and Eu(III), on extraction from two aliphatic and two aromatic diluents, for the independent and combined ligand systems. Finally, the stripping kinetics and distribution of Eu(III) and Am(III) are determined for the aliphatic and aromatic diluents. Extraction from a used nuclear fuel simulant allows determination of the effect of total metal concentration on Eu(III) and Am(III) distribution ratio, and the stripping value and kinetics are determined for this system with two polyaminocarboxylates.

Chapter 5 builds upon the results of Chapter 4, investigating the coordination of extracted Am(III) and Eu(III) complexes in the ALSEP organic phase using various spectroscopic methods. Coordination of the ligand is probed *via* infrared spectroscopy and NMR spectroscopy, and coordination at the metal center is probed using UV-vis spectroscopy. The dependence of organic phase metal coordination on HNO_3 concentration in the aqueous extraction phase is investigated.

Chapter 6 investigates the self-association and adduct formation of the ligands, HEH[EHP] and T2EHDGA, in *n*-dodecane using NMR spectroscopy *via* chemical shift analysis. Values for the dimerization constants and association constants are presented.

Chapter 7 presents the results of experiments using DOSY NMR to investigate changes in aggregation of the ligands, independently and in combination, upon self-association, adduct formation, and after equilibration with HNO_3 and extraction of Eu(III) from acidic solutions.

Chapter 8 provides a summary of the global conclusions and the key findings of this work, and is followed by the references used in this dissertation.

2 Background and Literature

2.1 The Nuclear Fuel Cycle

The United States currently adopts an open, or "once-through," fuel cycle. In this model, uranium fuel that has been removed from the core of a commercial light water reactor (LWR) is considered waste. The current strategy of the U. S. Department of Energy (U.S. DOE) is to permanently dispose of commercial LWR UNF in a geologic repository.[3] The siting and licensing of geologic repositories for commercial UNF has proven to be difficult, not only in the United States as demonstrated by Yucca Mountain, but worldwide.[4] Recently, construction began on the Onkalo repository in Finland, which is scheduled to open by 2020 and largely followed a consent-based siting approach.[4] The only operating geologic repository is of limited scope: the Waste Isolation Pilot Plant (WIPP), which began accepting waste in 1999, accepts only transurainc (TRU) waste from defense operations.[5]

In the closed fuel cycle, some fraction of the usable material that remains in the irradiated fuel is recovered and recycled into fresh fuel (*via* reprocessing), and the unusable material (e.g., fission products) are diverted for permanent disposal. The isotopic composition, and thus the usable fraction, of the LWR fuel after irradiation will depend on the initial fuel composition (i.e., enrichment), operating conditions, and burn-up.[6,7] Typically, the enrichment of ^{235}U has decreased from ca. 3% to ca. 1%, with a concomitant increase in activation and fission product inventory. The usable material remaining in the fuel is also determined by the existing political and technological frameworks, specifically concerning the recovery of Pu. U and Pu can be recovered by (i.e., by the industrially established Plutonium Uranium Reduction Extraction (PUREX) process) and converted into mixed oxide (MOX) fuels for use in commercial nuclear power plants.[8] This has several direct benefits: usable energy is recovered from the heretofore waste; the heat and radiotoxicity burden on the repository is reduced; and the Pu is destroyed, negating its proliferation risk. Recovery of

^{235}U alone has the benefit of reducing the front-end costs (mining, enrichment) of the nuclear fuel cycle – albeit at the expense of increased back-end costs. Various cost analyses suggest that reprocessing in the U. S. will not be favorable economically, given current uranium prices.[9,10] In the French twice-through system, where U and Pu are recovered for MOX fuel, recycling costs total only 2.9% of the final electricity cost, less than enrichment (5.2%) or mining (7.2%).[11] An analysis of the environmental impact of the once-through system compared to the French twice-through cycle found the recycling option to have a significantly smaller environmental impact.[12]

2.1.1 Advanced Reprocessing

Advanced reprocessing methods seek to separate the minor actinides (MA) from the used fuel, in order to decrease the long-term radiotoxicity and heat burden to the repository. The minor actinides are the main contributers to repository dose and thermal burden in the 100 – 10,000 year time frame.[1,13] Removing the MA from U, Pu, and fission products (FP) for irradiation in a fast reactor, or by an accelerator driven system, forms the basis of the partitioning and transmutation (P&T) strategy.[8,14] The radiotoxic inventory of a geologic repository can be reduced by a factor of 10 with full Pu recycle, and by a factor of 100 with full MA transmutation, with reductions in peak dose by as much as a factor of 100.[14] Transmutation of the MA significantly reduces their half-life, which in turn reduces their radiotoxitiy and thermal burden in waste repositories, as well as their impact on the local biosphere, should there be a breach in repository barrier.[15] Additionally, due to the reduction in radiolytic heat burden due to reduction of MA inventory, the footprint of repositories can be reduced by as much as a factor of 20.[14]

Efficient transmutation of the MA requires their separation from the lanthanides (Ln), which are abundant fission products with large neutron absorption cross sections.[16] The effective separation of the trivalent lanthanides (Ln) and minor actinides (MAs) remains a crucial technical challenge in advanced reprocessing. This separation has been the focus of a significant body of reprocessing research worldwide, resulting in the de-

velopment of many solvent extraction processes to accomplish the task. While some electrochemical methods (pyroprocessing) have been explored for this separation, the vast majority of the research has employed solvent extraction methods.[17]

The chemical separation of the MA, primarily Am and Cm, from the Ln is particularly challenging. Unlike the lighter actinides present in UNF, which have a rich redox chemistry and a wide range of easily accessible and stable oxidation states in solution, Am and Cm, like the lanthanides, adopt a stable, trivalent, oxidation state in solution.[a] Am, Cm, and the Ln have similar ionic radii, and are all hard Lewis acids; these properties contribute to the difficulty of their separation. The separation of MA from Ln in dissolved UNF is further complicated by the presence of many other metals, presenting a diverse chemical matrix, of which the composition depends on fuel burnup, fission product inventory, and decay time.[13] Nonetheless, separation of the minor actinides from Ln and other fission products has long been goal of advanced reprocessing schemes, dating at least to the introduction of the TALSPEAK process in 1964.[20] However, despite much research into TALSPEAK and many other[16,21] advanced solvent extraction schemes for MA/Ln separation, problems in accurate predictability, performance, reproducibility, and scalability have persisted in many of the solvent extraction separation methods that have been studied to date.

2.1.2 Chemistry of the f-Elements

The f-elements, comprised of the lanthanides (Ln) and actinides (An), are abundant constituents of UNF. Many of the Ln are prominent fission products (or fission decay products) of the thermal fission of ^{235}U, and several light Ln have mass number centered about A$\sim$140.[7] The f-elements heavier than uranium are produced in thermal reactors *via* successive neutron capture reactions of ^{235}U and ^{238}U. This results in the production of Pu, Np, Am, Cm, Bk and Cf; however, Bk and Cf are produced only in

[a] Am can be oxidized to Am(V) and Am(VI), but is easily reduced,[18] and undergoes reduction due to autoradiolysis in HNO_3.[19] Utilizing the higher oxidation states of Am to achieve Am/Ln separation is one of the research paths pursued by the U.§. DOE.[3]

low yield. Of these, Pu and Np have complex redox chemistry, and can adopt a wide range of oxidation states in solution, which can be controlled by solution conditions.[7] This redox chemistry had led to the development of methods for their separation, along with U, from the other components of dissolved UNF. Am and Cm adopt primarily trivalent oxidation states in solution, and behave in solution much like their trivalent lanthanide analogs, making their separation much more difficult.

Both the An and Ln are characterized as "hard" Lewis acids, which is a consequence of the behavior of the f electrons. In the Ln (An), the $4f$ ($5f$) orbitals are buried beneath the $5d$ and $6s$ ($6d$ and $7s$) orbitals, with very little density extending beyond the core electron configuration.[22,23] This results in the similar solution behavior of the trivalent lanthanides (and, consequently, for their difficult separation): because very little f electron density is available to participate chemical bonding, chemical properties change very little with Z (i.e., addition of valence shell f electron), as the chemical properties are largely determined by the $5d$ and $6s$ orbitals.[22,23] Most Ln separations methods take advantage of the decreasing size of the Ln across the series. The *lanthanide contraction* is a result of the non-spherical shape of the f orbtials. As Z increases, the outer most f electrons are not sufficiently shielded from the increasing nuclear charge, and the valence orbitals contract, resulting in the observed decrease in ionic radius of the trivalent Ln and An.[7,23]

2.2 Solvent Extraction

The primary means and most developed method of reprocessing UNF worldwide has been by solvent extraction. In this method, the irradiated fuel is dissolved in an acidic aqueous phase (typically 3 – 5 M HNO_3) and contacted with an organic phase consisting of a diluent (typically an alkane, such as *n*-dodecane or kerosene) bearing a metal complexing ligand (such as tri-*n*-butylphosphate, TBP). Metal ions partition from the aqueous into the organic phase by forming coordination complexes at the aqueous-organic interface with the organic-phase ligand. The choice of aqueous solution con-

ditions and metal complexing ligand(s) will determine the transport of different metal ions across the aqueous-organic interface, and hence determine the selectivity and effectiveness of the separation. Separation of a mixture of metal ions can be achieved when the metals partition differently to the organic phase (due to different thermodynamic favorability), or by non-selective group extraction followed by selective stripping from the organic phase. Stripping (or "back-extraction") refers to the partitioning of a complexed metal ion from the ligand-bearing organic phase to a new ("fresh") aqueous phase, by selecting conditions of the new aqueous phase to make partitioning of the metal to the aqueous phase thermodynamically favorable. Frequently, the stripping step of a process will be preceeded by a "scrub" step. The scrub step is essentially the same as a strip step. The difference in terminology reflects the intent of the scrub: of only removing an undesirable material that may interfere with subsequent process steps (e.g., extracted acid, or a metal that was not intended to be extracted, and is considered waste).

Most of the ligands (extractants) used in solvent extraction methods can usually be classified as acting by one of two mechanisms: either by a *netural solvate* or by an *ion exchange* mechanism, and for this reason, the ligands themselves are typically referred to as *neutral solvate ligands* or *ion exchange ligands*. Each is discussed briefly.

2.2.1 Neutral Solvate Ligands

The goal of solvent extraction is to selectively partition a target metal ion species across the aqueous-organic phase boundary.[b] This requires that the ligand (L) coordinate the metal ion (M) and that charge balance is achieved. For the lanthanides and actinides, which have coordination numbers of 8 – 9,[22] several multidentate ligands are typically needed to achieve sufficient coordination and displacement of the aqueous solvation shell to promote phase transfer of the metal ion. As there can be no net charge transfer

[b] Or, more generally: to partition the desired species (not necessarily a metal ion) across the phase boundary of two immiscible solvents.

across the phase boundary, the coordinated metal species must be neutral. In neutral solvate complexes, the charge balance is typically provided by the co-extraction of anions from the aqueous phase, which is referred to as the counterion. In fuel reprocessing schemes, where UNF is typically dissolved in HNO_3, the counterion is usually provided by $NO_3{}^-$. The overall reaction can be written

$$M^{z+} + zNO_3{}^- + \overline{nL} \rightleftharpoons \overline{M \cdot L_n(NO_3)_z} \tag{2.1}$$

Given Equation 2.1, it is clear that the concentration of anion in the aqueous phase then drives the extraction of metal into the organic phase for neutral extractants. Conversely, the metal can be back-extracted, or stripped, from the organic phase by driving the equation to the left, with introduction of an aqueous phase of low anion and metal concentration. Both of these techniques are applied in industrial solvent extraction processes, and in the process that is the subject of this dissertation, ALSEP.

2.2.2 Ion Exchange Ligands

Ion exchange ligands achieve charge balance not by co-extraction of an anion but by displacement of an ion of the ligand. The ion exchanged is usually a proton from a weakly acidic organic ligand, and as such, ligands in this class are often referred to as "acidic extractants." The reaction for a monoprotic ligand, HA, can be written

$$M^{z+} + \overline{zHA} \rightleftharpoons \overline{MA_z} + zH^+ \tag{2.2}$$

As the ligand must be deprotonated for the metal complexation to occur, the proton concentration in the aqueous phase determines the favorability of the reaction in Equation 2.2. Thus, as was the case for neutral solvates, metal extraction, and likewise, back-extraction, is determined by conditions of the aqueous phase. For a proton-exchange ligand, the proton concentration of the aqueous phase determines the metal transfer. Low proton (acid) concentration in the aqueous phase will make deprotonation of the ligand favorable, and thus drive metal transfer to the organic phase. Likewise, ex-

tracted metal can be stripped from the loaded organic phase by equilibration with an aqueous phase of high proton concentration, which will re-protonate the ligand, and cause the metal to partition to the aqueous phase.

2.3 Reprocessing Methods

Reprocessing of irradiated nuclear fuel began during the Manhattan Project, with the aim to separate plutonium for weapons production, performed at the Hanford site in Washington state.[24] Early reprocessing methods, such as the bismuth phosphate method, were based on multiple repeating steps of precipitation, oxidation and reduction to achieve a pure plutonium product.[25,26] Precipitation-based processes have many drawbacks compared to solvent extraction processes; they produce excessive solid waste, are often inefficient, do not scale well for continuous operation and must be operated in batch mode, and pose additional criticality safety risks that are avoided in solvent extraction systems. The development of solvent extraction methods that did not rely on precipitation was rapid,[27] and the bismuth phosphate method was soon replaced, first by Redox, and then by PUREX.

2.3.1 PUREX

One of the first solvent extraction methods developed for separating elements from irradiated nuclear fuel was the Plutonium Uranium Reduction Extraction (PUREX) process, which was developed in 1949 at Oak Ridge National Laboratory.[28] This process was developed as an alternative to the Redox process, which used methyl(isobutyl) ketone as an extractant from aqueous solutions of $Al(NO_3)_3$.[29] In the Redox process, high concentrations of $Al(NO_3)_3$ were necessary, as it served as the salting out agent, enabling phase transfer of metals to the organic phase. The development of PUREX, which uses tri-*n*-butyl phosphate (TBP) as the extractant in an aliphatic diluent, allows HNO_3 to be used without the addition of salts, which greatly reduced the waste of the process.

The PUREX solvent is ca. 30% TBP in an aliphatic diluent, such as *n*-dodecane or kerosene. The feed for the PUREX process is typically UNF dissolved in HNO_3 (ca. 3–5 M). The high concentration of HNO_3 serves to drive the extraction. TBP is a neutral solvate extractant, and metal ions are partitioned to the organic phase with accompanying counterion (e.g., nitrate): hence, the high concentration of HNO_3 drives the extraction. Under these conditions, hexavalent and tetravalent actinides are extracted, leaving the trivalent actinides and fission products in the raffinate. Further separation of the extracted tetra- and hexavalent actinides is achieved by control of their oxidation states, which has been achieved by a variety of methods.

Many derivative processes of PUREX have been developed to achieve various output streams, by adjusting the concentration of TBP, loading, or aqueous acidity.[30] Since the first PUREX plant-scale operations were built in 1954 and To date, PUREX remains the most widely used solvent extraction method in UNF reprocessing, and is used industrially in countries that reprocess commercial nuclear fuel (i.e., U.K., France, Russia, and Japan). As a result of the well-established industrial use of PUREX, a post-PUREX raffinate is often used as the aqueous feed for the development of advanced reprocessing schemes.

2.3.2 TALSPEAK

Separation of the trivalent minor actinides from irradiated nuclear fuel solutions has been a long-standing goal of separations chemists. The TRAMEX process, developed in 1961, used tertiary amines to extract MA from lithium chloride solutions to separate trivalent actinides for industrial purification.[31] Previous to this, separations methods using anion exchange resins, and exploiting the preferential formation of anionic actinide chloro complexes, had been employed.[31]

An improvement in the solvent extraction separation of MA and Ln came about in 1964, with the introduction of the TALSPEAK (Trivalent Actinide-Lanthanide Separations by Phosphorus reagent Extraction from Aqueous Complexes) process, developed

at Oak Ridge National Laboratory.[20] This process utilizes bis(2-ethylhexyl)phosphoric acid (HDEHP) as the extractant. This extractant was developed and investigated as a potential alternative to TBP,[32] and was found to have promising metal extraction properties.[33] As an ion exchange ligand, HDEHP is typically used to extract metals from aqueous phases of low acidity, but can also extract metal from high acidities.[32,34] From low acidity conditions of the extraction phase and under conditions of low metal loading, HDEHP, which dimerizes readily in apolar solvents (log K_2 = 4.5),[35] extracts metal *via* the cation-exchange process:

$$M^{z+} + \overline{z(HDEHP)_2} \rightleftharpoons \overline{M(HDEHP)_z(DEHP)_z} + zH^+ \tag{2.3}$$

where one proton of the dimer $(HDEHP)_2$ is exchanged for each charge of the metal, *M*, and the overbar denotes species in the organic phase. While HDEHP does show selectivity across the lanthanide series, and has been used as an industrial extractant for intralanthanide separations,[36] but as a hard donor ligand, is not sufficiently selective to efficiently perform MA/Ln separations.[20,37]

The approach in TALSPEAK is to use an aqueous-soluble soft-donor ligand to preferentially complex the MA, retaining them in the aqueous phase while allowing the Ln to be favorably extracted by HDEHP in 1,3-diisopropylbenzene diluent. Because the aqueous phase complexant prevents extraction (in this case, of the complexed actinides), it is often referred to as a "hold-back" reagent. The TALSPEAK process was found to operate reasonably with various polyaminocarboxylate ligands as the hold-back reagent, but was found to be most effective using 0.05 M DTPA (diethylenetriamine-*N,N,N′,N″,N″*-pentaacetic acid). As this ligand needs to be deprotonated to effectively complex metals in the aqueous phase, the use of a buffer increases performance and stability of the process. While several carboxylic acids were originally investigated, 1 M lactic acid, with operating range of pH 2.5 – 3.5, became the de facto TALSPEAK buffer. In addition to providing the appropriate conditions for DTPA to complex metals, the lactate buffer was also found to aid in solubilizing the complexant. Recovery of the MA from the DTPA solution is accomplished either

by oxalate precipitation, or by adjusting the pH of the aqueous buffer (to pH 1.5), such that they can be extracted by a fresh organic phase of HDEHP.

2.3.3 Advanced TALSPEAK

TALSPEAK was found to successfully perform the MA/Ln separation. However, the system is found to have a very complex chemistry, rich in interactions, not all of which can be adequately described or modeled by the measured thermodynamic constants.[37] Unpredictability in modeling, slow phase-transfer kinetics, acute pH-dependence, and complicated interactions between components have motivated the development of Advanced TALSPEAK.[38]

To alleviate the process difficulties presented by TALSPEAK, Advanced TALSPEAK retains the same basic chemistry, but achieves better pH stability and other properties by replacing the complexants. The organophosphoric acid, HDEHP, is replaced with its phosphonic acid analog, HEH[EHP] (mono 2-ethylhexyl phosphonic acid), and DTPA is exchanged for HEDTA (*N*-(2-hydroxyethyl)ethylenediamine-*N*,*N*′,*N*′-triacetic acid). HEH[EHP] is a more basic extractant than HDEHP, and consequently weaker; thus a weaker hold-back complexant, HEDTA, is necessary. Improved phase-transfer kinetics and better agreement with thermodynamic models have been demonstrated in this system than was observed in TALSPEAK. Various buffers have been evaluated for the system, including lactate, citrate, and malonate.[38–40] The process has recently been demonstrated to effectively separate Am(III) and Cm(III) from the Ln in a centrifugal contactor test.[41,42]

2.3.4 ALSEP

Since 2010, the USDOE's Fuel Cycle Research and Development (FCRD) initiative has investigated new methods for MA/Ln partitioning, in a multi-laboratory effort.[15] One of these methods is the Actinide Lanthanide Separation (ALSEP)[2] concept, a one-step

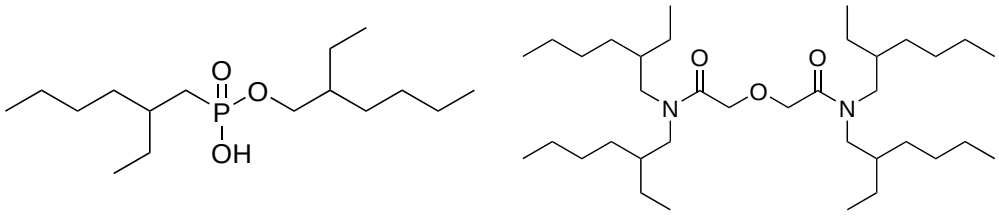

Figure 2.1: Left: structure of HEH[EHP]; right: structure of T2EHDGA.

MA/Ln separation method. ALSEP is the result of a joint project between Pacific Northwest National Laboratory (PNNL) and Argonne National Laboratory (ANL).

The ALSEP solvent combines two metal extracting ligands, *N,N,N′,N′*-tetra-2-ethylhexyl diglycolamide (T2EHDGA) and mono 2-ethylhexyl phosphonic acid (HEH[EHP]), shown in Figure 2.1, each having unique extraction properties and coordination behavior, in a single aliphatic diluent. The feed for the process is a nitric acid-based post-PUREX raffinate with uranium, plutonium, and neptunium removed. Trivalent MA and Ln are co-extracted by the ALSEP solvent and Ln/MA separation is achieved by subsequent selective stripping stages using buffered polyaminocarboxylic acid solutions. Little knowledge exists regarding the functionality of HEH[EHP] during the metal extraction step in the combined T2EHDGA–HEH[EHP] solvent system.

The ALSEP process consists of a single extraction step followed by two stripping stages. In the extraction stage, T2EHDGA is expected to be the active component of the ALSEP solvent, extracting trivalent Ln and MA from the highly acidic (3–5 M HNO_3) UNF solution. MA are then stripped from the loaded ALSEP solvent by contact with a fresh aqueous phase of buffered (pH 2–4) solution containing a soft-donor metal complexant (such as HEDTA or DTPA), which preferentially complexes the MA, partitioning them to the aqueous phase. Under these aqueous phase conditions, the Ln remain complexed by HEH[EHP] in the organic ALSEP solvent.

In the second stripping stage, an aqueous HNO_3 solution containing a strong aqueous metal complexant (such as TEDGA, *N,N,N′,N′*-tetraethyl diglycolamide) is used

to partition the Ln to the aqueous phase. Efficient Ln/MA separation in ALSEP relies on control of organic phase metal-ligand coordination, achieved *via* adjustment of the aqueous phases used to strip Ln and MA. However, little knowledge exists regarding the functionality of HEH[EHP] during the metal extraction stage in the combined T2EHDGA-HEH[EHP] solvent system. The ALSEP extraction step employs highly acidic feed solutions, and HEH[EHP] (a weak acid) remains fully protonated and presumably functions as a solvent modifier in the non-polar *n*-dodecane diluent. The exact extraction mechanism of the combined extractant system used in the ALSEP process is not yet fully understood. Furthermore, HEH[EHP] self-association tendencies, adduct formation with T2EHDGA, and solution structures formed with metal-DGA complexes are not yet determined. As a result, there is not a complete understanding of the effect of aqueous phase conditions on organic phase coordination complexes. Such an understanding is necessary to achieve greater control over ALSEP robustness and prevent upset conditions which may arise due to the changes in aqueous phase composition using industrial scale counter-current extraction flow systems.

One major problem that has been identified in ALSEP is associated with slow stripping kinetics of MA and heavier Ln. The molecular mechanism behind this phenomenon is unknown. Liquid-liquid extraction kinetics are governed by a number of chemical processes, including solvation changes, chemical complexation reactions, solute transport through the liquid-liquid interface, and aggregation of extracted solutes in the solvent. One likely limiting kinetic step is the rate of complexation/decomplexation of a metal ion by an organic extractant. It is anticipated that non-ideal behavior observed in ALSEP is due to complicated speciation of organic phase metal complexes, which has not been taken into account in chemical models to date.

2.4 Optimization of Extraction Processes

Any solvent extraction system, in order to scale from the bench to the industrial level, must be robust to process conditions. Solvent extraction process are complex systems,

with multiple chemical equilibria, some of which are not always well understood. Unintended interactions between various components may lead to conditions that result in deviation from ideal operation, causing diminished performance *via* decreased separation factors or slow kinetics, for example.

2.4.1 Aggregation of Extractants

Aggregation of organic-phase extractants can affect the metal ion selectivity as well as the efficiency of extraction.[43,44] Additionally, extensive aggregation can lead to detrimental "third phase" formation, the splitting of the organic phase into a light, diluent-rich, and heavy, extractant-rich, phase, which is problematic for process-scale operation.[45] Process-scale solvent extraction is run in equipment (e.g., centrifugal contractors or mixer-settlers) in which the formation of any solids, or heavier phases, poses a problem to efficiency and normal operation. Additionally, in the scenario in which fissionable material would be present, the formation of third phase introduces the risk for criticality incidents by concentrating the material in a smaller volume of the organic phase.

It is anticipated that the HEH[EHP] extractant will self-organize to form reverse micelles or larger aggregates in the organic phase before and/or after contact with metal-containing aqueous feed solutions, based on the results of investigations with its phosphoric acid analog, HDEHP.[36,46–50] Similarly, TODGA has been found to form reverse micelles when contacted with moderate concentrations of HNO_3.[43,51–53] However, data in the published literature for the aggregation behavior for HEH[EHP] under conditions relevant to the ALSEP process are lacking. Additionally, no results are published for aggregation in the ALSEP solvent, that is, on aggregation with the combination of DGA and HEH[EHP] in aliphatic diluents.

In other extraction systems, certain conditions have been found to promote or induce third phase formation. For example, partitioning of HNO_3 from highly acidic aqueous phases into the organic phase has been previously shown to facilitate aggregation

and third phase formation in such processes utilizing tributyl phosphate (TBP).[54] On the other hand, at the pH of the citrate buffer (3–5), a portion of HEH[EHP] will be converted to the sodium salt, which is prone to micelle formation.[46,47] In both cases, it is not known if the acid and/or anions that may partition into the organic phase will be involved in the metal coordination with HEH[EHP] or not.

2.4.2 Partitioning of Water and Acid

It has been observed in systems of various different extractants (malonamides, diglycolamides, and netutral orgaonophosphorus extractants) that the uptake or co-extraction of water and acid can have significant effects on the aggregation of extractant molecules and third phase formation.[44,52,55–57]

Nave and co-workers[52] observed that aggregation of TODGA into tetrameric reverse micelles is accelerated by extraction of HNO_3, with increased HNO_3 extraction resulting in the formation of additional aggregates (i.e., a shift of the monomer:dimer:tetramer equilibrium toward higher n-mers). These authors also claim that increased extraction of HNO_3 results in an increase in the interaction and attractive force between micelles, which arises from the increased polarity of the acid-loaded micellar core, leading to enhanced third phase formation.

The extraction of acid, in absence of metal, can promote the formation of third phase in various solvent extraction systems. Formation of third phase in the TODGA system has been reported under various conditions. Sasaki[58] reported that TODGA contacted with 6 M HNO_3 did not form third phase; Nave[52] reported third phase formation after contact with 3 M HNO_3; and Modolo[59] reported third phase after contact with 4–6M HNO_3. The cause for the discrepancy in these results is unknown. A study by Jensen[43] reports the formation of TODGA reverse micelles after contact with 0.7 M HNO_3, and observes a drastic increase in organic phase water concentration, diagnostic of reverse micelle formation, after equilibration with HNO_3 above this concentration.

Acid uptake has been determined for TODGA[53,60] and T2EHDGA systems.[61,62] To the best of knowledge, there are no published reports of nitric acid uptake by HEH[EHP], nor of the HEH[EHP]-T2EHDGA system. The concentration of water co-extracted with metal has been reported for various HEH[EHP] concentrations with select Ln,[63] as has the extraction of water into HEH[EHP] from variable concentration lactic acid.[64]

3 Effect of HEH[EHP] Impurities on the ALSEP Solvent Extraction Process

3.1 Preface

This contents of this chapter have been published as an article in the journal *Solvent Extraction and Ion Exchange*, DOI:10.1080/07366299.2017.1412111

3.2 Abstract

In solvent extraction processes, organic phase impurities can negatively impact separation factors, hydrolytic performance, and overall system robustness. The resulting inconsistent performance can affect the process-level viability of a separation concept, and thus knowledge of the impurities present, their effects on the process, and how to remove them are vital. Deleterious impurities may be introduced into a system from reagent synthesis, or result from degradation via radiolysis and hydrolysis during use. In this work, the acidic extractant, 2-ethylhexylphosphonic acid mono-2-ethylhexyl ester (HEH[EHP]) –proposed for application in extractive processes aimed at separating trivalent minor actinides from lanthanides and other fission products – is characterized with respect to its common impurities and their impact on Am(III) stripping in the Actinide Lanthanide SEParation (ALSEP) system. To control impurities in HEH[EHP], existing purification technologies commonly applied for the acidic organophosphorus reagent were assessed and a new chromatographic purification method specific to HEH[EHP] is presented.

3.3 Introduction

Successful transition of solvent extraction processes, which are developed and validated in laboratory settings, to large-scale industrial implementation relies on consistent and predictable performance of the system components. The solvents are the most important components, and even low levels of impurities can alter their extractant properties, which can have a significant impact on the overall performance of the system. Most notably, acidic impurities present in neutral extractants manifest themselves by interfering with the partitioning of metal cations from loaded organic solvents into the aqueous stripping solution, obstructing solvent regeneration and quantitative recovery of the product of interest. For example, the presence of small amounts of dibutylphosphoric acid (HDPB) and monobutylphosphoric acid (H2MBP), impurities and degradation products of tributylphosphate (TBP), interfere with ura-

nium stripping in the Plutonium Uranium Reduction Extraction (PUREX) process.[65] Acidic impurities present in (diisobutylcarbamoyl)methyloctylphenylphosphine oxide (CMPO) have been found to affect Am(III) stripping efficiency in the TransUranic Extration (TRUEX) process.[66] In the Caustic-Side Solvent Extraction (CSSX) process, a trace-level impurity, dodecylsulfonate, significantly suppresses cesium stripping.[67] In processes based on di(2-ethylhexyl) phosphoric acid (HDEHP), 2-ethylhexanol and the diacid radiolytic degradation product of HDEHP, mono(2-ethylhexyl)phosphoric acid (H2MEHP), have been found to depress extraction of Ln(III), U(VI), and Sr(II).[68] Given the significant impact that impurities have been found to have on various solvent extraction systems, it is clear that sufficiently pure extractants are necessary for the robust and predictable performance of solvent extraction systems as well as for optimization of their performance via fundamental studies.

The acidic extractant, 2-ethylhexylphosphonic acid mono-2-ethylhexyl ester, HEH[EHP], is currently being investigated for application in the Advanced TALSPEAK (Trivalent Actinide Lanthanide Separation by Phosphorus-reagent Extraction from Aqueous Complexes) and ALSEP (Actinide Lanthanide SEParation) concepts developed for trivalent minor actinide (MA) recovery in used nuclear fuel reprocessing.[2,39,41,42,64,69] HEH[EHP] impurities are expected have different effects on the process chemistry of the Advanced TALSPEAK and ALSEP systems. In Advanced TALSPEAK, trivalent lanthanide/actinide separation is achieved using a polyaminocarboxylate hold-back reagent to retain the trivalent MA in the buffered (pH 2 – 4) aqueous phase while the lanthanides (Ln) are extracted by the weakly acidic HEH[EHP] into an aliphatic diluent.[39,40,64] Because this system operates via a cation exchange mechanism, neutral and minor-constituent acidic impurities in HEH[EHP] are not expected to significantly affect its separation performance. Indeed, the Advanced TALSPEAK concept was successfully demonstrated using unpurified commercial HEH[EHP] reagent under single- and multi-stage dynamic flow conditions.[41,42] In contrast, ALSEP combines the neutral diglycolamide *N,N,N′,N′*-tetra-(2-ethylhexyl) diglycolamide (T2EHDGA) with HEH[EHP] in an aliphatic diluent. The ALSEP solvent co-extracts trivalent actinides and lanthanides from a post-PUREX raffinate,

which are subsequently separated in a stripping step using a buffered polyaminocarboxylic acid solution, such as *N*-(2-hydroxyethyl)ethylenediamine-*N*,*N*′,*N*′-triacetic acid (HEDTA) in citrate buffer. During the MA stripping stage, a balance between MA coordination affinity toward the aqueous buffered polyaminocarboxylic acid solution and organic phase HEH[EHP] governs the separation process. Consequently, acidic impurities in the organic solvent may have a significant impact on the performance of the ALSEP solvent. Increased retention of the MA in the loaded ALSEP solvent due to acidic impurities present in the source HEH[EHP] may result in insufficient MA stripping by HEDTA and therefore compromise separation factors. This problem is difficult to address and limits the efficiency of the overall process.

HEH[EHP] is offered by only a few commercial suppliers and typically contains multiple phosphorus-bearing impurities. In addition to phosphorus-bearing organic impurities, non-phosphorus organic impurities and transition metals, such as iron, are common. Two methods originally developed for the purification of the phosphoric acid HDEHP are most commonly applied to the purification of the phosphonic acid HEH[EHP].[70,71] The copper salt precipitation method is successfully used for the purification of HDEHP to remove neutral phosphorus-containing impurities.[70,72] However, as demonstrated in this work, when applied to HEH[EHP], this method does not separate the impurities that form copper complexes which co-precipitate with the copper HEH[EHP] complex, notably, HDEHP and other acidic impurities which are found to be problematic in ALSEP. Modifications to the copper salt method have been developed to improve the yield and reproducibility of HDEHP purification;[73] these optimizations do not fundamentally alter the separation chemistry, and are not anticipated to significantly improve HEH[EHP] purity. The "third phase" purification method[71] achieves purification by forming the sodium salt of HEH[EHP] in a middle phase microemulsion, and, as shown in this work, fails to completely remove neutral impurities and HDEHP.

Alternate methods for the purification of HDEHP and other extractants proposed for reprocessing flowsheets have been published.[66,72,74–78] A procedure for HDEHP pu-

rification similar to the "third phase" method first forms the sodium salt, followed by distillation under reflux, and finally washing with ethylene glycol to remove the 2-ethylhexyl phosphoric acid (H2MEHP) impurity.[74] Conversion to the sodium salt followed by caustic scrubs is found to remove some impurities, but these methods are found to suffer from inconsistencies in purity of the final product.[72] With judicious choice of organic diluent, a simple water wash may provide effective removal of mono-alkyl acidic impurities from the more hydrophobic HDEHP.[75] Vacuum distillation of HDEHP was found to provide little improvement in purity.[72] Macroporous anion exchange resins have been used to remove acidic impurities from neutral extractants, such as CMPO.[66,76] Similarly, removal of neutral impurities from HDEHP by macroreticular anion exchange resin has been reported.[77,78] However, in the case where both acidic and neutral impurities are present in an acidic solvent, ion exchange methods may be challenging to implement.

Due to the variability in the impurities present in commercially available HEH[EHP], which may be acidic, neutral, or both, the common purification methods do not consistently produce HEH[EHP] of sufficient purity for fundamental studies nor robust solvent extraction performance. Additionally, it was found in the course of the present work that certain impurities present in commercially available HEH[EHP] can have significant impact on solvent extraction systems, particularly ALSEP. To develop an improved purification procedure, we characterized the impurities present in commercially available HEH[EHP] and evaluated the performance of existing purification methods. The present study presents a new purification method for HEH[EHP] that can remove all phosphorus-bearing impurities. The method reported here applies the copper salt precipitation method to remove a neutral impurity, followed by column chromatography to remove the remaining impurities that are not removed by the first method. The effect of HEH[EHP] impurities on the ALSEP flowsheet are determined and quantified.

3.4 Experimental

Experimental solvent extraction studies were conducted both at the Pacific Northwest National Laboratory (PNNL) and at Idaho National Laboratory (INL). Significant differences in the materials and methods used at these two institutions are indicated in the experimental description below.

3.4.1 Materials

T2EHDGA was obtained from Eichrom Technologies, LLC (Lisle, IL) and either used as received (INL) or purified before use (PNNL) as described elsewhere.[62] Samples of HEH[EHP] were obtained from four suppliers: BOC Sciences (Shirley, NY), Marshallton Research Laboratories, Inc. (King, NC), CarboSynth (U.K.) and Yick Vic Chemicals & Pharmaceuticals (Hong Kong). In the text, these suppliers are identified as A, B, C, and D (assigned randomly). Two different manufacturing lots from supplier A were used, and are identified as A-1 and A-2. Reagent grade *n*-dodecane was obtained from Alfa Aesar and used as received. Octylphosphonic acid was obtained from Strem and used as received. HDEHP was obtained from Sigma-Aldrich and purified[71] before use. Radiotracer ^{241}Am (7.4 MBq/mL) was purchased from Eckert & Ziegler as $AmCl_3$ in 1 M HCl (PNNL) or obtained from laboratory stocks (INL). Citric acid (Fluka) and HEDTA (Aldrich) were of ACS grade. Aqueous HNO_3 solutions were prepared using TraceSELECT 16 M HNO_3 (Fluka) and standardized using Titrando Metrohm 905 Automatic Titrator against NaOH. The pH of citrate buffer solutions was adjusted by addition of NaOH and checked by pH electrode (Orion Ross). Except as indicated in specific procedures, all other reagents were of analytical grade and used as received. All aqueous solutions were prepared using distilled water deionized to at least 18 MΩ-cm resistivity.

3.4.2 Solvent extraction procedures

Unless otherwise noted, solvent extraction experiments were performed in at least duplicate by batch contact. The PNNL experimental protocol consisted of the following procedure. Equal volumes of the ALSEP solvent organic phase (0.05 M T2EHDGA + 0.75 M HEH[EHP] in *n*-dodecane) were equilibrated with 3 M HNO_3 spiked with ^{241}Am tracer (a typical sample contained 3.5 – 10 kBq ^{241}Am) and agitated on a hand-motion shaker (Sonics SHK-COCK2) at ambient temperature (19 $\pm$ 1 °C) in screw-top plastic vials (2.0 mL, Axygen Scientific). After centrifugation, the organic phase was removed to a fresh vial and scrubbed with an equal volume of 0.2 M Na-citrate solution (pH = 3) under the same equilibration conditions as the extraction step. After phase separation by centrifugation, an aliquot of the scrubbed organic phase was removed to a fresh vial containing the stripping solution (0.125 M HEDTA + 0.2 M Na-citrate, pH = 3) and equilibrated as before. Equilibration times for the extraction, scrub, and stripping steps were 5, 15, and 60 minutes, respectively. A phase volume ratio of organic/aqueous = 1 was maintained at each step. The INL experimental protocol differed from the PNNL procedure as follows. Samples were agitated using a large capacity mixer (Glass-Col) at ambient temperature (19 $\pm$ 1 °C). Equilibration times for extraction, scrub, and stripping steps were 30 minutes.

Between each step, aliquots of each phase were removed for radiometric analysis to determine ^{241}Am distribution ratios. ^{241}Am activity was determined by gamma spectroscopy (NaI(Tl), PerkinElmer Wizard^2 Model 2480 or a high purity germanium detector). The distribution ratio, D, defined as

$$D = \frac{[\mathrm{Am}^{3+}]_{\mathrm{organic}}}{[\mathrm{Am}^{3+}]_{\mathrm{aqueous}}} \tag{3.1}$$

was calculated as the ratio of the organic phase ^{241}Am activity concentration to that in the aqueous phase. D values from 0.001 to 100 could be reliably measured by this technique.

3.4.3 Purification methods

HEH[EHP] was purified following existing literature procedures,[70,71] by column chromatography, and by vacuum distillation. Silica gel (60 Åpore size, 70-230 mesh, Alfa Aesar) was sonicated in the selected eluent (e.g., 80% dichloromethane:20% acetone (v:v)) and slurry packed into glass columns (1.7 cm or 6 cm diameter, 15 or 25 cm length, respectively). The compound to be separated was dissolved in a minimal volume of the eluent and loaded onto the column. Flow was controlled using the column stopcock to 1-2 drops per second. Eluate fractions were collected in glass vials for analysis. Vacuum distillation was performed using a Kugelrohr apparatus (Buchi) at 0.1 torr and a maximum temperature of 190 °C.

3.4.4 Analytical methods

^{31}P NMR measurements were performed on a Varian VNMRS spectrometer operating at a field strength of 17.6 T (^{1}H ν_0 = 748.4 MHz, ^{31}P ν_0 = 303.0 MHz) with a Varian 5mm direct, broadband tuneable, pulsed-field gradient (PFG) probe. The temperature was regulated at 25 °C for all experiments. Unless otherwise specified, each ^{31}P spectrum was acquired using a 90° pulse width of 13.375 μs, an acquisition time of 0.89 s, and a recycle delay of 30 s. The number of transients collected varied from 64 to 256. Broadband ^{1}H decoupling employing the WALTZ-16 composite pulse scheme was applied during acquisition only. The resulting free induction decays were zero-filled to 64k points and multiplied by an exponential decay function to give 1 Hz line broadening. Spectra were referenced to zero ppm using an external reference of 85% phosphoric acid. For quantitative studies, spectra were referenced using the ^{31}P signal of 50 mM tetraphenylphosphonium chloride in $CDCl_3$ contained in a coaxial insert. Processing was performed using VNMRJ 4.0 and Mestrenova 10.0.

ESI-MS was performed on a Finnigan MAT TSQ-7000 in positive and negative mode, using a flow rate of 10.0 μL/minute, capillary temperature of 250 °C, and spray voltage of 4.50 kV. Samples were prepared in CHROMASOLV HPLC grade acetonitrile (Riedel-

de Haën) and diluted to nominal concentration of 0.1 mM.

GC-FID was performed using a Thermo Scientific Trace ULTRA gas chromatograph and FID detector. The chromatograms were processed using Thermo Scientific Xcalibur software. The chromatographic separations were carried out utilizing a Thermo Scientific TG-35MS capillary column (30 m x 0.32 mm ID x 0.5 μm film) with helium carrier gas. Samples were derivatized using diazomethane in hexane in conjunction with dilution in hexane and addition of 0.5 mM tributyl phosphate (TBP), as an internal standard, prior to analysis.

GC/MS analysis was performed using an Agilent 7890A gas chromatograph equipped with a 7693A automatic liquid sampler, an HP-5ms capillary column (30 m long x 0.25 mm inside diameter with a 0.25-μm capillary film of 5% phenyl methylsilicone) and a 5975C mass-sensitive detector. Splitless injections of 1 μL were made at an inlet temperature of 270 °C with a 15-s dwell time (needle left in the inlet after injection), an initial column temperature of 50 °C and helium carrier gas at a constant flow of 1 mL/min. After 2 min at 50 °C, the temperature was ramped at 15 °C/min to 300 °C and held for 2 min. The detector was operated with a transfer line temperature of 300 °C, source temperature of 230 °C and quadrupole temperature of 150 °C. After a 6-min solvent delay, electron-impact mass spectra from 50 – 550 amu were collected continuously (3/s) for the duration of the run.

Samples of HEH[EHP] were dissolved at 2 mg/mL in chloroform (stabilized with amylene), and a 5-μL (10-μg) sample of each was transferred to a 2-mL glass autosampler vial. Samples were then treated with a silylating agent, N,O-bis(trimethylsilyl)trifluoroacetamide (BSTFA) containing 1% trimethylsilyl chloride (TMSCl), to produce trimethylsilyl (TMS) derivatives of all hydroxyl-containing compounds. To each vial was added 100 μL of this reagent, after which the vials were sealed and heated at 60 °C for 30 min. Prior to analysis, each sample was diluted with 900 μL of *n*-hexane.

Data were analyzed using the instrument manufacturer's ChemStation software. Due

to the presence of ions from background or co-eluting compounds, targeted compounds were analyzed on the basis of distinctive ions. Peak integrals from these ions were scaled according to the fractional abundance of the ion in the mass spectrum of the compound, creating an approximated total ion integral. The ions (scaling factors) were as follows: 2-ethylhexanol(TMS), *m/z* 187 (5.72); di(2-ethylhexyl) ether, *m/z* 112 (10.82); EHP(TMS)$_2$, *m/z* 243 (4.40); HEH[EHP](TMS), *m/z* 267 (5.97); HDEHP, *m/z* 171 (2.57); and DEH[EHP], *m/z* 195 (2.94).

3.5 Results and Discussion

Samples of HEH[EHP] obtained from suppliers A, B, and C were characterized using quantitative $^{31}P\ \{^1H\}$ NMR, GC/MS, and ESI-MS. Multiple impurities were observed in each sample and their relative concentrations were found to vary between lots and between manufacturers. The objective of this investigation was three-fold:

1. determine the structural identity of the most abundant impurities and examine the efficiency of their removal by the two most commonly applied purification methods, namely the copper salt precipitation and sodium salt third phase methods

2. evaluate the impact of the individual impurities on the ALSEP process

3. develop an improved purification method to quantitatively remove impurities that are the most detrimental for the ALSEP process.

3.5.1 Characterization of HEH[EHP] impurities by GC/MS and ESI-MS

A survey of commercial samples of HEH[EHP] was undertaken to identify major impurities. As-received materials from suppliers A, B, and C were trimethylsilylated to improve chromatographic behavior and analyzed by GC/MS. Impurities identified in all samples include 2-ethylhexanol, di(2-ethylhexyl) ether, 2-ethylhexylphosphonic

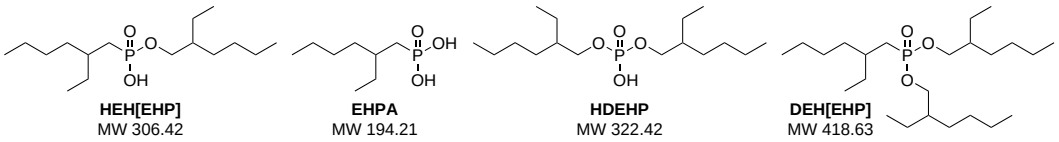

Figure 3.1: Structures and molecular weights of HEH[EHP] and principal P-bearing impurities.

acid (EHPA), di(2-ethylhexyl)2-ethylhexyl phosphonate (DEH[EHP]), and HDEHP (Figure 3.1). Of these compounds, only 2-ethylhexanol(trimethylsilyl ether) could be identified on the basis of a matching reference spectrum in the NIST Mass Spectral Database. Mass spectra for the identified impurities are provided in the supporting information (Figure 3.7). HDEHP was assigned on the basis of comparison to an authentic sample, and the remaining compounds were assigned on the basis of molecular weight, fragmentation pattern, retention time, and sample history. The assignment for di(2-ethylhexyl) ether ($C_{16}H_{34}O$, exact mass 242.26) was made based on the following. The fragmentation pattern is consistent with that expected of a long-chain ether,[79] and its mass spectrum is very similar to that of the isomeric n octyl ether, with no parent ion observed and the largest significant fragment having *m/z* 113 ($C_8H_{17}^+$). However, the observed material elutes earlier than authentic *n*-octyl ether (t_R 11.2 vs. 12.4 min), consistent with a branched structure. Furthermore, the compound did not form a trimethylsilyl derivative, and hence is unlikely to be an alcohol. Di(2-ethylhexyl) ether could plausibly form from 2-ethylhexanol in several ways during the synthesis and purification of HEH[EHP], for example, from acid-catalyzed condensation or alkylation during the base-catalyzed hydrolysis of DEH[EHP] to HEH[EHP]. Together, these factors support the assignment of di(2-ethylhexyl) ether.

GC/MS chromatograms of four as-received commercial samples are shown in Figure 3.2, and a summary of the analyses for these samples as well as purified forms is presented in Table 3.1. It is important to note that the reported relative peak areas are not corrected for differential response of the detector to the various compounds and are thus not true molar or mass percentages. Many of the suspected impurities are not available in pure form commercially, limiting the choice of standards for quantitative

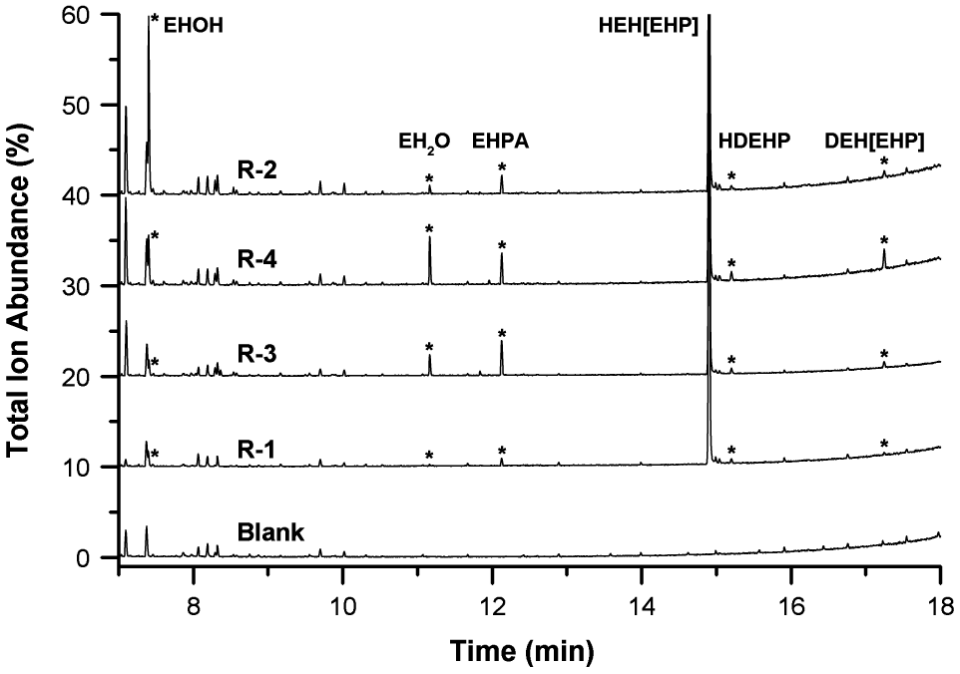

Figure 3.2: GC/MS Analysis of commercial HEH[EHP]. Total ion chromatograms are shown for four samples of commercial materials from three different suppliers (A, B and C), along with a blank, to illustrate the variations in purity. Samples A-1 and A-2 are different production lots received from the same supplier. The chromatograms are scaled such that the HEH[EHP] peak at 14.9 min has a relative intensity of 100%. Samples were trimethylsilylated prior to analysis, converting 2-ethylhexanol (EHOH), HEH[EHP] and HDEHP to monosilyl derivatives and EHPA to a disilyl derivative. Di(2-ethylhexyl) ether (EH_2O) and DEH[EHP] are unmodified.

GC/MS analysis. While this lack of standards makes exact quantification by GC/MS difficult, the concentration of a given impurity relative to HEH[EHP] can be compared among samples, which makes the technique valuable for testing different production lots of material and evaluating the efficacy of purification procedures. As discussed below, relative impurity concentrations determined by GC/MS correlate well with those determined by ^{31}P NMR, which directly provides mole ratios for P-containing impurities.

The two non-phosphorus containing impurities, 2-ethylhexanol and di(2-ethylhexyl) ether, were found in widely varying relative concentrations. Notably, the sample from supplier B was found to contain significantly more 2-ethylhexanol, nominally 20%

Table 3.1: Retention time and assignments from GC/MS analysis of HEH[EHP]. Impurities found in HEH[EHP] material obtained from three suppliers (A, B, and C), prior to and after various purification procedures. Ion intensities have been normalized to the HEH[EHP] total ion signal.

Compound	2-ethylhexanol	di(2-ethylhexyl) ether	2-ethylhexyl phosphoric acid	HEH[EHP]	HDEHP	DEH[EHP]
Retention time (min)	7.4	11.16	12.13	14.90	15.21	17.25
A-2, as received	5.89	5.67	3.54	100	1.14	2.63
A-1, as received	1.94	2.55	2.83	100	0.72	0.86
A-1, third phase purified	0.09	0.38	1.48	100	2	2.15
A-1, copper salt purified	0.2	0	1.04	100	2	0
A-1, column purified	1.99	2.6	0.92	100	0.45	0.96
B, as received	20.2	0.7	1.83	100	0.55	0.82
B, third phase purified	7.36	0.8	0.73	100	0.88	0.27
B, copper salt purified	0.22	0	0.64	100	0.41	0.03
C, as received	1.64	0.13	0.82	100	0.66	0.41

relative to HEH[EHP], than samples from other suppliers, which contained 1.6-5.9%. Di(2-ethylhexyl) ether was found at levels ranging from 0.1-5.7%. EHPA, the phosphonic acid hydrolysis product of HEH[EHP], occurs at levels ranging from 0.8-3.5%, with a much higher relative concentration in the samples from supplier A, and with lowest concentration in the sample from supplier C. DEH[EHP], the neutral phosphonic diester, was present in all samples at similar levels of 0.6-2.4% with lowest relative concentration in the supplier C sample, and at higher concentrations in samples from the other suppliers. Relative concentrations of the phosphoric diester, HDEHP, were lower and in a narrower range of 0.55-1.1%. Analysis of material from two different production lots received from a single supplier (samples A-1 and A-2) showed significant batch-to-batch variation in the concentration of the various impurities, with one batch having 25-200% more of each impurity.

Analysis of one commercial sample (supplier B) of HEH[EHP] by ESI-MS confirmed the GC/MS identification of 2-ethylhexanol, EHPA, DEH[EHP], and HDEHP (Figure 3.3 and Table 3.2). The ESI-MS data showed the typical proton, sodium and solvent adducts, as well as dimer, trimer, and higher order oligomers of HEH[EHP]. Detection of intact DEH[EHP] as $[M+H]^+$ at *m/z* 419 substantiated the assignment in GC/MS, where the parent ion fragmented completely. While the phosphonic acids (EHPA and HEH[EHP]) were detected in both negative- and positive-ion mode, HDEHP was detected only in negative ion mode, where its greater acidity likely enhances its signal with respect to other components.

3.5.2 Characterization of HEH[EHP] impurities by ^{31}P NMR

^{31}P NMR reveals the oxidation state of P-containing molecules through chemical shift and directly provides their molar ratios through integration, while also providing valuable information about the chemical environment of the analytes. Quantitative ^{31}P NMR was used to determine the nature and relative abundance of the P-bearing impurities in HEH[EHP] samples received from suppliers A, B, and C (Table 3.3 and Figure 3.4). ^{31}P NMR spectra typically showed four resonances in addition to the

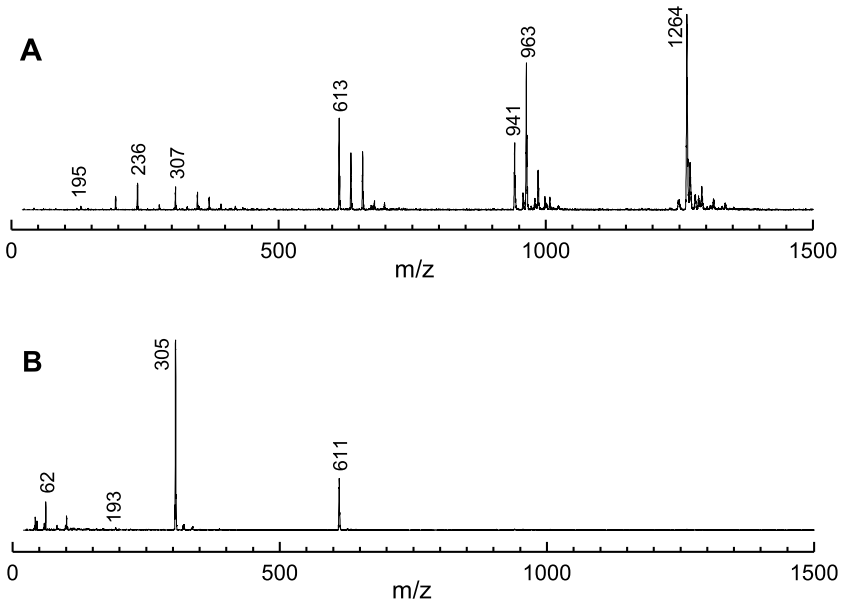

Figure 3.3: ESI-MS spectrum of HEH[EHP] (supplier B, 0.01 mM in MeCN) in (A) positive ionization mode and (B) negative ionization mode. Peaks are identified in Table 3.2.

Table 3.2: Assignments of peaks in ESI-MS spectrum of HEH[EHP] (supplier B, 0.01 mM in MeCN). In the table,"X" refers to the parent species of that row, i.e., in the first row, X = EHPA.

m/z (positive mode)	Assignment
195.2, 236.3, 277.3	EHPA + H, X + H + MeCN, X + H + 2MeCN
307.3, 348.3, 370.0	HEH[EHP] + H, X + H + MeCN, X + MeCN + Na
392.3	HEH[EHP] - H + 2Na + MeCN
419.3	DEH[EHP] + H
613.4, 635.5, 657.3, 679.3	$HEH[EHP]_2$ + H, X + Na, X - H + 2Na, X - 2H + 3Na
941.7, 963.8, 985.7	$HEH[EHP]_3$ + Na, X - H + 2Na, X - 2H + 3Na
1247.9, 1270.0	$HEH[EHP]_4$ + Na, X - H + 2Na
1263.9	$HEH[EHP]_4$ + K
m/z (negative mode)	**Assignment**
62.4	NO_3^-
193.1	EHPA - H
305.1, 610.9	HEH[EHP] - H, $HEH[EHP]_2$ - H
321.3	HDEHP - H

main HEH[EHP] resonance at δ 35.8 ppm. Structural assignments were made based on the observed chemical shifts and information obtained from GC/MS and ESI-MS characterizations. On the basis of chemical shift, the impurity appearing at δ 1.8 ppm (in $CDCl_3$) can be assigned to the only significant phosphoric impurity, HDEHP; this assignment is consistent with the oxidation state, the observed chemical shift of pure HDEHP and the observation of HDEHP by GC/MS and ESI-MS. Similarly, the resonance at δ 32.6 ppm (slightly upfield of HEH[EHP]) can be assigned as the neutral species DEH[EHP] identified in the GC/MS and ESI-MS. Substitution of additional alkyl groups onto oxygen bonded to phosphorus is known to cause upfield shifts;[80] and the structurally similar diamyl(amyl) phosphonate has a reported chemical shift of 31.6 ppm in dichloromethane.[81] The good correlation ($R^2 \geq 0.95$) between impurity concentrations found by ^{31}P NMR and GC/MS, shown in Figure 3.8, supports the ^{31}P NMR assignments for DEH[EHP] and HDEHP.

The chemical shifts and line shapes of the remaining two resonances at δ 36.4 ppm and δ 36.6 ppm (downfield of HEH[EHP] in $CDCl_3$) were found to depend on the diluent. Of these, the impurity appearing at δ 36.4 ppm was generally sharper and

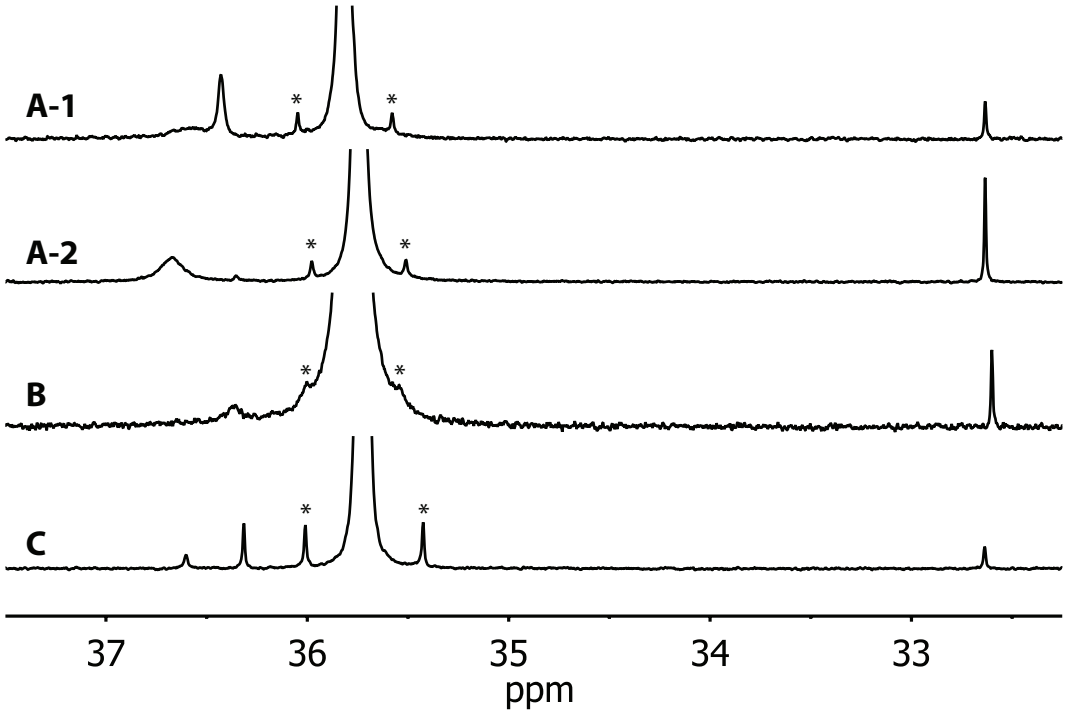

Figure 3.4: ^{31}P $\{^{1}H\}$ NMR of HEH[EHP] material as-received (unpurified) from three different suppliers (A, B and C). Samples A-1 and A-2 are different production lots received from the same supplier. The region about the HEH[EHP] resonance at δ 35.7 ppm is expanded. ^{13}C satellites are marked by (*). All spectra were recorded in $CDCl_3$.

Table 3.3: Phosphorus-containing impurities in HEH[EHP] from various suppliers, as determined by quantitative ^{31}P $\{^{1}H\}$ NMR spectroscopy. Integrations are reported as atom-% relative to HEH[EHP] (assumes 1 P-atom per chemical environment). NQ indicates the resonance was not quantifiable by this detection method.

Sample	DEH[EHP] (δ 32.6 ppm)	HDEHP (δ 1.8 ppm)	Acidic Impurity (δ 36.6 ppm)	EHPA (δ 36.4 ppm)
A-1, as received	0.75	1.19	0.73	2.91
A-1, third phase purified	1.47	2.93	NQ	2.83
A-1, copper salt purified	NQ	2.9	NQ	2.24
A-1, column purified	0.79	0.83	NQ	NQ
B, as received	0.64	0.65	NQ	0.8
B, third phase purified	0.16	1.52	NQ	0.076
B, copper salt purified	NQ	0.87	NQ	0.26
C, as received	0.1	0.64	0.1	0.36

is assigned as the acidic impurity EHPA. No specific structural assignment is made for the resonance at δ 36.6 ppm, as no correspondence was found with a specific P-bearing impurity identifiable in the GC/MS or ESI-MS. Rather, this peak might result from association of one or more species in solution, with chemical exchange causing the broadening. Both the broadness and position of the peak in this scenario are expected to depend on the solvent and nature of impurities present. In support of this hypothesis, only sharp peaks were observed in the strongly polar, dissociating solvent methanol-d_4 or the non-polar, strongly associating solvent *p*-xylene (Figure 3.9). The broad peak was observed only in $CDCl_3$, which has intermediate polarity. Furthermore, addition of up to a 1.5 times molar excess of 2-ethylhexanol had little effect on the ^{31}P chemical shift of neutral DEH[EHP] but caused a pronounced upfield shift of the acidic phosphonic species (HEH[EHP] and EHPA) and the resonance at δ 36.6 ppm (Figure 3.10). These observed shifts may be caused by either association between the acidic species and 2-ethylhexanol, or by the change in the solvent polarity resulting from addition of the 2-ethylhexanol.[82] It is apparent that the presence of 2-ethylhexanol, which is present as an impurity in some samples, has a significant effect on the position of the acidic phosphonic species resonances.

3.5.3 Evaluation of copper precipitation and third phase purification methods

The results of GC/MS, ESI-MS and ^{31}P NMR characterization showed that HEH[EHP] obtained from various suppliers, including two batches from a single supplier, contained the same major neutral and acidic impurities, albeit at different relative concentrations. The total levels of P-bearing impurities ranged from 1 –5 mole percent (as measured by ^{31}P NMR), and significant levels of non-P-bearing impurities were also present, including 2–20% 2-ethylhexanol and 1–5% di(2-ethylhexyl) ether (as measured by GC/MS). These impurities and the variability in the purity of commercial materials have the potential to impact solvent-extraction protocols significantly. Therefore, a model separation was used to assess the performance of HEH[EHP] and determine the effects of the impurities, as well as the ability of existing purification methods to

remove them.

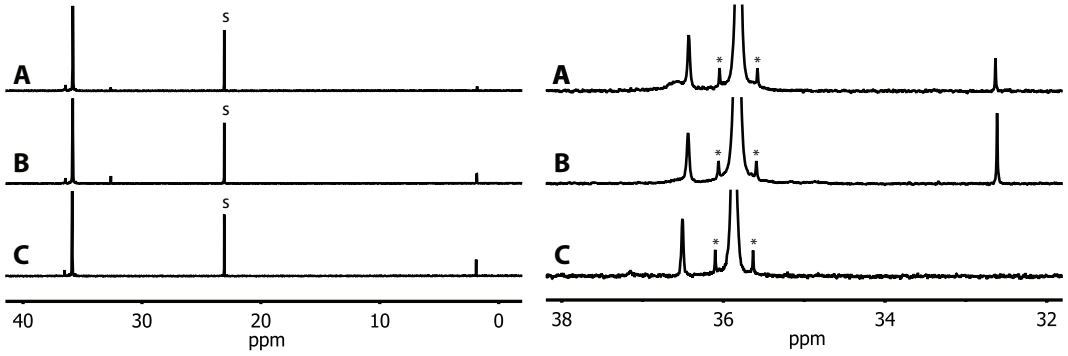

Figure 3.5: t
o paramagnetic impurities]Left: $^{31}P\{^{1}H\}$ NMR spectra of HEH[EHP] (supplier A-1) (a) as-received; (b) after purification by third phase method; (c) after purification by copper salt precipitation method. Right: expanded region around HEH[EHP] resonance of the same traces. Chemical shift standard, tetraphenylphosphonium chloride, is denoted by (s); ^{13}C satellites are denoted by (*). All spectra recorded in $CDCl_3$.

HEH[EHP] was purified using the copper salt and third phase methods[70,71] and comparatively assessed through quantitative ^{31}P NMR and GC/MS analysis. As shown in Tables 3.1 and 3.3, both methods remove significant fractions of 2-ethylhexanol, di(2-ethylhexyl) ether and EHPA, but neither method completely removes all of the phosphorus-bearing impurities. The residual impurities are clearly observed in the ^{31}P NMR spectra of HEH[EHP] of sample A-1 purified by each method (Figure 3.5).

Additionally, these purification methods may concentrate particular impurities during purification. For example, while the third phase and copper salt precipitation methods[70,71] effectively remove some acidic impurities, they are observed to concentrate the HDEHP impurity in material from suppliers A and B. In the copper salt precipitation method, copper complexes of both HDEHP and HEH[EHP] co-precipitate, resulting in poor separation. Similarly, in the third phase method, HDEHP can form a sodium salt in the microemulsion layer, preventing its separation from the HEH[EHP] sodium salt. The copper salt purification method was found to remove the neutral impurities DEH[EHP], 2-ethylhexanol and di(2-ethylhexyl) ether to at or near the limits of detec-

tion of the analytical methods, and appears to be more effective overall at removing impurities than the third phase method. The efficiency of the third phase method may depend on the initial concentration of neutral impurities, which may affect the solubility of other impurities in the organic and/or third phase, as observed by Hu and coworkers.[71] This comparison shows that both methods improve the purity HEH[EHP] but do not eliminate all impurities, so the purity of the final material depends, at least partially, on the concentration of impurities present in the starting material.

3.5.4 Effect of HEH[EHP] impurities and purification methods on ALSEP performance

HEH[EHP] obtained from suppliers A-1, B and C was used as-received to prepare three ALSEP solvent samples for a parallel examination. In these experiments, the previously described ALSEP solvent formulation of 0.75 M HEH[EHP] and 0.05 M T2EHDGA in *n*-dodecane was used.[69] These extraction experiments were designed to evaluate the variations in the distribution behavior of Am(III) among samples due solely to the different sources and purification methods of the HEH[EHP] used to prepare the ALSEP solvent constituent. The same T2EHDGA material purified as described previously[62] was used in all solvent samples. An aqueous 3 M HNO_3 solution containing trace quantity of Am(III) was equilibrated with the prepared ALSEP solvents. The Am(III)-bearing extraction solvent was then subjected to a scrubbing step with 0.2 M aqueous Na-citrate solution (pH 3) to remove HNO_3, followed by an Am(III) stripping step with aqueous 0.125 M HEDTA/0.2 M Na-citrate solution (pH 3). The same scrub and strip solutions were used in all parallel measurements.

In the ALSEP process, separation of the lanthanides and minor actinides is achieved via selective stripping of MA after their co-extraction with Ln. The D_{Am} values of each stage (extraction, scrub, and strip) provide metrics of the efficiency and performance of the process. High extraction D values allow Ln and MA to be extracted from molar HNO_3 solutions into the ALSEP solvent in a minimal number of stages. A high scrub D_{Am} is desired in order to prevent loss of MA to the scrub solution. To achieve a practical MA/Ln separation factor, the MA stripping D values must be minimized

Table 3.4: Extraction and stripping D_{Am} values of ALSEP solvent (0.05 M T2EHDGA + 0.75 M HEH[EHP] in *n*-dodecane) using HEH[EHP] from various suppliers. HEH[EHP] was used as received, or purified by a literature method[70,71] or as described in the text. Values in parentheses are $\pm\sigma$. Values outside the quantifiable range of D values (0.001 – 100) are reported as $\leq$0.001 or $\geq$100, respectively.

HEH[EHP] source	D_{Am}, extraction	D_{Am}, scrub	D_{Am},strip
A-1, as received	29.4 ($\pm$ 0.5)	$\geq$ 100	3.9 ($\pm$ 0.1)
A-1, purified (third phase)	30.17 ($\pm$ 0.03)	56.1 ($\pm$ 0.4)	1.13 ($\pm$ 0.01)
A-1, purified (copper salt method)	30.8 ($\pm$ 1.3)	54.82 ($\pm$ 0.08)	0.91 ($\pm$ 0.01)
A-1, purified (silica column)	26.3 ($\pm$ 0.7)	15 ($\pm$ 5)	0.44 ($\pm$ 0.02)
A-1, enriched in neutral impurity	21.0 ($\pm$ 0.3)	0.70 ($\pm$ 0.01)	0.18 ($\pm$ 0.02)
B, as received	25.32 ($\pm$ 0.07)	44 ($\pm$ 2)	0.73 ($\pm$ 0.05)
B, purified (third phase, PNNL)	27.4 ($\pm$ 0.4)	20.7 ($\pm$ 0.4)	0.37 ($\pm$ 0.01)
B, purified (third phase, INL)	19.5 ($\pm$ 0.6)	13.8 ($\pm$ 0.7)	0.34 ($\pm$ 0.01)
B, purified (copper salt method)	27.0 ($\pm$ 1.4)	26.17 ($\pm$ 0.01)	0.40 ($\pm$ 0.01)
C, as received	30.3 ($\pm$ 0.6)	27.4 ($\pm$ 0.8)	0.51 ($\pm$ 0.05)
D, as received	22.2 ($\pm$ 1.1)	60 ($\pm$ 3)	1.2 ($\pm$ 0.1)
D, purified (third phase, INL)	30.7 ($\pm$ 1.5)	40 ($\pm$ 2)	0.42 ($\pm$ 0.02)

and maintained well below unity. The process becomes less efficient as the MA strip D value increases, leading to an increase in the number of strip stages are required to partition MA from the organic phase to maintain a target separation factor in the process.

The results reveal that the extraction and stripping distribution ratios of Am(III) in the ALSEP process are highly dependent upon the commercial supplier of HEH[EHP], as shown in Table 3.4. Solvents prepared using HEH[EHP] as-received from suppliers A-1, B, C and D all exhibit extraction D_{Am} values over 20, which is acceptable for this process. The D_{Am} values during stripping with the citrate-buffered HEDTA solution vary from 0.51 to 3.9 for these solvents. The sample with the highest strip D_{Am} value is prepared with HEH[EHP] from supplier A-1, which GC/MS and ^{31}P NMR analysis showed contains the greatest relative concentrations of various impurities. The lowest D_{Am} stripping value corresponds to sample prepared with material from supplier C, which was found to have the lowest overall impurity levels.

To evaluate whether existing purification methods provide sufficient refinement of

HEH[EHP] to provide effective MA stripping, the ALSEP extraction/scrub/strip contact sequence was repeated using ALSEP solvent prepared with HEH[EHP] obtained from suppliers A-1, B and D that was purified by the copper salt precipitation and/or third phase methods. As evident from the results presented in Table 3.4, these purification methods have little effect on the extraction D_{Am} values. With all three materials, a large decrease in the scrub D_{Am} value is observed relative to the unpurified material, which is most pronounced with the material from supplier A. The D_{Am} strip values decrease substantially when using solvent prepared with HEH[EHP] purified by either literature method,[70,71] indicating the removal of some of the problematic impurities. However, the correlation between impurity concentration (determined by ^{31}P NMR and GC/MS) and Am(III) stripping behavior is not entirely clear. The pairs of purified samples from suppliers A-1 and B are an illustrative case, as each contains different relative amounts of the various impurities and yet exhibit either similar or dissimilar D_{Am} stripping values. The identification of which impurities are responsible for the anomalous stripping behavior and hence which are the most crucial to remove through purification is necessary. To this end, ALSEP solvent prepared using purified HEH[EHP] was doped with likely impurities (or analogues thereof) and a masking complexant to allow an examination of their role.

3.5.5 Addition of a basic complexant: trioctylamine

The results of extraction/scrub/strip tests using ALSEP solvent prepared with purified HEH[EHP] indicated that acidic impurities contribute to the Am(III) retention during stripping. A masking agent was selected to complex acidic impurities in the organic phase, in order to evaluate of the D_{Am} values under these conditions. Trioctylamine (TOA) is an organic base, and as such, reacts with a phosphorus oxyacid to form a lipophilic ion pair containing the trioctylammonium cation and the phosphorus oxyanion. Additionally, TOA has been reported to form complexes with organic acids in various organic diluents.[83–86] TOA (10 mM) was therefore added to four ALSEP solvent samples prepared with HEH[EHP] from suppliers A-1 and B, used either as

Table 3.5: Stripping D_{Am} values of ALSEP solvent (0.05 M T2EHDGA + 0.75 M HEH[EHP] in *n*-dodecane) prepared using HEH[EHP] from different sources, with and without the addition of 10 mM TOA modifier. Values in parentheses are estimates of the experimental error (± 3%).

HEH[EHP] Source	D_{Am}, strip 0 mM TOA	D_{Am}, strip 10 mM TOA
A-2, as received	7.3 (± 0.2)	2.20 (± 0.07)
A-1, purified (third phase)	1.18 (± 0.03)	0.75 (± 0.02)
B, as received	0.72 (± 0.02)	0.46 (± 0.01)
B, purified (third phase)	0.38 (± 0.01)	0.29 (± 0.01)

received (unpurified) or purified by the third phase method.[71] The solvents were subjected only to extraction and stripping steps for this test, and single replicates were performed. The extraction and strip D_{Am} values were determined as described previously.

Significant decreases in D_{Am} stripping values are observed with the addition of TOA for both purified and non-purified HEH[EHP] (samples A-1, A-2 and B), as shown in Table 3.5. The effect was greatest in samples that had the largest concentration of acidic impurities, with up to a 70% relative decrease in the D_{Am} strip value observed. This result suggests that addition of TOA inhibits the action of the acidic impurities EHPA and/or HDEHP, which have concentrations ranging from less than 0.1% to 3 mol-% and 0.65 to 3 mol-%, respectively, in the different samples, as determined by ^{31}P NMR (Table 3.3). The purified HEH[EHP] (supplier B) used in this experiment was found to have a minimal EHPA impurity by ^{31}P NMR, and yet still showed an improvement in the D_{Am} strip value from 0.38 to 0.29 upon the addition of TOA. This indicates that the addition of TOA likely results in either (a) formation of non-complexing adducts with both EHPA and non-EHPA impurities, such as HDEHP, present in the solvent and/or (b) participates in formation of MA coordination complexes that are more easily stripped than those formed in the absence of TOA. The exact mechanism by which TOA functions in this scenario is not clear, and is likely complex. Addition of TOA to the ALSEP solvent (in lieu of or in addition to solvent purification) may sufficiently mitigate the effects of acidic impurities, but such a change in solvent composition

Table 3.6: Extraction and stripping D_{Am} values of ALSEP solvent (0.05 M T2EHDGA + 0.75 M HEH[EHP] in *n*-dodecane) with the addition of varying amounts of HDEHP (14 – 73 mM). Values in parentheses are $\pm\sigma$. Values outside the quantifiable range of D_{Am} values (0.001 – 100) are reported as $\leq$0.001 or $\geq$100, respectively.

	D_{Am}, extraction	D_{Am}, scrub	D_{Am}, strip
B, as received	25.3 ($\pm$ 0.1)	44 ($\pm$ 2)	0.73 ($\pm$ 0.05)
B, 14 mM HDEHP added	25.0 ($\pm$ 0.5)	53 ($\pm$ 3)	0.99 ($\pm$ 0.01)
B, 45 mM HDEHP added	26.8 ($\pm$ 0.3)	90 ($\pm$ 28)	2.00 ($\pm$ 0.03)
B, 56 mM HDEHP added	26.1 ($\pm$ 1.5)	$\geq$100	2.38 ($\pm$ 0.02)
B, 73 mM HDEHP added	27.0 ($\pm$ 0.2)	$\geq$100	3.20 ($\pm$ 0.01)

would necessitate a thorough and careful investigation, which is beyond the scope of this work. The addition of the basic complexant TOA demonstrates that acidic impurities are deleterious to strip D_{Am} values, and we next examine the individual effects of the acidic impurities.

3.5.6 Addition of HDEHP

Solutions of ALSEP solvent (0.75 M HEH[EHP] + 0.05 M T2EHDGA) were prepared using purified T2EHDGA and unpurified HEH[EHP] (supplier B), with purified HDEHP added in varying concentration (14 – 73 mM). These solvent samples were used in the same extraction/scrub/strip procedure described previously.

Addition of HDEHP to the ALSEP solvent results in an increase in the D_{Am} scrub and stripping values, as shown in Table 3.6. As HDEHP is a more acidic complexant than HEH[EHP], it is expected that Am(III) might remain more fully complexed by HDEHP under the stripping conditions, resulting in the increased stripping D_{Am} values as HDEHP concentration increases. However, even when HDEHP was added in concentrations (73 mM) far exceeding those present in any source of HEH[EHP] tested (less than 25 mM), the D_{Am} stripping values were below those observed in solvents prepared without added HDEHP. This finding indicates that the HDEHP impurity likely contributes to Am(III) retention, but is not solely responsible for the observed high D_{Am} stripping values.

Table 3.7: Stripping D_{Am} values for the batch contact flowsheet test using ALSEP solvent prepared using purified HEH[EHP] (supplier D) containing varying concentrations of added octylphosphonic acid (0 – 17 mM). [Phos] denotes total concentration of phosphonic acid (i.e., added OPA and phosphonic acid impurity present in the sample), as determined by GC-FID. Values in parentheses are $\pm\sigma$.

[Phos], wt%	[Phos], M	D_{Am}, strip
0.04	3.31 E -4	0.43 ($\pm$ 0.01)
0.26	1.64 E -3	0.42 ($\pm$ 0.01)
0.31	2.33 E -3	0.49 ($\pm$ 0.01)
0.58	4.33 E -3	0.55 ($\pm$ 0.02)
1	7.33 E -3	0.72 ($\pm$ 0.04)
1.6	1.23 E -2	1.1 ($\pm$ 0.1)
2.3	1.73 E -2	1.6 ($\pm$ 0.1)

3.5.7 Addition of octylphosphonic acid

To assess whether the enhanced retention of Am(III) in the ALSEP solvent leading to ineffective stripping can be largely attributed to the phosphonic acid impurity, EHPA, a series of extraction/scrub/strip experiments was performed using ALSEP solvent with an added monoalkyl phosphonic acid. Since EHPA is not readily available as a pure compound, the commercially available, isomeric compound *n*-octylphosphonic acid (OPA) was chosen as an analog of EHPA. Samples of ALSEP solvent (0.75 M HEH[EHP] + 0.05 M T2EHDGA) were prepared using purified[71] HEH[EHP] from supplier D, with varying amounts of added octylphosphonic acid (2 – 17 mM). The organic solvents were first pre-equilibrated with 3 M HNO_3, and then were subjected to the same extraction, scrub, and strip procedure described previously.

The addition of OPA to the ALSEP solvent results in increased D_{Am} stripping values, as shown in Table 3.7. For this portion of the study, the total concentration of phosphonic acid (OPA + EHPA) in each solvent composition was determined by GC-FID, and is reported in Table 3.7. The D_{Am} strip value is observed to increase minimally when OPA concentration is under $2\mathrm{x}10^{-3}$ M. However, the data presented in Table 3.7 suggests that concentrations of phosphonic acid impurities in excess of ca. $3\mathrm{x}0^{-3}$ M may lead to unacceptably high Am(III) stripping distribution ratios, in excess of 0.5. While a

D_{Am} strip value of 0.5 is likely acceptable, lower values of strip D_{Am} allow for a more efficient and robust ALSEP process.

3.5.8 Effect of diethylhexyl ethylhexyl phosphonate (DEH[EHP])

DEH[EHP] is the neutral, P-bearing impurity found in most commercial samples of HEH[EHP]. While the exact synthetic route used in HEH[EHP] production by a given supplier is unknown, one reported synthetic route is from the basic hydrolysis of DEH[EHP].[87] It was not expected, *a priori*, that neutral impurities would be responsible for the anomalous stripping behavior. Under the conditions of the Am(III) stripping step (citrate buffered HEDTA solution at pH 3), complexation by acidic (proton-exchange) complexants is expected to be favored over complexation by neutral complexants, such as the dialkyl phosphonate DEH[EHP]. While a neutral complexant may alter the extraction step chemistry, behaving either as a synergist or antagonist of HEH[EHP], or as an independent neutral extractant, it is not expected to retain Am(III) during the stripping step, and hence is expected to have a minor, if any, effect on the Am(III) stripping D value. To verify this prediction, HEH[EHP] enriched in the neutral impurity, DEH[EHP], was prepared by contacting a 1 M solution of unpurified HEH[EHP] (supplier A-1) in hexane diluent with 1 M Na_2CO_3. The acidic HEH[EHP] selectively partitions to the aqueous phase, forming the sodium salt, leaving the organic phase enriched in neutral species. The DEH[EHP]-enriched organic phase was then washed with 3 M HCl and DI water before removal of solvent. ^{31}P NMR and GC/MS analysis verified enrichment of DEH[EHP] to 36% relative to HEH[EHP] in this sample. This material was used to prepare an ALSEP solvent which was used in the same extraction/scrub/strip batch contact tests of the ALSEP flowsheet as described previously, with results shown in Table 3.4.

A decrease in the extraction D_{Am} value was observed, as well as low D_{Am} scrub and stripping values, in the solvent prepared with enriched neutral impurity. The scrub and strip step distribution ratios of 0.70 and 0.18, respectively, show that this impurity is not responsible for retention of Am(III) in the organic phase, but instead con-

tributes to decreased retention. In this prepared solvent, the HEH[EHP] concentration was approximately 0.4 M (compared to 0.75 M in all other ALSEP solvent samples) and the concentration of the impurity is approximately 0.24 M. The lower HEH[EHP] concentration does not account for the exceedingly low D_{Am} of 0.70 observed in the scrub step, nor for the low strip D_{Am} value. It is suspected that the neutral impurity forms an adduct with HEH[EHP], similar to the adduct formed between HDEHP and tri-*n*-octylphosphine oxide (TOPO),[88] which would reduce the concentration of free HEH[EHP] available to complex metal during the scrub and strip steps. Adduct formation with HEH[EHP] would allow partitioning of metal to the aqueous phase resulting in the observed low scrub and strip D_{Am} values. The existence of such an adduct between HEH[EHP] and DEH[EHP] is also consistent with results of column chromatography (*vide infra*).

3.5.9 Purification of HEH[EHP]

Many of the studies using HEH[EHP] to date have applied existing literature methods[70,71] to purify the extractant. As described above, these methods do not effectively remove all impurities, and fail to sufficiently purify the HEH[EHP] material obtained from some suppliers. To address these drawbacks and to obtain high purity material, alternative purification methods were evaluated. Initially, purification was attempted by vacuum distillation (0.1 torr, 190 °C). However, degradation of HEH[EHP], confirmed by ^{31}P NMR, occurred before P-bearing impurities could be separated. Purification of HEH[EHP] via column chromatography was found to be more effective. A wide range of eluent compositions were studied, including various mixtures of hexanes:ethyl acetate, dichloromethane:acetone, and dichloromethane:ethyl acetate.

Eluent systems were evaluated with respect to their ability to separate the compounds of interest, as well as toward total separation time and necessary solvent volume. Less polar solvent systems, while providing acceptable separation of impurities, significantly increased the retention time of HEH[EHP]. A less-polar eluent system thus requires a greater volume of solvent to elute the material without a significant im-

provement in separation. An eluent composition of moderate polarity was found to be optimal for this system, to perform the separation in a time and resource efficient manner, while still maintaining optimal separation of impurities.

In all solvent systems evaluated, the acidic impurities that appear downfield of HEH[EHP] in the ^{31}P NMR were completely removed. These impurities appear to interact strongly with the silica column and are not readily eluted from the column after the addition of many bed volumes of eluent, nor after gradient elution to more polar solvents (e.g., 100% acetone). Their high affinity for silica gel indicates that these impurities are significantly more polar than HEH[EHP], and supports their assignment as acidic compounds.

To determine the effectiveness of the column purified HEH[EHP] toward Am(III) stripping, an ALSEP solvent sample was prepared using HEH[EHP] (supplier A-1) purified using 50:50 dichloromethane/acetone (v/v) eluent on a silica column. Quantitative ^{31}P NMR analysis (Table 3.3) of the material obtained showed only two detectable phosphorus-bearing impurities: DEH[EHP] at δ 32.6 ppm and the HDEHP at δ 1.84 ppm (0.79% and 0.83% relative to HEH[EHP], respectively). GC/MS analysis (Table 3.1) of this sample revealed a small amount of EHPA, and no removal of 2-ethylhexanol or di(2-ethylhexyl) ether. This solvent was used in the extraction/strip/scrub procedure as described previously, and the distribution results are shown in Table 3.4. The strip D_{Am} value obtained using the column-purified material from supplier A-1 is significantly lower than those obtained with either unpurified A-1 or A-1 material purified by the literature methods, representing a substantial improvement in purification of the material relative to the literature methods. While the GC/MS results showed the column-purified A-1 material to contain the neutral impurity DEH[EHP] and some non-P impurities, the concentrations of HDEHP and EHPA were substantially reduced relative to other purified samples of A-1 material. This finding indicates that the neutral and non-P impurities do not substantially contribute to the high D_{Am} stripping value, but that instead, the acidic impurities HDEHP and EHPA are problematic.

Optimal separation was achieved with 70–230 mesh silica gel and an eluent of

80:20 (v/v) dichloromethane:acetone using gravity flow. In this system, removal of all P-bearing impurities can be achieved with the exception of the neutral dialkyl phosphonate, DEH[EHP]. Aliphatic non-P containing impurities elute first, followed by HEH[EHP] co-eluting with DEH[EHP], followed by HDEHP. There is a narrow window in which HEH[EHP] elutes without co-elution of the HDEHP impurity. The observed co-elution could be a result of either (a) similar interactions of DEH[EHP], HEH[EHP] and HDEHP on the column, or (b) formation of an adduct between HDEHP and HEH[EHP], and/or between DEH[EHP] and HEH[EHP]. The latter explanation is consistent with the results of the previous section.

Neither chromatography alone nor either of the literature methods effected complete removal of impurities in HEH[EHP]. The problem is challenging as a result of the co-existence of neutral and acidic impurities, and the targeted chemical methods of the existing purification methods. By applying purification techniques with orthogonal modes of operation, material of increased purity can be obtained. HEH[EHP] free of any of P-bearing impurities (as detectable by ^{31}P NMR) was attained by combining the copper salt precipitation method[70] with subsequent column chromatography. In the first purification method, the phosphonic acid-copper precipitation step was repeated three times. Repeating this step allows for better separation of impurities that may otherwise co-precipitate with the metal-ligand complex or that have limited solubility in the supernatant. The HEH[EHP] thus obtained was reconverted to the acid form before purification on a silica column using 80:20 (v/v) dichloromethane:acetone eluent. Prior to NMR analysis, the purified sample was washed three times with 3 M HCl and DI water to remove any residual complexed metal originating from the silica column. ^{31}P NMR of the sample is shown in Figure 3.6. While this method results in a product that is found to be free from any P-bearing impurities, the overall yield is low (ca. 20%).

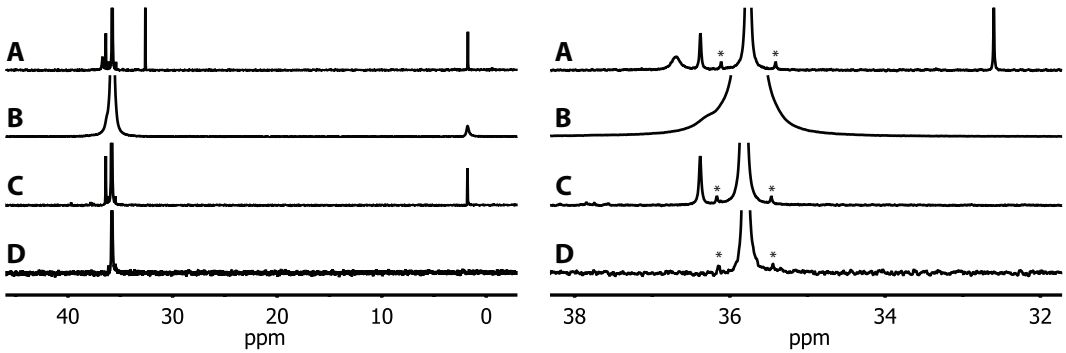

Figure 3.6: Left: $^{31}P\{^{1}H\}$ NMR spectra of HEH[EHP] from supplier A-1 (a) as-received; (b) purified by copper salt precipitation and washed with 0.2 M H_2SO_4; (c) the fraction shown in (b) after subsequent washing with 3 M HCl; and (d) after purification by copper salt precipitation and silica chromatography. Right: expanded region around HEH[EHP] resonance of the same traces. ^{13}C satellites are marked by (*). All spectra recorded in $CDCl_3$ and externally referenced to H_3PO_4.

3.5.10 Analytical Methods Suitable for Determination of HEH[EHP] Purity

These experiments have demonstrated that small variations in solvent composition (vis-à-vis impurity inventory) can have a significant impact on the ALSEP process chemistry. Information regarding the purity of HEH[EHP] on a batch-to-batch basis is needed for both fundamental studies and process development. It is therefore necessary to have an accurate, reliable, and robust method to determine the purity of HEH[EHP] purified in-lab on the preparatory scale.

HEH[EHP] purity is routinely determined by ^{31}P NMR, a method which is fast, sensitive, and requires minimal sample preparation. This method is able to easily determine the presence of phosphorus-containing impurities (qualitative analysis). However, for quantitative analysis of the P-bearing impurities to determine the degree of purity, it is crucial that both (a) the HEH[EHP] sample is properly prepared for analysis and (b) appropriate NMR pulse sequences and parameters are used. Phosphorus nuclei typically have long T_1 relaxation times;[89] accurate integration of phosphorus resonances (and hence accurate comparison of integrals) requires a relaxation delay of at least $5T_1$. Other standard practices for quantitative-NMR spectroscopy apply.[90–93] The presence of paramagnetic impurities (such as Cu(II), spin 3/2), residual from purifi-

cation or from the raw material, may cause line broadening.[94] Line broadening from paramagnetic metal complexation may occur to such an extent that minor impurities become indistinguishable from the spectral baseline or are otherwise obscured.[95] This is demonstrated in the spectra presented in Figure 3.6, which shows the ^{31}P NMR of HEH[EHP] before and after purification by the copper salt precipitation method. The spectrum presented in trace (B), which was washed 6 times with 0.2 M H_2SO_4 to reconvert the copper salt to the acid form, showed significant broadening of the HEH[EHP] resonance due to the presence of residual metal. After further washing with 3 M HCl, shown in trace (C), the HEH[EHP] resonance narrowed substantially, which revealed the previously obscured resonance of the impurity.

For the accurate quantitative determination of impurities in HEH[EHP] by ^{31}P NMR, the following methods are suggested. First, the HEH[EHP] sample should be in the acid form, and free of complexed metal. Depending on the purification method used, metal removal may require dissolution of the sample in an appropriate diluent (e.g., hexanes) followed by multiple washings with acid (e.g., 3 M HCl) to strip any complexed metal followed by DI water washes, followed by removal of the solvent and residual water prior to NMR analysis. The ^{13}C satellites ($^1J_{C-P}$ = 143 Hz) of HEH[EHP] should appear clearly in the spectra. Excessive line broadening, which is diagnostic of metal complexation, will obscure the carbon satellites. The line width of pure HEH[EHP] in $CDCl_3$ was observed to be ca. 5 Hz. Second, the NMR pulse parameters must be appropriate for quantitative NMR, with delay time sufficient to allow complete relaxation of the slowest relaxing nuclei. Specifically, a pulse delay of at least 5 times the T_1 of the slowest relaxing nuclei must be used, and T_1 must be measured, as it depends on the field strength of the spectrometer.[90–92] Third, the deuterated solvent should be chosen, if possible, to maximally separate the resonances of the impurities on the instrument being used. The chemical shift of HEH[EHP] and the typical impurities is solvent-dependent, and, in some solvents, some impurities are not well resolved from the HEH[EHP] resonance. We have found that $CDCl_3$ provides good separation of the observable P-bearing impurities at fields from 11.7 – 17.6 T.

Potentiometric titration is commonly used to determine the purity of both HDEHP and HEH[EHP].[63,64,96,97] This method is only able to determine acidic impurities, and is not particularly sensitive to minor impurities, nor those with pK_a near the main constituent. A critical analysis of this method for the determination of H_2MEHP in HDEHP estimated the sensitivity of this method to be about 1 wt-% H_2MEHP in HDEHP and noted that quantitative analysis is difficult when small amounts of impurity were present.[74] Errors were on the order of 0.5 to 3 wt-% when known amounts of H_2MEHP were added to HDEHP. Given the deficiencies of potentiometric titration in determining non-acidic and acidic impurities, it is not recommended as a sole quantitative test of purity for HEH[EHP].

GC/MS can be used to determine the impurities present, and with appropriate standards, the method can provide quantitative results. However, such standards are not readily available commercially for all of the typical impurities, which limits the use of this method for absolute quantitation. Furthermore, GC/MS analysis of HEH[EHP] and its impurities requires derivatization to make the compounds sufficiently volatile, and incomplete derivatization will skew the results. Even with these limitations, GC/MS offers a number of advantages that make it a valuable complement to ^{31}P NMR. These include accurate relative quantitation of impurities, high overall sensitivity, detection of non-P-bearing impurities, suitability for samples that give broad NMR peaks, and establishing the identity of impurities.

3.6 Conclusions

Commercially available HEH[EHP] contains a number of impurities at concentrations that are sufficiently high to be chemically detrimental to the ALSEP process. The impurities consistently found in all commercial samples are 2-ethylhexanol, di(2-ethylhexyl) ether, DEH[EHP], EHPA and HDEHP. In the samples from several manufacturers examined, significant differences were noted in the levels of impurities, both among suppliers and between lots from a single supplier. Existing purification methods remove

these impurities partially and to varying degrees. Both acidic and neutral impurities are found in commercially available HEH[EHP]. The acidic impurities (EHPA and HDEHP) were found to have the largest impact on Am(III) stripping D values in the ALSEP concept flowsheet, and hence should be the primary targets for removal when developing solvent purification schemes. However, the potential for interactions of the other impurities with HEH[EHP] argues for eliminating them where possible.

DEH[EHP] is a lingering synthetic precursor of HEH[EHP], whereas EHPA results from its hydrolysis, and HDEHP likely results from its oxidation (or oxidation of the precursor DEH[EHP]). The latter two problematic impurities, once removed, may reform in use through acid-catalyzed hydrolysis and oxidation by chemical or radiochemical pathways. Regular analysis is therefore warranted, and periodic repurification may be necessary. Stripping is the step in ALSEP most affected by the impurities, and the stripping D_{Am} value is a good criterion for assessing HEH[EHP] performance. When the stripping D_{Am} is unacceptably high for process applications (e.g., over 0.5), purification of the solvent is indicated. A purification method to substantially remove all P-bearing and non-P-bearing impurities was presented, in which an initial copper salt precipitation is followed with column chromatography on silica gel. The copper salt method effectively removes both P-bearing and non-P-bearing neutral impurities, while column chromatography removes all acidic impurities. Purification efficacy can be verified by solvent extraction tests or by quantitative ^{31}P NMR. ^{31}P NMR should be performed only on metal-free samples, with proper choice of NMR parameters, and with careful attention to the linewidth of the HEH[EHP] resonance.

3.7 Supplemental Information

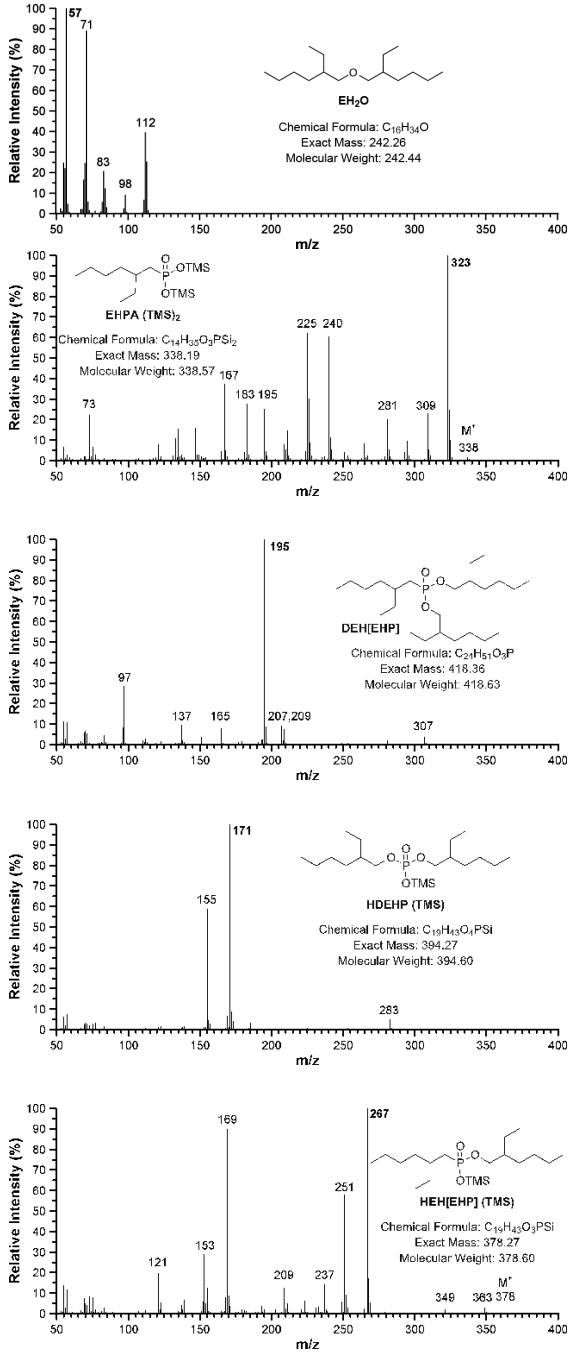

Figure 3.7: Mass spectra of compounds (or their trimethylsilyl derivatives) identified by GC/MS in commercially avaiable HEH[EHP]. Structures, chemical formula, exact mass and molecular weight of each compound is inset.

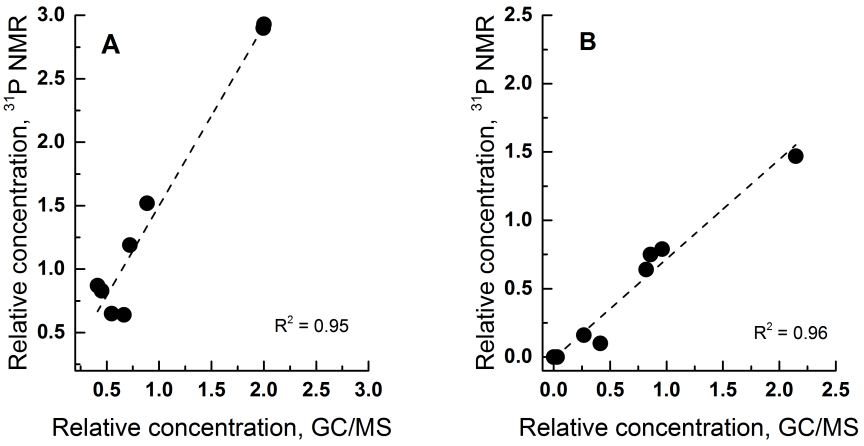

Figure 3.8: Correlation between the relative concentration of impurities found by GC/MS and ^{31}P NMR for (a) HDEHP (b) DEH[EHP]. Individual points correspond to unique samples of HEH[EHP] material, either as-received or purified by various methods, from various suppliers, as described in the text.

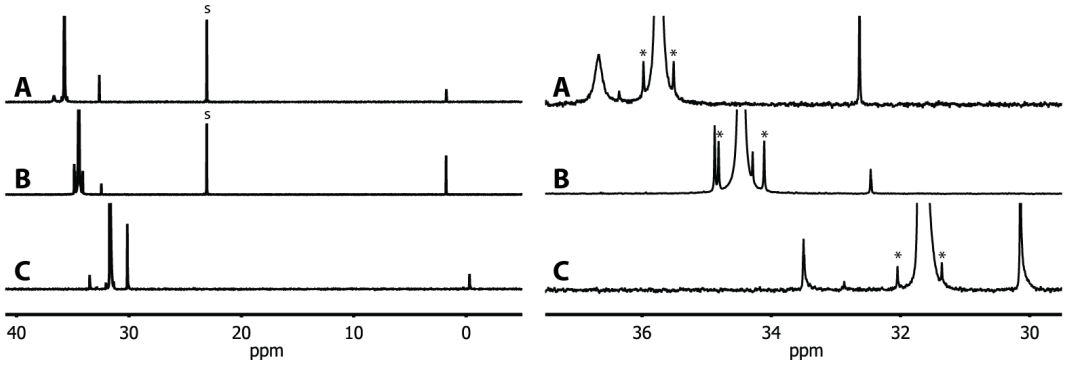

Figure 3.9: Left: Variation in position and linewidth of ^{31}P NMR δ 36.6 ppm resonances in as-received HEH[EHP] (supplier B-1) in various diluents (a) $CDCl_3$; (b) *p*-xylene, and (c) MeOH-d_4. Right: Expanded region of the same traces. Spectra A and B are referenced to tetraphenylphosphonium chloride in coaxial insert (marked by s); spectra C is referenced externally to H_3PO_4. ^{13}C satellites are marked by (*).

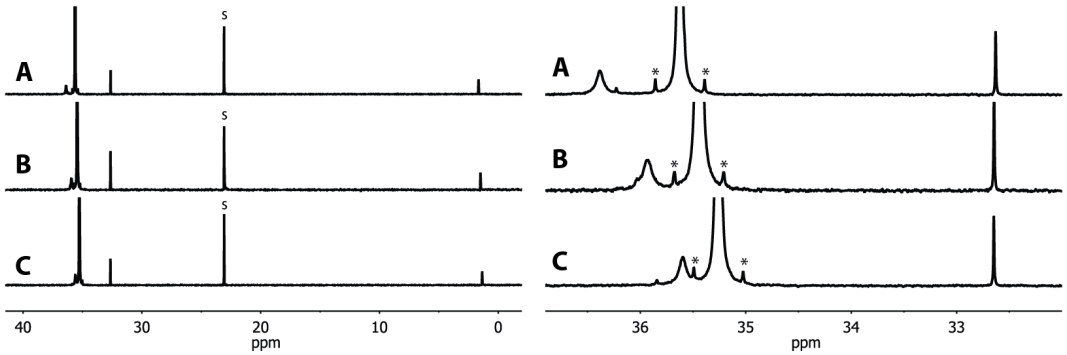

Figure 3.10: Left: Effect of added 2-ethylhexanol on ^{31}P resonances of HEH[EHP] and its impurities. Sample is material as-received from supplier B-1. Upfield shifts of acidic components (HDEHP, EHPA, and HEH[EHP]) are observed as 2-ethylhexanol concentration is increased. Notably, the $\Delta\delta$ (ppm shift) between EHPA and HEH[EHP] decreases with increasing 2-ethylhexanol concentration, and, for some concentrations of 2-ethylhexanol, the resonances of impurities downfield of HEH[EHP] become coincident and indistinguishable (trace B). Concentration of HEH[EHP] in all samples is nominally 0.17 M. Concentration of 2-ethylhexanol in the samples corresponding to traces A, B, and C is: (A) 0.05 M; (B) 0.12 M and (C) 0.26 M. Right: expanded region around HEH[EHP] resonance of the same traces. ^{13}C satellites are marked by (*) and tetraphenylphosphonium chloride ^{31}P chemical shift reference (in coaxial insert) is marked by (s).

3.8 Contribution of Authors

Emily L. Campbell (WSU, PNNL) contributed data in section 3.5.5, addition of the TOA complexant, and assisted in editing the manuscript.

Dean R. Peterman (INL) contributed data in section 3.5.7, addition of OPA complexant, and assisted in editing the manuscript.

Robert F. Standaert (ORNL, UT-Knoxville) contributed GC/MS data, GC/MS interpretation, and assisted in editing the manuscript.

Alena Paulenova (OSU) and Gregg J. Lumetta (PNNL) assisted in editing the manuscript. Tatiana G. Levitskaia (PNNL) assisted in experimental design and in editing the manuscript.

All other data collection and preparation of the manuscript was done by the author.

4 Distribution studies of the ALSEP system

4.1 Introduction

Motivation for the ALSEP concept,[2] as for all advanced reprocessing methods, was to develop a robust process for MA/Ln separation with a simplified flowsheet. Two commercially available extractants, T2EHDGA and HEH[EHP], are combined in an aliphatic diluent to create the ALSEP solvent. A body of literature exists on metal extraction by each individual ligand.[61,98–103] There are fewer published studies on the ligands under conditions relevant to the ALSEP concept, or regarding ALSEP directly.[62,63,69,104–106] To fill knowledge gaps in the ALSEP system, the effect of ligand concentration and aqueous phase extraction conditions on metal extraction have been studied. This chapter presents the results of acid, water, and metal distribution studies on the ALSEP system.

4.2 Methods

All solvent extraction experiments were performed in at least duplicate by batch contact. Due to differences in available equipment and procedural requirements, experimental protocol varied slightly between experiments performed at OSU and PNNL. The protocol for experiments performed at OSU (Section 4.3.2) consisted of the following. Equal volumes of the organic phase solvent (0.005 M T2EHDGA + (0.05 – 1 M) HEH[EHP] in *n*-dodecane) were combined in 2 mL screw-top plastic vials and pre-equilibrated twice with HNO_3 (0.1 – 5 M). The pre-equilibration step consisted of agitation for 10 minutes (VWR vortexer) followed by centrifugation, after which the aqueous phase was completely removed. Fresh HNO_3 (of the same concentration to be used in the extraction step) was added to the pre-equilibrated organic phase, followed by an aliquot of ^{152,154}Eu or ^{241}Am radiotracer (10 μL). ^{152,154}Eu radiotracer was prepared by neutron activation of $Eu(NO_3)_3$ (99.99%, Alfa Aesar) in the Oregon State

University TRIGA reactor. The activated $Eu(NO_3)_3$ was dissolved in HNO_3 to produce a radiotracer solution containing 10 μM Eu in 1 M HNO_3, with activity of 60 Bq/μL. ^{241}Am radiotracer (0.7 MBq/mL) was obtained from Isotope Product Laboratories as $AmCl_3$ in 1 M HCl. Samples were agitated for 10 minutes on a vortexer (VWR) at ambient temperature (19 $\pm$ 1 °C). Phases were disengaged by centrifugation, separated to fresh vials, and equal volume aliquots of each phase sampled for gamma analysis (NaI(Tl), Packard COBRA II).

The protocol for experiments performed at PNNL (Sections 4.3.3, 4.3.4, and 4.3.5) consisted of the following. Equal volumes of the organic phase solvent (0.05 M T2EHDGA + 0.75 M HEH[EHP] in *n*-dodecane, 2,2,4,6,6-pentamethylheptane ("branched dodecane"), *p*-xylene, or 1,4-diisopropylbenzene (1,4-DIPB) were combined with the desired aqueous phase (0.1 – 3 M HNO_3) spiked with $^{152,154}Eu$ and/or ^{241}Am tracer in screw-top plastic vials. $^{152,154}Eu$ (3.7 MBq/mL) was obtained from Eckert & Ziegler as $EuCl_3$ in 0.5 M HCl. Distribution studies using Eu(III) contained an added non-radioactive carrier concentration of 0.3 mM $Eu(NO_3)_3$. ^{241}Am (7.4 MBq/mL) was purchased from Eckert & Ziegler as $AmCl_3$ in 1 M HCl. No carrier was added to ^{241}Am solutions. Samples were agitated on either a hand motion-shaker (Sonics SHK-COCK2) or on an orbital mixer (J-KEM Scientific) for 60 minutes at 25 $\pm$ 1 °C, after which phases were disengaged by centrifugation. For all experiments, equal volume aliquots of each phase were collected for gamma analysis. Experiments of Sections 4.3.4 and 4.3.5 were further subjected to scrub and strip steps. In this protocol, the metal-loaded organic phase was removed to a fresh vial and equilibrated with an equal volume of the scrub solution (0.2 M Na-citrate, pH 3 or 0.2 M Na-citrate + 1 M acetohydroxamic acid (AHA), pH 3) under the same conditions as the extraction step. After phase separation by centrifugation, an aliquot of the scrubbed organic phase was removed to a fresh vial containing an equal volume of the stripping solution (0.125 M HEDTA + 0.2 M Na-citrate, pH = 3) and equilibrated as before. Equal volume aliquots of each phase were removed at each step for gamma analysis (NaI(Tl), PerkinElmer Wizard^2 Model 2480 or HPGe). Equilibration times for the extraction, scrub, and stripping steps were 60, 15, and 15 minutes, respectively, unless stated otherwise. A phase volume ratio of

organic/aqueous = 1 was maintained at each step.

4.2.1 Karl Fischer and Nitric Acid Determination

Experiments were performed in at least duplicate by batch contact. Equal volumes of the organic phase solvent (0.05 M T2EHDGA + 0.75 M HEH[EHP] in *n*-dodecane) were combined in screw-top plastic vials and equilibrated with deionized H_2O ($\geq$ 18 MΩ resistivity) or HNO_3 (0.1–5 M). Samples were agitated for 60 minutes on an orbital shaker (J-KEM Scientific) at (25 $\pm$ 1 °C). Phases were disengaged by centrifugation and separated to fresh vials. Water content of the organic phase was determined by Karl Fischer (KF) titration (Photovolt Aquatest 2010). KF titrations were done in at least triplicate for each sample. Extraction of HNO_3 by HEH[EHP] was determined by potentiometric titration (Metrohm Titrando 905) of the post-contact aqueous phase. Potentiometric titrations were performed in at least duplicate. Extraction of HNO_3 by T2EHDGA and ALSEP solvent was determined by ion chromatographic analysis of the stripped organic phases and post-contact aqueous phases. Details of this procedure were described previously.[62]

4.2.2 Distribution Ratio and Slope Analysis

The distribution ratio of metal M, D_M, is defined as the ratio of the analytical concentration of M in each phase:

$$D = \frac{[M^{3+}]_{organic}}{[M^{3+}]_{aqueous}} \tag{4.1}$$

D was calculated as the ratio of the organic phase ^{241}Am or ^{152,154}Eu activity concentration to that in the aqueous phase.

When a set of extractions is performed with exactly one experimental parameter (such as ligand concentration or acid concentration) varied, the dependence of the varied parameter can be determined *via* slope analysis. Given a neutral organic-phase ligand,

L, extracting an aqueous-phase metal ion, M, with counterion Y:

$$\mathrm{nM} + \mathrm{jL} + \mathrm{pY} \rightleftharpoons \mathrm{M}_n\mathrm{L}_j\mathrm{Y}_p \tag{4.2}$$

The conditional equilibrium constant, K_{ex} and D value of the reaction are

$$K_{ex} = \frac{[\mathrm{M}_n\mathrm{L}_j\mathrm{Y}_p]}{[\mathrm{M}]^{\mathrm{n}}[\mathrm{L}]^{\mathrm{j}}[\mathrm{Y}]^{\mathrm{p}}} \tag{4.3}$$

$$\tag{4.4}$$

$$D_M = \frac{[\mathrm{M}_n\mathrm{L}_j\mathrm{Y}_p]}{[\mathrm{M}]} \tag{4.5}$$

which assumes the species $\mathrm{M}_n\mathrm{L}_j\mathrm{Y}_p$ is the only species containing metal M formed in the organic phase. Combining the equations and taking the logarithm yields the expression[107]

$$\log(D) = \log K_{ex} + j\log([\mathrm{L}]) + \mathrm{p}\log([\mathrm{Y}]) \tag{4.6}$$

From Equation 4.6, it is clear that a plot of $\log D$ vs. $\log[\mathrm{L}]$ gives the number of ligands in the complex, and a plot of $\log D$ vs. $\log[\mathrm{Y}]$ yields the dependence on the concentration of the counterion, Y. This method is commonly referred to as *slope analysis*.

4.3 Results and Discussion

4.3.1 Water and HNO_3 extraction by ALSEP solvent

Karl Fischer (KF) titration and ion chromatography or potentiometric titration was used to determine the concentration of extracted water and HNO_3, respectively, in 0.1 M T2EHDGA, 0.75 or 1 M HEH[EHP], and ALSEP (0.05 M T2EHDGA + 0.75 M HEH[EHP]) organic phases after equilibration with varying concentrations of HNO_3. The results of water and HNO_3 extraction by T2EHDGA have been reported in a previous publication.[62]

As shown in Figure 4.1, each ligand extracts a relatively constant amount of water until the aqueous HNO_3 concentration exceeds ca. 1 mol L^{-1}. Thereafter, water concentration in the organic phase increases sharply with increasing aqueous HNO_3 concentration, most notably for T2EHDGA, where nearly 0.05 mol L^{-1} water is observed in the organic phase after contact with 3 mol L^{-1} HNO_3, yielding a stoichiometric ratio of H_2O:T_2EHDGA_2, while the organic phase HNO_3 concentration under the same conditions exceeds 0.1 M, equal to the concentration of T2EHDGA.[62] Under these conditions, it is likely that T2EHDGA forms supramolecular species architectures, such as small polar core aggregates, containing the extracted water and HNO_3. Such behavior has been observed for the octyl-derivative, TODGA.[43,51,52] HEH[EHP] has been reported to extract low ($\leq$10% loading) and nearly constant amounts of water after contact with variable concentrations of lactic acid[64] (0.5 – 2 M) and HNO_3[108] (0.01 – 2.5 M). Consistent with these results, little dependence on HNO_3 concentration was observed until ca. 2 M HNO_3. However, a drastic increase in water extraction by HEH[EHP] is observed with progressive increase of HNO_3 concentration (Figure 4.1, left).

In the ALSEP solvent, the profile of water uptake follows that of the bulk-constituent HEH[EHP], with a moderate increase in water partitioning occurring only at high aqueous HNO_3 concentration. There is indication of synergistic water partitioning in the mixed ligand system.[c] Throughout the acid concentration range studied, additional water is partitioned by the ALSEP system relative to the sum of the individual extractants.

In the ALSEP solvent, the partitioning of HNO_3 into the organic phase is observed to be linear (slope of 1.8) with increasing aqueous phase HNO_3 concentration (Figure 4.1, right). The constant slope suggests that there is no change in the mechanism of

[c]Due to the concentrations of ligands used in the experiments, a direct comparison is not made. Ligand concentrations above the ALSEP concentrations (0.05 M T2EHDGA, 0.75 M HEH[EHP]) were used for KF experiments in order to have $[H_2O]_{org}$ above the detection limit of the method. However, it is still clear that the ALSEP solvent extracts water synergistically: the sum of water extracted by the individual ligand solutions, 0.1 M T2EHDGA and 0.75 M HEH[EHP], is less than that extracted by the ALSEP solvent (0.05 M T2EHDGA + 0.75 M HEH[EHP].

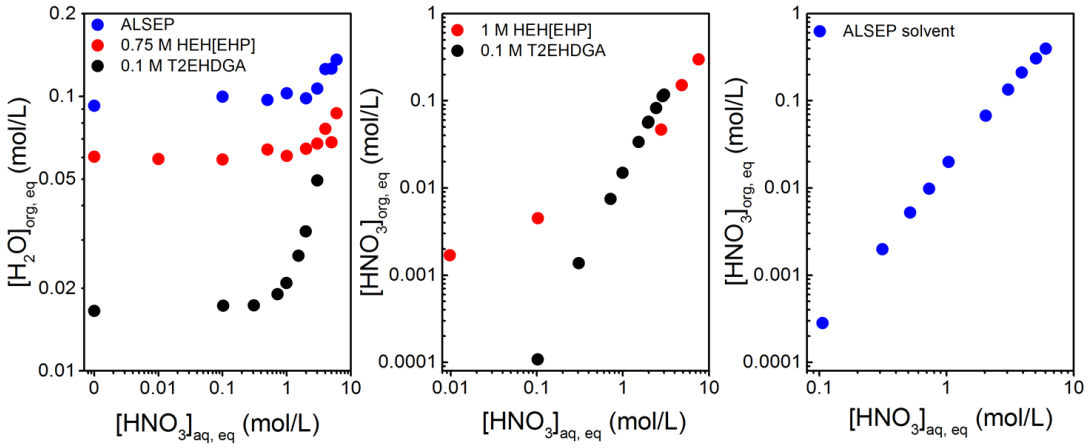

Figure 4.1: Left: Partitioning of H_2O into organic phases of 0.1 M T2EHDGA, 0.75 M HEH[EHP], and ALSEP (0.05 M T2EHDGA + 0.75 M HEH[EHP]) solvent after equilibration with variable concentration HNO_3. Center: Partitioning of HNO_3 into organic phases of 0.1 M T2EHDGA and 1 M HEH[EHP] solvent after equilibration with variable concentration HNO_3. Right: Partitioning of HNO_3 into ALSEP (0.05 M T2EHDGA + 0.75 M HEH[EHP]) solvent after equilibration with variable concentration HNO_3. Data for T2EHDGA and ALSEP reproduced with permission of E. Campbell.

acid extraction over the range of acid concentration studied. In the absence of metal, significant amounts of HNO_3 have been shown to be extracted by T2EHDGA.[62] The extraction of HNO_3 by T2EHDGA was also found to be linear with acid concentration. Extraction of HNO_3 by HEH[EHP] was measured from 0.01 – 6 M and determined by potentiometric titration of the pre- and post-contact aqueous phases. Acid concentrations from 0.5 – 1 M were found to have high standard errors and are omitted from further analysis. In the limited data set, the apparent slope change in the HEH[EHP] acid extraction suggests a change in the stoichiometry and mechanism with the change in aqueous HNO_3 concentration.

4.3.2 Dependence of metal extraction on HEH[EHP] concentration

One of the first published papers on the ALSEP concept[2] reports the dependence of D_{Am} (extraction from 3 M HNO_3) on TODGA concentration, in solvents containing 1 M HDEHP or 1 M HEH[EHP]. A second order dependence is found with HDEHP, and

Table 4.1: Slopes of D_{Am} and D_{Eu} vs. [HEH[EHP]] (50 mM – 1 M) for extraction from variable concentration HNO_3.

$[HNO_3]$	slope, Eu(III) ($\pm \sigma$)	slope, Am(III) ($\pm \sigma$)
0.1 M	2.4 (0.08)	2.3 (0.02)
0.5 M	1.6 (0.02)	1.5 (0.03)
1 M	1.1 (0.05)	1.2 (0.03)
3 M	0.42(0.01)	0.46 (0.01)
5 M	0.04 (0.01)	0.1 (0.02)

dependence of order 2.4 reported for HEH[EHP], indicating 2 to 3 TODGA molecules are present in the extracted metal complex. This differs from the expected third order dependence of a homoleptic T2EHDGA complex,[109–114] suggesting the participation of the acidic extractant in the complex. The T2EHDGA and TODGA dependence is reported to be ca. 1.4 in an HDEHP system[2] upon extraction from 1 M HNO_3, indicating a change in the extraction mechanism of the ALSEP solvent compared to extraction from 3 M HNO_3.

To further explore the role of each ligand in metal complexation of the ALSEP organic phase, extractions of Eu(III) and Am(III) were performed from 0.1 – 5 M HNO_3, using organic solvent prepared with varying concentration HEH[EHP] (50 mM – 1 M). The concentration of T2EHDGA was held constant at 5 mM in all experiments. While this concentration of T2EHDGA differs from that used in the process solvent formulation (50 mM), this scoping study still provides relevant and interesting results. A later study performed with 50 mM T2EHDGA with variable concentration HEH[EHP] was found to be in good agreement with these results.

The dependence of D_{Eu} and D_{Am} on HEH[EHP] concentration is shown in Figures 4.2 and 4.3, respectively. The change in slope (shown in Table 4.1) with aqueous phase HNO_3 concentration indicates a change in the extraction mechanism (i.e., change in the organic speciation of the extracted metal) dependent on the aqueous phase extraction conditions. The changes in slope indicate that the ligand driving the extraction switches, from HEH[EHP] at low $[HNO_3]$, to T2EHDGA at high $[HNO_3]$. This phe-

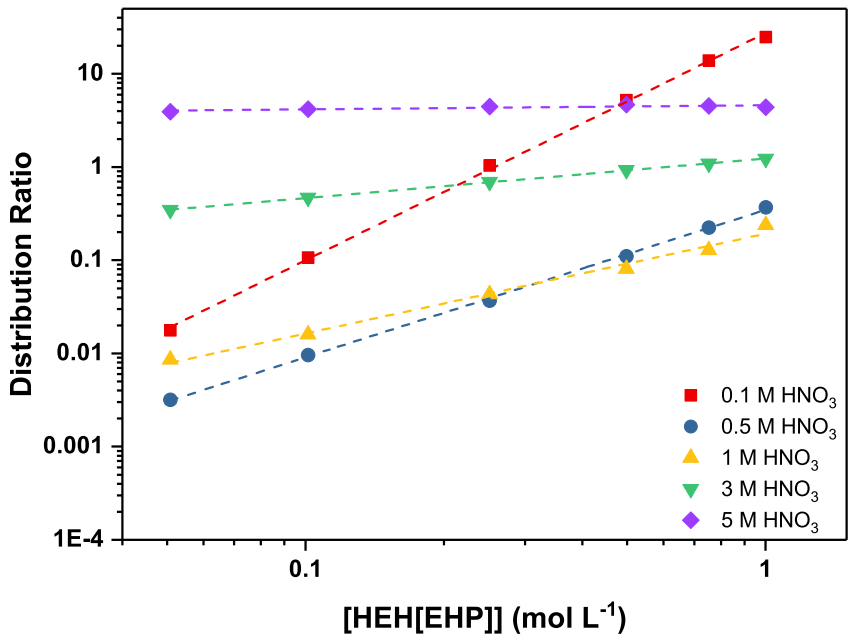

Figure 4.2: Eu(III) extraction by 5 mM T2EHDGA + HEH[EHP] as a function of HEH[EHP] concentration (50 – 1000 mM), for extractions from 0.1 – 5 M HNO_3. Dashed lines are linear regression fits.

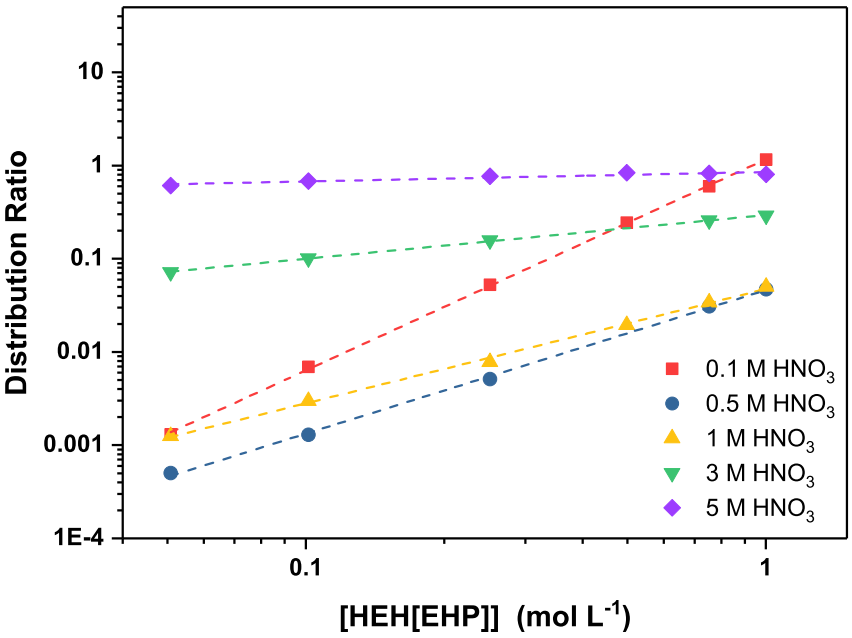

Figure 4.3: Am(III) extraction by 5 mM T2EHDGA + HEH[EHP] as a function of HEH[EHP] concentration (50 – 1000 mM), for extractions from 0.1 – 5 M HNO_3. Dashed lines are linear regression fits.

nomenon is explored in greater detail in section 4.3.3.

The dependence of D_{Am} or D_{Eu} extraction from low acid concentrations on HEH[EHP] concentration is excepted to be third order[106,115] but has been observed to be order 2.5.[39] Third order dependence corresponds to, and is typically interpreted as, coordination of the metal by three HEH[EHP] dimers (each dimer singly de-protonated), but is indistinguishable by slope analysis from coordination by three monomers (each monomer deprotonated) of the ligand. Additionally, it has been found that non-ideal behavior and/or self-aggregation of the extracting ligand can cause erroneous results in the slope analysis.[50] Correction for non-ideality and self-aggregation was found to be a necessary correction for extraction by HDEHP and thiophosphinic ligands.[50,116] In the studied system, extraction from increasing concentration of HNO_3 results in a progressive decrease in the slope. This indicates a change in the number of HEH[EHP] molecules present in the extracted complex and hence a change in the extraction mechanism. The deviation from the expected third order dependence at low acid concentrations may be due to non-ideal behavior of the ligand, similar to the non-ideal behavior that has been observed with HDEHP.[117] The present data are consistent with the formation of mixed-ligand adducts, the composition of which are dependent upon the aqueous extraction conditions. Together with the slope, the magnitude of D_M at each aqueous acid concentration suggests the dominant ligand. At 3 and 5 M HNO_3, the flat dependence on HEH[EHP] concentration indicates that T2EHDGA is the dominant extractant. At 0.5 and 1 M HNO_3, the dependence on [HEH[EHP]] shows HEH[EHP] participates in these metal complexes, but to a lesser degree than at the extraction from 0.1 M HNO_3, where the slope is steeper (indicating stronger dependence on ligand concentration). Extraction by the independent ligands is discussed in section 4.3.3.

A synergistic effect of the ALSEP solvent was indicated (Figures 4.4 and 4.5) in plots of D_M vs. [HNO_3]. In these figures, it is clear to see the same U-shaped dependence of D_{Eu} and D_{Am} on acid concentration that will be discussed in Section 4.3.3. It is also apparent that under these conditions (5 mM T2EHDGA), a significant synergistic

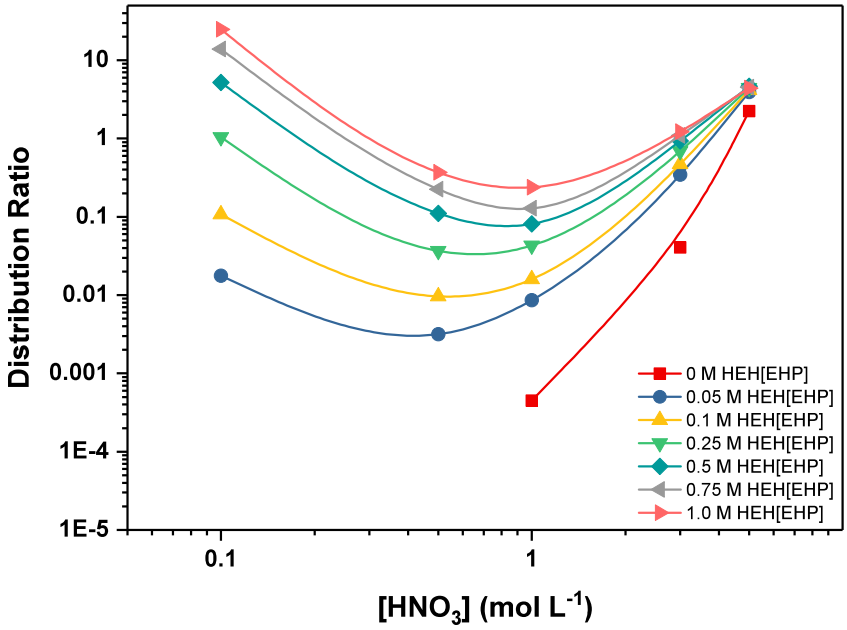

Figure 4.4: Eu(III) extraction by 5 mM T2EHDGA + HEH[EHP] as a function of HNO_3 concentration (0.1 – 5 M). Solid lines are a guide for the eye, and have no theoretical significance.

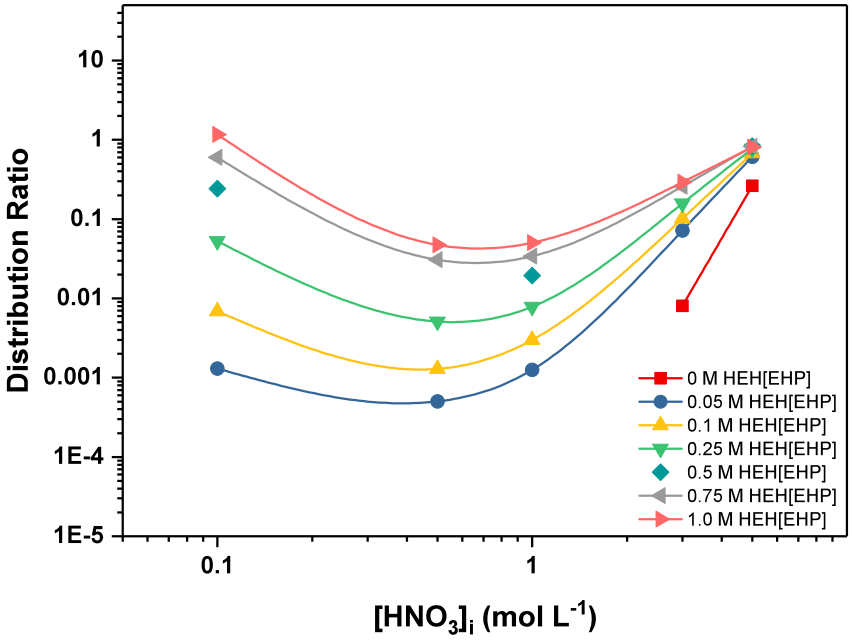

Figure 4.5: Am(III) extraction by 5 mM T2EHDGA + HEH[EHP] as a function of HNO_3 concentration (0.1 – 5 M). Solid lines are a guide for the eye, and have no theoretical significance.

effect exists at 3 M HNO_3, which was not observed as keenly in the 50 mM / 750 mM ALSEP formulation. This feature could be caused by two different mechanisms. In one, the metal loading capacity of the (5 mM) T2EHDGA is reached, and the increased extraction at 3 M HNO_3 is due to extraction by HEH[EHP] by formation of neutral solvates, as has been observed with HDEHP.[34] However, if this were the case, we would expect the same synergistic effect to be observed at 5 M HNO_3, as well, but it is not. A second possible mechanism is that in the combined system, T2EHDGA and HEH[EHP] form a ternary, mixed-ligand complex which is more efficient at metal extraction. A mixed complex is indicated (but not confirmed) by the slope analysis: the decrease in slope indicates that a smaller, but non-zero, number of HEH[EHP] molecules are involved in the metal complex as aqueous [HNO_3] increases.

To further explore the effects of each ligand and the aqueous phase extraction conditions on the ALSEP system, a systematic study was performed, and is the subject of the next section.

4.3.3 Synergism in ALSEP

Figures 4.6 and 4.7 illustrate the dependence of D_{Am} and D_{Eu} on the aqueous extraction conditions (HNO_3 concentration) for each ligand independently and combined in the ALSEP solvent. This study was performed under the same conditions in four different diluents: *n*-dodecane, 2,2,4,6,6-pentamethylheptane (which will be referred to as "branched dodecane"), *p*-xylene, and 1,4-diisopropylbenze (1,4-DIPB). The impact of the diluent will be discussed subsequently.

The extraction profiles of Figures 4.6 and 4.7 are described by the mechanism of the extractants. The acidic extractant, HEH[EHP], which must exchange a proton to complex metal exhibits maximum distribution ratios at low acid concentrations, where proton exchange is favorable. The D_{M} decrease rapidly with increasing acid concentration, reaching its minimum around 1 M HNO_3. The D_{M} of the neutral T2EHDGA follows the opposite trend of the acidic extractant, with metal extraction increasing with HNO_3

concentration. This is classically explained by the increased concentration of nitrate anions in the aqueous phase, which are co-extracted with the metal to attain charge neutrality of the extracted species, assumed to be the species $M{\cdot}(T2EHDGA)_3(NO_3)_3$.[109–114] However, recent work[104] demonstrates the role of co-extracted HNO_3 on T2EHDGA metal extraction, and indicates the $HNO_3{\cdot}$T2EHDGA adduct as an extracting species.

In the ALSEP solvent (0.05 M T2EHDGA + 0.75 M HEH[EHP]), the dependence of D on HNO_3 concentration breaks into three regimes. One, at low concentrations of acid ($\leq$ 0.1 to ca. 0.3 M), metal extraction of the ALSEP solvent is driven by the acidic extractant. Second, at high concentrations of acid (above 3 M), metal extraction is driven by the neural extractant. In both of these regimes, extraction of the mixed-ligand system, measured by the D_M, closely mimics that of the independent ligands. However, the third acid regime, which exists between ca. 0.2 M to 2 M HNO_3 in the *n*-dodecane/Eu(III) system, shows a D value which is greater than that can be explained by the extraction of HEH[EHP] or T2EHDGA alone, nor by the summation of the D_M of the two extractants. For example, with an aqueous phase of 0.75 M HNO_3, 0.05 M T2EHDGA has a D_{Eu} of 0.02 and the D_{Eu} of 0.75 M HEH[EHP] is 0.03, while the combined system of 0.05 M T2EHDGA and 0.75 M HEH[EHP] shows a D_{Eu} of 2.3, much greater than the sum of the D_{Eu} for the two individual extractants. This clear synergistic effect is observed for the extraction of both Eu(III) and Am(III) in the moderate-acidity regime. The synergism can be quantified by defining a synergistic ratio (SR),

$$SR = \frac{D_{AB}}{D_A + D_B} \tag{4.7}$$

as the quotient of the distribution ratios of the ligand mixture (D_{AB}) to the sum of the independent ligands A and B (D_A and D_B). Similar degrees of synergism were observed in all four diluents studied, with a slight enhancement in SR observed in the aromatic diluents relative to the alkane diluents (Figure 4.8).

Additionally, in the aromatic diluents, increased SR are observed extending to higher acid concentrations than in the alkane solvents. This may suggest that deprotonated

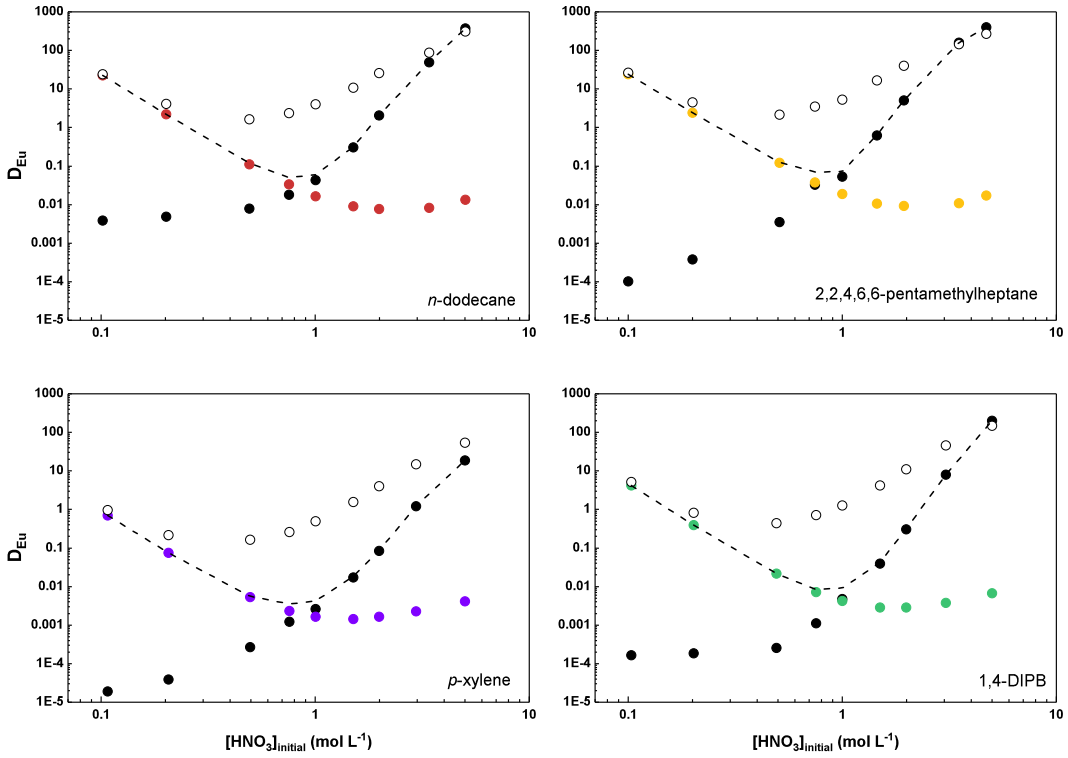

Figure 4.6: Distribution ratio, D_{Eu}, of Eu(III) is shown for extraction by T2EHDGA (black circles), HEH[EHP] (color circles) and ALSEP solvent (open circles) in four diluents (indicated in the figure). Dashed line indicates the sum, D_{Eu} (T2EHDGA) + D_{Eu} (HEH[EHP]).

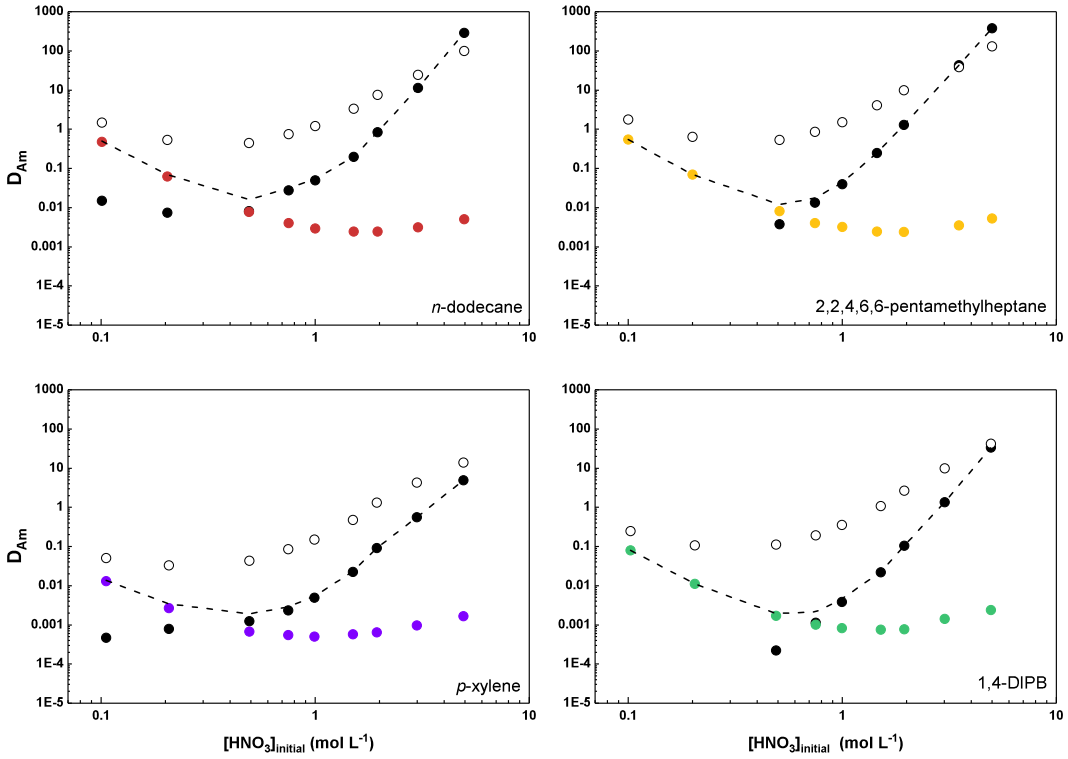

Figure 4.7: Distribution ratio, D_{Am}, of Am(III) is shown for extraction by T2EHDGA (black circles), HEH[EHP] (color circles) and ALSEP solvent (open circles) in four diluents (indicated in the figure). Dashed line indicates the sum, D_{Am} (T2EHDGA) + D_{Am} (HEH[EHP]).

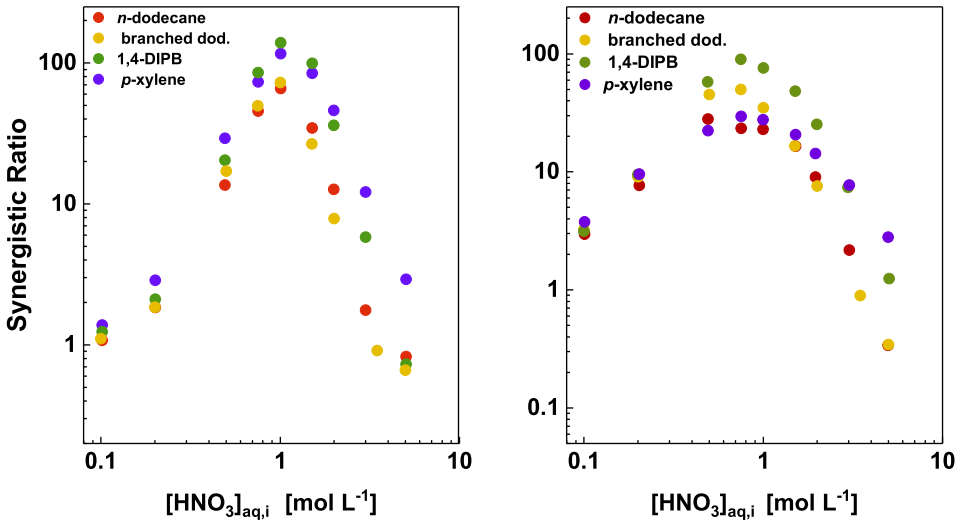

Figure 4.8: Dependence of the synergism ratio, SR, on HNO_3 concentration for extraction of Eu(III) (left) and Am(III) (right), for the four diluents studied.

HEH[EHP] monomers replace nitrate as the charge balancing anions in the extracted metal complex under these conditions, permitting enhanced extraction at higher concentrations of HNO_3.

For both metals and in all three ligand combinations, there was very little difference in D_M between the straight chain and branched alkane diluents. This indicates that there is little effect of the branching of the aliphatic diluent on the formation of the extracted metal complex, suggesting that it does not influence ligand coordination.

The similar trends in extraction of metal between diluents, as evidenced by the preservation of synergism and SR as the aqueous nitric acid concentration is varied, suggests that the structure and speciation of the extracted metal complex is similar in the different diluents. This is not too surprising, as the coordination of Eu(III) and uranyl to HDEHP is observed to be the same in *n*-dodecane and in an ionic liquid.[118]

For both Eu(III) and Am(III), a significant decrease in D_M is observed in the aromatic diluents relative to the alkane diluents. While the magnitude of D_M is decreased, the trends exhibited across the acid regimes are maintained in the aromatic diluents, and

synergism is still observed at moderate acid concentrations.

4.3.4 ALSEP Stripping Kinetics

For ALSEP to operate efficiently at the process scale, strip D_{Am} must be less than unity, and ideally less than 0.5, while at the same time the strip D_{Eu} value sufficiently high to maintain an Am/Eu separation factor of at least 10. Additionally, this value of D_{Am} must be achieved within the residence time of the industrial-scale equipment used (e.g., centrifugal contactor or mixer-settler), which may range from seconds to minutes.[41] Such short residence times may be insufficient to reach equilibrium,[119] resulting in decreased process performance. The ALSEP Am(III) stripping step has previously been observed to suffer from slow kinetics, and, depending on the impurities present in HEH[EHP], unacceptably high D_{Am}.[105]

Am(III) was extracted under identical conditions from 3 M HNO_3 into ALSEP solvent prepared in in *n*-dodecane, branched dodecane, and 1,4-DIPB diluents to determine the effect of the diluent on stripping kinetics. After the extraction step, all solutions were first subjected to a scrub step (0.2 M citrate, pH 3) to remove excess HNO_3 from the organic phase. The scrubbed, loaded organic phase was then subjected to stripping by equilibration with a solution of 0.125 M HEDTA + 0.2 M citrate (pH 3). The stripping contact time for the kinetic study was 1, 5, 10, 15, 30, 60, or 180 minutes.

The alkane diluents reached equilibrium D_{Am} within similar times (ca. 10 minutes), and achieved a similar equilibrium value of D_{Am}: 0.3 and 0.4 for *n*-dodecane and branched dodecane, respectively (Figure 4.9). The aromatic diluent 1,4-DIPB exhibits both faster equilibrium stripping kinetics (ca. 5 minutes) and a lower equilibrium strip D_{Am} of 0.05. These data can be rationalized within the context of the extraction distribution values. From 3 M HNO_3, the value of the extraction D_{Am} decreases in the order branched dodecane > *n*-dodecane > 1,4-DIPB > *p*-xylene. The extraction D_{Am} values provide an indication of the relative thermodynamic stability of the extracted metal complex in each diluent (as well the thermodynamics of desolvating the aque-

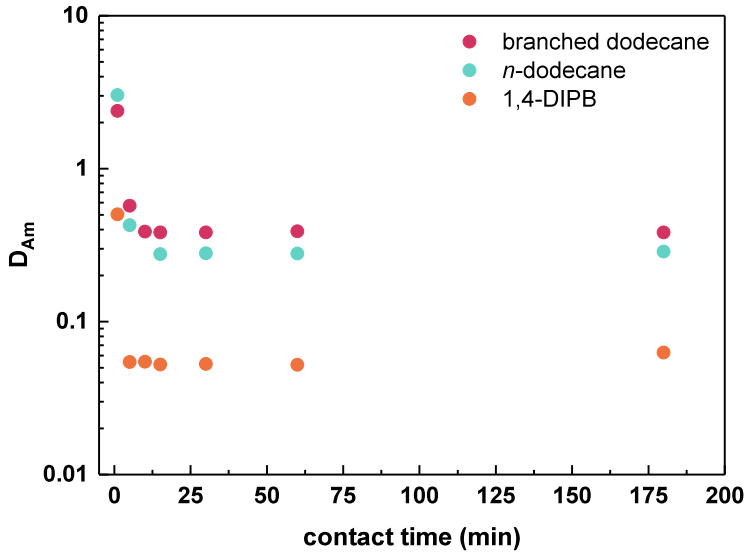

Figure 4.9: Kinetics of Am(III) stripping from ALSEP solvent in various diluents (indicated in the figure legend). ALSEP solvent was loaded from 3 M HNO_3, scrubbed with 0.2 M citrate (pH 3), and stripped using 0.125 M HEDTA in 0.2 M citrate buffer (pH 3).

ous metal species). In this system, it appears that the greatest stability of the metal complex is achieved in branched dodecane. It then follows that the expected order of stripping D_{Am} would be follow the extraction D_{Am}: branched dodecane > *n*-dodecane > 1,4-DIPB, which is observed. A higher strip D_{Am} indicates a greater fraction of Am(III) is retained in the organic phase.

Assuming the speciation of the extracted metal complex does not change significantly in the different diluents, the difference in extraction and stripping D_{Am} values indicate the influence of the diluent on the thermodynamics of metal extraction.

4.3.5 ALSEP extraction and stripping kinetics from used fuel simulant

Distribution studies are typically performed with trace, or near-trace concentrations of the metal being investigated, present as radiotracers. In some cases, using trace-concentrations is necessary, due to radiological concerns regarding the nuclide being studied (e.g., it is possible to safely use millimolar concentrations of ^{243}Am, but not of

^{241}Am, which is used only at tracer concentration). However, frequently, even when the concentration of a metal can be increased by adding a carrier (e.g., adding stable Eu to ^{152,154}Eu) to approximate the concentration of metal that would be expected in the target process stream, experiments are still performed using radiotracer concentrations.

The presence of other metals, or of a higher concentration of a single metal, in the aqueous feed can significantly alter the distribution of species that are formed in the organic phase.[49,120] This can be due to a change in the mode of ligand binding as a consequence of metal loading (low loading vs. high loading),[49] or as a result of the extraction of other metals. In initial studies of the ALSEP system,[69] extraction from a solution containing a mixture of lanthanides and transition metals revealed that Mo(VI), Zr(IV), and Fe are extracted, in addition to Am and the lanthanides. Lumetta[69] et al. found that Mo and Zr are quantitatively extracted by the ALSEP solvent from HNO_3. Favorable extraction of non-target metals (such as Mo or Zr) may suppress the extraction of the desired metals and/or negatively affect separation factors. The organic phase concentration, $[\mathrm{M}]_{\mathrm{org,f}}$, of an extracted metal depends on the distribution ratio, D, and the initial aqueous concentration, $[\mathrm{M}]_{\mathrm{aq,i}}$:

$$[M]_{org,f} = \frac{D[M]_{aq,i}}{1 + [M]_{aq,i}} \tag{4.8}$$

Thus, metals with moderate D_{M} may partition significantly to the organic phase, given a substantial the $[\mathrm{M}]_{\mathrm{aq,i}}$. The separation factor, SF, between two metals A and B is defined as the ratio of their D values:

$$\mathrm{SF_{A,B}} = \frac{\mathrm{D_A}}{\mathrm{D_B}} \tag{4.9}$$

In the ALSEP concept, separation of Ln and MA is accomplished in the stripping step (alternatively called back-extraction). When additional metals are extracted into the

solvent in the extraction step (e.g., transition metals), the chemistry of the strip step may be perturbed, potentially altering separation factors. In the ALSEP system, selective MA stripping is achieved using a polyaminocarboxylate complexant (i.e., HEDTA or DTPA) in citrate buffer (ca. pH 3). This allows for deprotonation of HEH[EHP], and also strips HNO_3 from the organic phase. This induces a switch in the dominant ligand involved complexation, from neutral T2EHDGA to acidic HEH[EHP]. Selective separation is achieved due to the difference in affinity of the the soft-donor polyaminocarboxylate complexant for the MA, while the harder Ln are retained in the organic phase in HEH[EHP] complexes. When additional metals are introduced to the system, this balance could be perturbed. For example, a transition metal that is well-extracted (by the same mechanisms as the MA and Ln, i.e, by DGA or DGA·HEH[EHP]) and which is retained by HEH[EHP] during the MA strip will act to displace Ln to the aqueous strip solution. The result will be a decrease in the MA/Ln SF, as both MA and Ln will partition to the MA strip solution.

To determine the performance of the ALSEP solvent toward solutions of post-PUREX dissolved used nuclear fuel (UNF), batch contacts using a simulated post-PUREX UNF solution were performed. The motivation of this test was twofold: to determine D_{Am} and D_{Eu} under process-like conditions, and to determine the Am/Eu separation factor and kinetics obtained using two different polyaminocarboxylate complexants (HEDTA and DTPA). The composition of the simulant solution is provided in Table 4.2. ^{241}Am and ^{152,154}Eu were added to this simulant, and a batch contact test of the ALSEP flow sheet was performed using a modified composition of the ALSEP solvent (0.05 M T2EHDGA + 0.5 M HEH[EHP]). At each step of the flowsheet, D_{Am} and D_{Eu} were determined by counting (*via* HPGe) equal-volume aliquots of each phase (Table 4.3).

Extraction Step. The extraction D_M values obtained in this study are very comparable to those reported using another ALSEP solvent composition (0.05 M T2EHDGA + 0.75 M HEH[EHP]), which found D_{Am} of 8 and D_{Eu} of 30 on extraction from a UNF simulant in 2.8 M HNO_3.[69] Comparing the extraction D_{Am} and D_{Eu} of the present experiment to the extraction of D_{Am} and D_{Eu} in the tracer study (D_{Am} = 25 and D_{Eu} = 88), it

Table 4.2: Initial composition of UNF simulant solution. Solution prepared with nitrate salts of all of the metals listed, with the exception of Mo ($NaMoO_4$), Sn (dissolved Sn metal), and Te (Na_2TeO_4). Concentrations determined by ICP-OES analysis.

Component	Concentration (mmol L^{-1})
Ce	4.12
Cs	4.99
Eu	0.29
Fe	0.11
Gd	0.19
La	2.31
Mo	4.54
Nd	7.51
Pd	0.03
Pr	1.34
Rb	1.03
Rh	0.00
Ru	2.79
Sm	1.42
Sn	0.18
Sr	2.41
Te	0.53
Y	1.38
Zr	8.17
Total Ln	9.68
HNO_3	3 mol L^{-1}

Table 4.3: D_{Am} and D_{Eu} of ALSEP batch contact flowsheet test using UNF simulant. D_{Am} and D_{Eu} for HEDTA and DTPA are equilibrium values.

Process step	Aqueous phase	D_{Am} $(\pm\sigma)$	D_{Eu} $(\pm\sigma)$
Extraction	UNF simulant in 3 M HNO_3	5.6 (0.1)	32.0 (0.5)
Scrub (1)	3 M HNO_3	12.6 (0.6)	47.2 (0.5)
Scrub (2)	1 M AHA + 0.175 M citrate, pH 3.3	15 (1.4)	350 (47)
Strip (HEDTA)	0.125 M HEDTA + 0.2 M citrate, pH 3	0.16 (0.01)	11.01 (0.07)
Strip (DTPA)	0.015 M DTPA + 0.2 M citrate, pH 2	0.16 (0.01)	11.83 (0.01)

is observed that the extraction of both f-elements is significantly suppressed by the UNF matrix. This is a result of the competitive extraction of other metals in the UNF simulant, and a reflection of the limited loading capacity of the ligands in the organic solvent. This significant difference in the extraction D values in the two experiments highlights the need and value of validating process flowsheets with simulated aqueous feeds, in addition to tests using tracer concentrations.

Scrub Steps. Each scrub step in the ALSEP flowsheet serves a different purpose. The purpose of the HNO_3 scrub is to remove metals that have low extraction D_M, but which may interfere with later steps or contaminate the final product. As the concentration of metal in the 3 M HNO_3 scrub solution is essentially zero, this step can be imagined as the extraction step performed with an infinitely dilute feed solution, hence, metals with low D_M will favorably partition to the scrub. The purpose of the second scrub step, comprised of 1 M AHA and 0.175 M citrate, is twofold. One is to remove excess extracted HNO_3 from the organic phase, in preparation for the stripping step (if this step is not performed, excess HNO_3 partitions to the strip solution, where it may overload the capacity of the citrate buffer). The second is to scrub Mo from the organic phase. The D_{Am} and D_{Eu} of both scrub steps show that Am(III) and Eu(III) are retained in the organic phase in each step, as desired, and are sufficiently large for process operations.

MA Stripping Step. The stripping efficacy and kinetics of two different proposed MA strip solutions, each a polyaminocarboxylate complexant in a citrate buffer, were evaluated. The composition (concentration and pH) of each solution has been optimized previously.[69,121] The pH of the stripping solution is maintained by the citrate buffer, and chosen to allow deprotonation of the polyaminocarboxylate ligand for metal complexation. The composition of the stripping solutions were 0.125 M HEDTA + 0.2 M citrate (pH 3), and 0.015 M DTPA + 0.2 M citrate (pH 2).

The results of the kinetic experiment show that while the values of D_{Am} and D_{Eu} are not constant with time, for both DTPA and HEDTA solutions, the equilibrium values are attained within 5 minutes of equilibration (Figure 4.10). Both results are inter-

esting. The stripping kinetics (in experiments using UNF simulant) have previously been reported as "slow" when using DTPA and HEDTA, with an improvement using HEDTA.[121] In this experiment, the two complexants show almost no difference in kinetics over the time regime studied (5 – 120 minutes), and result in equivalent Am/Eu separation factors. The increase in strip D_{Am} at the third time point (15 minutes) is likely due to the experimental design of the experiment. The method of agitation for the first two time points (5 and 10 minutes) was hand-shaking, to be consistent with a follow-up experiment performed using genuine dissolved fuel in the PNNL hot cell facility, where mechanical agitation was not available. For longer time points, a "wrist-action" mechanical shaker was used. As phase transfer is highly dependent on the interfacial contact area of the phases,[122] the difference in agitation methods could account for the slight difference in kinetic values. The strip D_{Am} is expected to be more sensitive to this change than the strip D_{Eu}, as the Eu(III) predominantly stays complexed in the organic phase, but the majority of Am(III) crosses the phase boundary to be complexed by the aqueous polyaminocarboxylate. The values of D_{Am}, D_{Eu} and SF obtained using HEDTA and DTPA to strip the ALSEP solvent loaded from UNF simulant solution demonstrate that the process performs adequately. In particular, the D_{Am} is well less than 0.5, which allows efficient stripping of Am(III).

Overall, the results of this experiment using a post-PUREX UNF simulant show that the D_{Am} and D_{Eu} values of each step of the ALSEP flowsheet are viable for process implementation: Am(III) and Eu(III) are sufficiently extracted, are retained during the scrubs, and are efficiently separated during the MA strip step.

4.4 Conclusions

The synergism observed in the ALSEP solvent (0.05 M T2EHDGA + 0.75 M HEH[EHP]) was found to depend on the aqueous phase extraction conditions, with maximal synergism occurring on extraction from 1 M HNO_3. The synergistic effect persists upon change of diluent to the aromatic diluents *p*-xylene and 1,4-DIPB. The mechanism re-

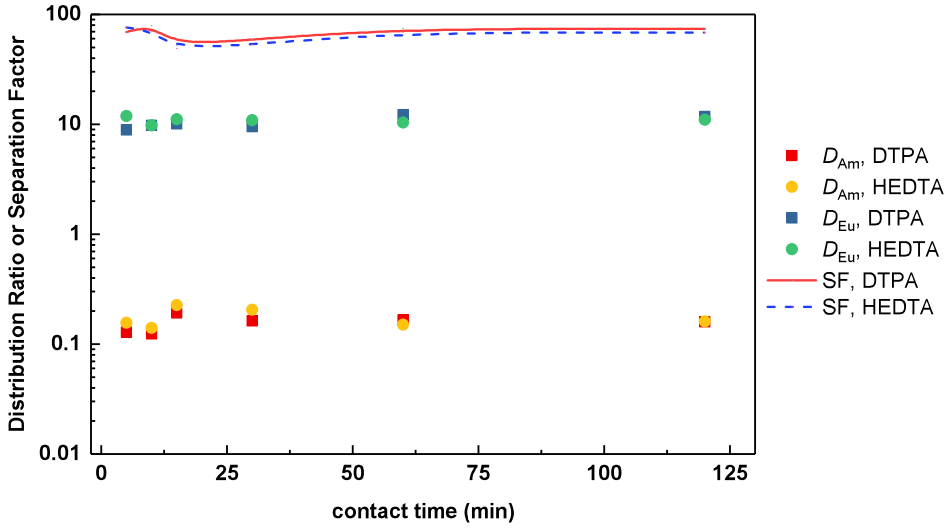

Figure 4.10: Stripping kinetics of Am(III) and Eu(III) by HEDTA (circles) and DTPA (squares). ALSEP solution extracted from simulated UNF solution (3 M HNO_3) and scrubbed per ALSEP flowsheet. Also shown is the SF attained with each stripping solution (lines).

sponsible for the synergism cannot be determined by slope analysis alone, but results of the variable ligand study indicate that a mixed-ligand species may be involved. While the change to aromatic diluent did not affect the synergism, it did affect the value of D_M, as has been observed in other systems. As a consequence, the strip D_{Am} from the aromatic diluent, 1,4-DIPB, was found to be much lower than that from *n*-dodecane or branched dodecane, and with slightly faster kinetics.

The slope analysis results of the variable HEH[EHP] experiment are consistent with the formation of a ternary, mixed-ligand complex. However, the results are also consistent with two independent extraction mechanisms (i.e., T2EHDGA extraction and HEH[EHP] extraction), as the slope analysis method cannot distinguish between the these. In order to better understand the mechanism of extraction and the organic phase speciation, the system was investigated by various spectroscopic techniques, which is the focus of the next chapter.

4.5 Contribution of Authors

Emily L. Campbell contributed Karl Fischer titration and HNO_3 extraction data on T2EHDGA and ALSEP systems, distribution ratio extraction data for *n*-dodecane (^{241}Am and ^{152,154}Eu), and distribution ratio ^{241}Am extraction data for 2,2,4,6,6-pentamethylheptane.

The UNF simulant solution was prepared by Gabriel B. Hall. ICP-OES analysis of the solution was performed by the Subsurface Science and Technology Group, Life Sciences Laboratory, PNNL.

5 Spectroscopic Investigation of ALSEP

5.1 Introduction

The distribution slope analysis experiments presented in Chapter 4 revealed synergism in the ALSEP solvent, which was dependent on the aqueous phase extraction conditions. The participation of ternary complexes in the metal extraction step was indicated, but not confirmed, by the results of section 4.3.2. The distribution experiments and slope analysis are macroscopic techniques, and are unable to probe the ligand or metal speciation of the complex. Further studies using various spectroscopic methods were undertaken in order to determine the metal speciation in the ALSEP extraction step, its dependence on acid concentration, and the mechanism of synergism in the system.

5.2 Methods

For the spectroscopy (IR, UV-vis, and EXAFS) experiments of this section using Am(III), millimolar concentrations were needed. This required the use of ^{243}Am, which has a lower specific activity than ^{241}Am. ^{243}Am was obtained from PNNL stocks in concentrated HNO_3. The nitrate salt was obtained by evaporating the stock to dryness, after which solutions were made in the desired concentrations of HNO_3.

Metal-bearing organic phase samples were prepared by solvent extraction, as described in section 4.2. Equal volumes of organic and aqueous phases were contacted for 60 minutes by orbital shaker (Eu(III) samples) or by a wrist-action shaker (Am(III) samples). Phases were disengaged by centrifugation and physically separated to fresh vials prior to analysis.

IR spectra were collected on a Bruker Alpha-P spectrometer using a diamond ATR

plate, with a minimum of 32 scans averaged for each spectrum using a resolution of 4 cm^{-1}.

Electronic spectra were collected using an Ocean Optics HR-4000 spectrometer using a 1 cm quartz cuvette (Starna). An integration time of 55 ms was used, and 25 spectra were averaged for each sample. All UV-vis spectra were normalized by metal concentration in the organic phase. Organic phase metal concentration was approximately 2 mM Am(III) in each organic phase sample. Exact concentration of ^{243}Am in each sample was determined *via* gamma spectroscopy (HPGe). Since organic phase speciation is not strictly known in these samples, the normalized UV-vis spectra are presented with an ordinate of absorbance/concentration (A/C) instead of the extinction coefficient.

5.3 Results and Discussion

5.3.1 Vibrational Spectroscopy

Infrared spectroscopy was used to probe the ligand environment in solutions of T2EHDGA, HEH[EHP], and the ALSEP solvent. This section is broken into two parts. First, changes in the IR spectra of each of the independent ligand solutions are examined after equilibration with water and variable concentration HNO_3. Then, the same is done for the ALSEP solvent. In the second part, spectral changes that arise as a result of complexation of T2EHDGA, HEH[EHP], and the ALSEP solvent with Eu(III) and Am(III) are investigated. This part is subdivided into two sections, each focusing on each metal. Building on the results of Chapter 4, the effect of aqueous extraction phase conditions on metal extraction and organic-phase metal coordination was studied, and extractions were performed from either 0.1, 0.75, or 3 M HNO_3.

Each ligand has several IR-active groups, which allow the changes due to water, acid, and metal complexation to be monitored (Figure 5.1). The major vibrational bands of the T2EHDGA ligand are assigned to the C=O (1660 cm^{-1}) and C-O-C (1118 cm^{-1}).[123,124] The major bands in HEH[EHP] arise from the P=O (1198 cm^{-1}), P-O-C

(1036 cm^{-1}), P-O-H (984 cm^{-1}), and O-H (1680 cm^{-1}, br).[87,125,126] The main features of each ligand are observable in the ALSEP solvent. The prominent vibrational bands of each ligand and their assignments are presented in Table 5.1.

5.3.1.1 Extraction of H_2O and HNO_3

The IR spectra of solutions of T2EHDGA, HEH[EHP], and ALSEP did not show significant changes after equilibration with water. After equilibration with variable concentration HNO_3, yielded significant changes in the IR spectra of each ligand solution were observed, allowing for determination of the functional groups participating in acid coordination, discussed below.

The IR spectra of T2EHDGA in *n*-dodecane diluent after equilibration with HNO_3 have been recently reported.[62] In particular, a new band is observed at 1604 cm^{-1}, showing coordination of extracted HNO_3 to the C=O group (Figure 5.2). Additionally, new bands at 1293 and 945 cm^{-1} correspond, respectively, to the O-N-O symmetric and N-OH symmetric stretches of HNO_3, with the intensities of these bands increasing with aqueous HNO_3 concentration.

The spectra of HEH[EHP] solutions showed significant changes after equilibration with increasing concentration of HNO_3 (Figure 5.3). The P-O-H stretch at 981 cm^{-1} was observed to broaden and decrease in intensity (Figure 5.4). The appearance of a new peak on its shoulder at 933 cm^{-1} was attributed to the N-OH symmetric stretch of HNO_3. New bands attributed to HNO_3 appear at 1654 cm^{-1} and 1301 cm^{-1}, and may be assigned as the asymmetric and symmetric stretching vibrations, respectively, of coordinated HNO_3. The maximum of the broad band of the P=O group was observed to shift to only slightly lower wavenumber (from 1196 cm^{-1} to 1193 cm^{-1}), while the overall shape changes such that the shoulder at 1221 cm^{-1} disappears and a new band at 1165 cm^{-1} appears: indeed, the overall center of mass of the band shifts to lower wavenumber. Four isosbestic points were observed, at 1252, 1188, 996, and 966 cm^{-1}, indicating the presence of two distinct solution species in the acid-equilibrated solu-

Table 5.1: Major bands in the IR spectra of 0.75 M HEH[EHP], 0.05 M T2EHDGA, and ALSEP solvents, in pristine solvent, and after equilibration with H_2O, 0.1 or 3 M HNO_3, Eu(III) in 0.1 or 3 M HNO_3, and Am(III) in 0.1 or 3 M HNO_3.

Solvent	Aqueous phase	O-H (cm^{-1})	P=O (cm^{-1})	P-O-C (cm^{-1})	P-O-H (cm^{-1})	C=O (cm^{-1})	C-O-C (cm^{-1})
HEH[EHP]	pristine	1680	1198	1036	984	—	—
	0.1 M HNO_3	1680	1196	1036	982	—	—
	Eu + 0.1 M HNO_3	1680	1196	1036	982	—	—
	Am + 0.1 M HNO_3	1675	1197	1035	982	—	—
T2EHDGA	pristine	—	—	—	—	1660	1118
	3 M HNO_3	—	—	—	—	1660, 1602	1116
	Eu + 3 M HNO_3	—	—	—	—	1662, 1608	1116
	Am + 3 M HNO_3	—	—	—	—	1657, 1604	1118
ALSEP	pristine	1680	1198	1036	984	1660	1116
	3 M HNO_3	1680	1197	1035	982	1658	1116
	Eu + 3 M HNO_3	1680	1197	1035	982	1646, 1609	1116
	Am + 3 M HNO_3	1675	1196	1035	982	1651, 1607	1116

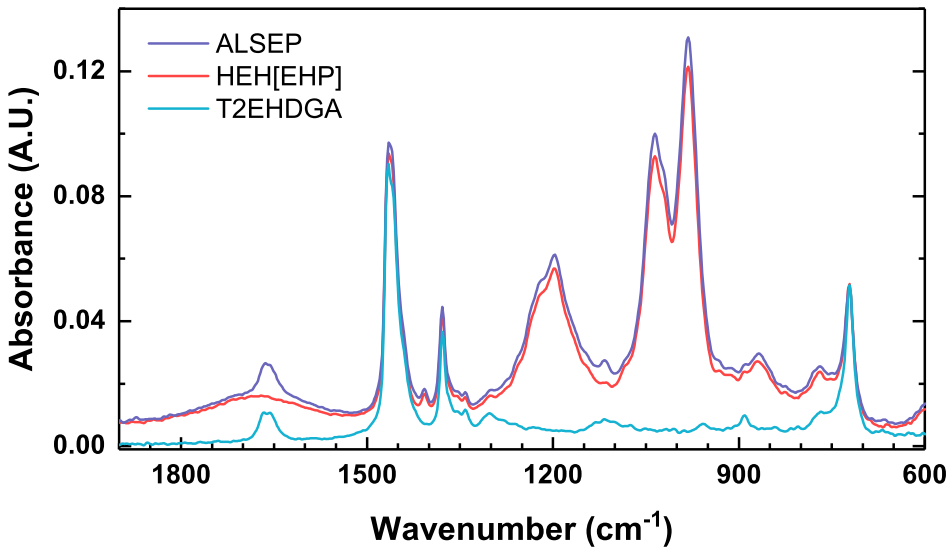

Figure 5.1: IR spectra of 0.05 M T2EHDGA, 0.75 M HEH[EHP], and ALSEP (0.05 M T2EHDGA + 0.75 M HEH[EHP]) in *n*-dodecane.

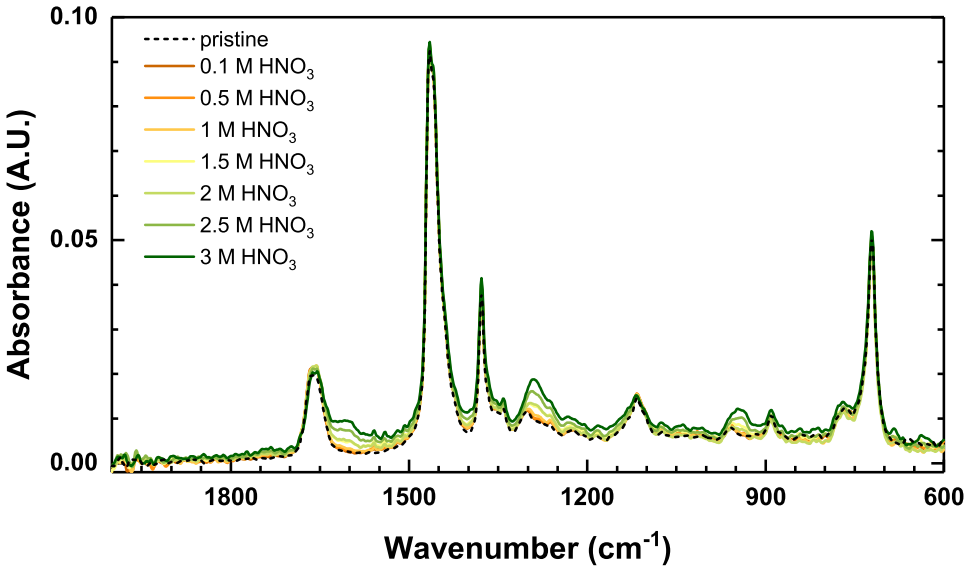

Figure 5.2: IR spectra of 0.1 M T2EHDGA (in *n*-dodecane) after equilibration with 0.1 – 3 M HNO_3. Data courtesy of E. Campbell.

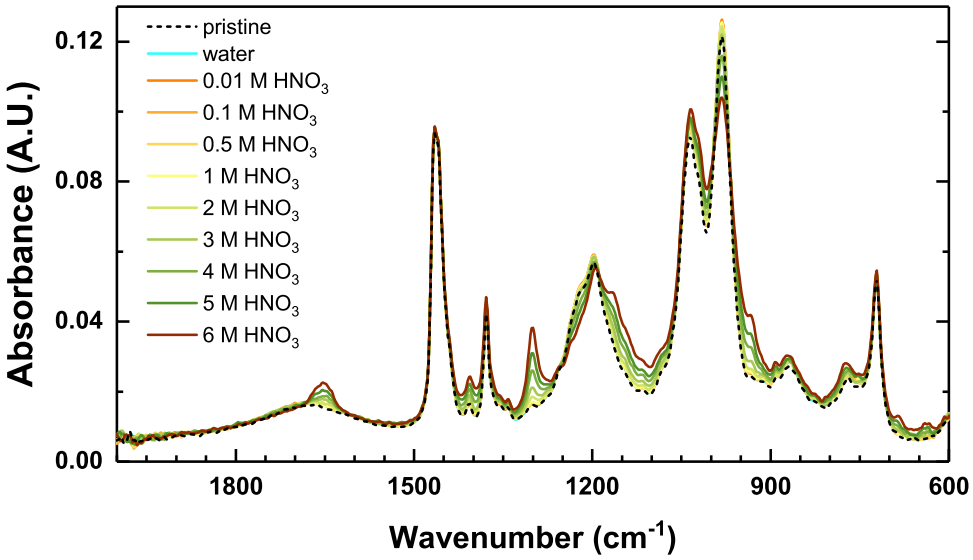

Figure 5.3: IR spectra of 0.75 M HEH[EHP] (in *n*-dodecane) after equilibration with water or 0.01 – 6 M HNO_3.

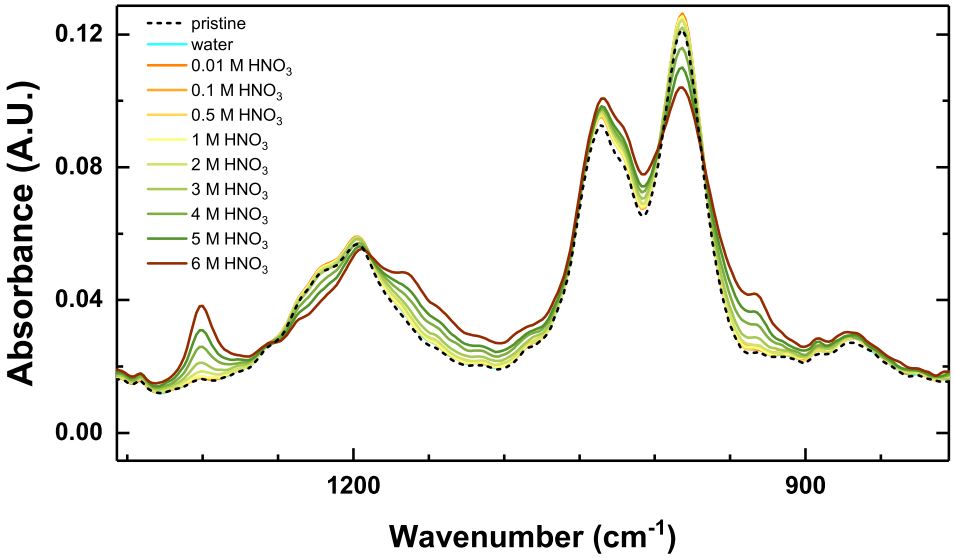

Figure 5.4: P=O, P-O-H, and P-O-C bands of the IR spectra of 0.75 M HEH[EHP] (in *n*-dodecane) after equilibration with water or 0.01 – 6 M HNO_3.

tions. Together, these spectral changes suggest coordination of HNO_3 to HEH[EHP] through the P=O and P-O-H, possibly at the expense of the disruption of HEH[EHP] dimers. Extraction of HNO_3 by TBP has been well studied,[127–129] and extraction of HNO_3 by HDEHP is also reported.[128] In these similar ligand systems, new bands attributed to HNO_3 are observed at frequencies similar to this work (1675, 1300, and 925 cm^{-1} for the HDEHP-HNO_3 system), together with a frequency shift of the P=O bond to 67 cm^{-1} lower energy, indicating HNO_3 bonding *via* breaking the HDEHP dimer in that system.[128] It is likely that the present system behaves similarly.

HEH[EHP], like the phosphoric acid HDEHP, readily forms strong dimers in apolar diluents.[35] Changes in the relative intensities of the P-O-H and P-O-C bands is indicative of a change in dimerization. With increasing concentration of HNO_3, intensity of the P-O-C band increased slightly, while the intensity of the P-O-H band decreases significantly, which suggests a decrease in the dimer concentration. In the absence of acid, a similar change in the ratio of P-O-C and P-O-H bands was observed due to concentration change of HEH[EHP], illustrating the dependence of the P-O-H band intensity on the concentration of HEH[EHP] dimer. Lumetta et al. observed a similar decrease in the HEH[EHP] P-O-H band, together with a slight shift to lower/higher wavenumber, upon Nd(III) complexation, which was attributed to disruption of hydrogen bonds in the dimer.[120] Similar changes in the P-O-C and P-O-H bands were observed by Johnson[130] in a study of the association between HEH[EHP] and Cyanex-923, and were attributed to the disruption of HEH[EHP] dimers as the two ligands formed adducts.

Upon contact with HNO_3, the ALSEP solvent showed pronounced spectral changes, indicating association with HNO_3 (Figure 5.5). As in the HEH[EHP] system, four isosbestic points were observed, at 1241, 1192, 993, and 969 cm^{-1}, again indicating the presence of two distinct solution species. The prominent band at 1300 cm^{-1}, attributed to the O-N-O symmetric stretch of HNO_3, increased in intensity with concentration of HNO_3 in the contacting aqueous phase. Spectral changes in the P=O group at 1196 cm^{-1} generally follow the trend observed with the individual extractant, HEH[EHP],

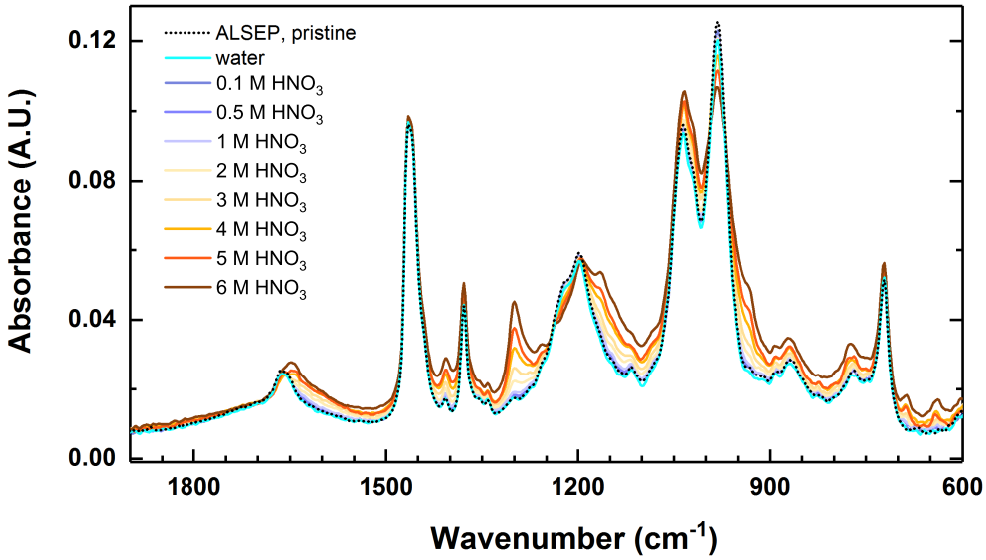

Figure 5.5: IR spectra of ALSEP solvent (in *n*-dodecane) after equilibration with water or 0.1 – 6 M HNO_3.

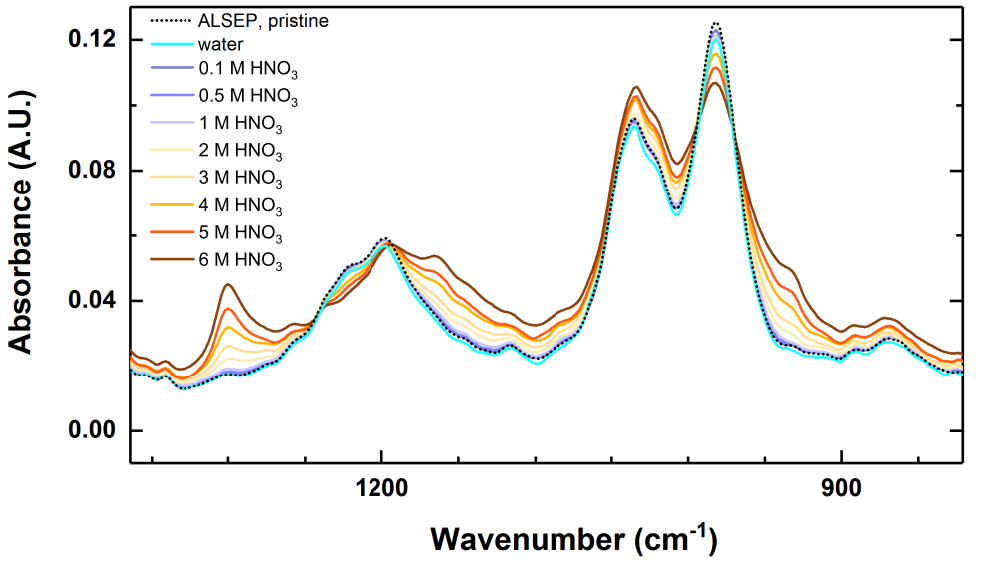

Figure 5.6: P=O, P-O-H, and P-O-C bands of the IR spectra of ALSEP solvent (in *n*-dodecane) after equilibration with water or 0.1 – 6 M HNO_3.

indicating that coordination of acid to the P=O group is similar in the ALSEP solvent as in HEH[EHP], i.e., that it is not strongly affected by the presence of T2EHDGA. Given the molar excess of HEH[EHP] relative to T2EHDGA in the ALSEP solvent, this is to be expected. As observed in the HNO_3-equilibrated HEH[EHP] solutions, equilibration with low concentrations of HNO_3 resulted in a minimal spectral change, with pronounced spectral changes observed only after contact with HNO_3 concentrations in excess of 2 M. Comparison of HEH[EHP] and ALSEP spectra after contact with 3 M HNO_3 (Figure 5.7) indicate increased extraction of acid in the ALSEP system, as evidenced by the intensity of the HNO_3 vibrational bands as well as the broadening and shift of the P=O band to lower energy. The decrease in intensity of the P-O-H band of the ALSEP solvent again indicates disruption of HEH[EHP] dimers in this system (Figure 5.8). In the congested spectral region from 1650 to 1560 cm^{-1}, the T2EHDGA C=O broadens and shifts to lower energy and the O-N-O band from nitric acid appears.

5.3.1.2 Extraction of Eu(III) and Am(III)

To better understand the mechanism responsible for the synergism observed upon extraction from moderate concentrations of HNO_3 (0.5 – 2 M), IR spectra of the ALSEP solvent were collected after extraction of Eu(III) and Am(III) from low (0.1 M), moderate (0.75 M), and high (3 M) concentrations of HNO_3. Similar extractions with HEH[EHP] were done only from 0.1 M HNO_3, and with T2EHDGA only from 3 M HNO_3. The most significant changes in the IR spectra of the ligands were observed in the regions of the C=O band of T2EHDGA, and in the P=O and P-O-H bands of HEH[EHP].

5.3.1.3 Extraction of Eu(III)

To investigate the effect of aqueous conditions on organic phase speciation, extractions using the individual ligand solutions and the ALSEP solvent from variable concentration HNO_3 were performed. The concentration of Eu(III) in the aqueous phase was

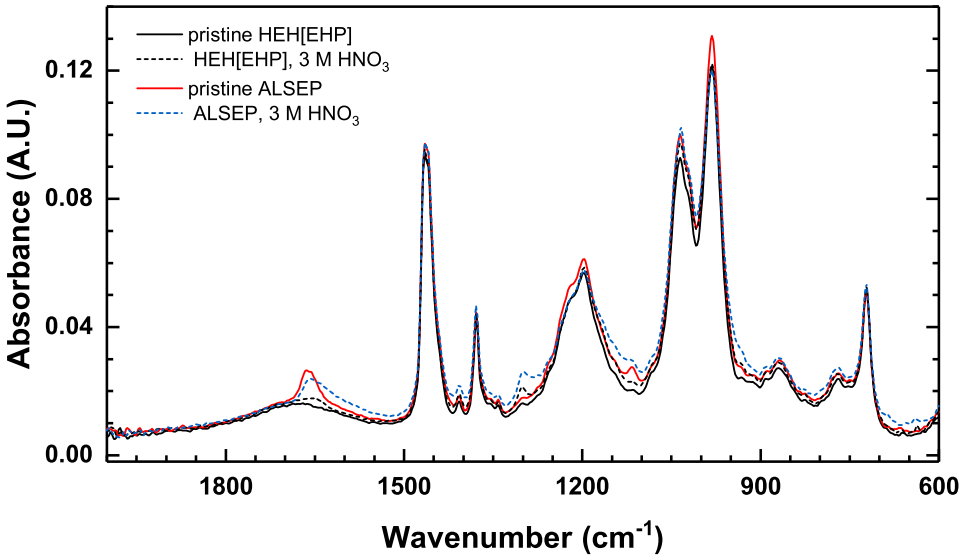

Figure 5.7: Comparison of IR spectra of HEH[EHP] and ALSEP solvent (in *n*-dodecane) before (pristine) and after equilibration with 3 M HNO_3.

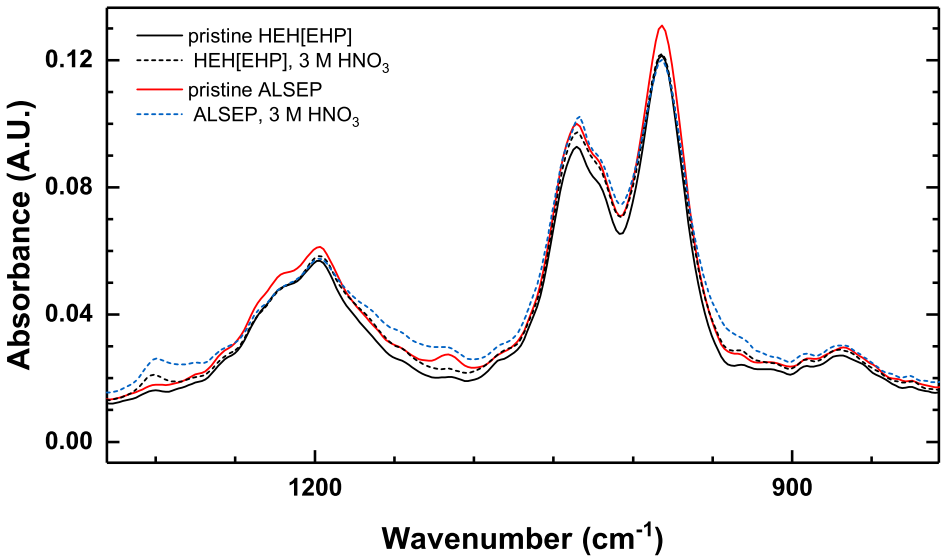

Figure 5.8: P=O, P-O-C, and P-O-H bands of IR spectra of HEH[EHP] and ALSEP solvent (in *n*-dodecane) before (pristine) and after equilibration with 3 M HNO_3.

kept constant at 15 mM, except in solutions of 3 M HNO_3, where [Eu(III)] was 3 mM.[d] Due to the dependence of D_{Eu} on HNO_3 concentration, the concentration of Eu(III) in the organic phase is not constant in the organic phases of this study.

After extraction of Eu(III) by the ALSEP solvent, the greatest change in the P=O stretch was observed upon extraction from 3 M HNO_3 (Figures 5.9, 5.10). This indicates a greater participation of the P=O in the extraction as HNO_3 increases. However, this conclusion cannot be established conclusively, as the effect of acid-equilibration on the ALSEP solvent is not taken into account. A direct comparison of the metal-extracted organic phases to acid-equilibrated organic phases (color and gray traces, Figure 5.9) shows that the change in the P=O may be mostly attributed to changes that occur upon acid equilibration, for each acid concentration. This effect is also observed for the individual extractant, HEH[EHP], for extractions from 0.1 M HNO_3 with and without Eu(III). This indicates that either association of the metal to HEH[EHP] results in the same changes to the P=O band as associated HNO_3, or that any change in the P=O due to metal complexation is not observable due to the presence of the HEH[EHP]·HNO_3 species. The change in intensity of the P-O-H stretch may be a better indicator of the involvement of HEH[EHP] in metal complexation in the ALSEP solutions (Figure 5.11). In all of the metal-equilibrated ALSEP solutions, the P-O-H band was observed to decrease relative to its intensity in the pristine ALSEP solvent, indicating dissociation of HEH[EHP] dimers.

In ALSEP solutions, the P-O-H stretch showed a greater decrease in intensity (relative to the pristine ALSEP solvent) after extraction from Eu(III)-containing 0.1 and 0.75 M HNO_3 aqueous phases than from 0.1 and 0.75 M HNO_3 without Eu(III). This is also observed in the independent HEH[EHP] ligand after metal extraction. The decrease in intensity of the P-O-H band can be explained by an increase in monomerization of the ligand, or by an increase in the concentration of deprotonated dimers due to an increase in metal complexation. The decrease in the P-O-H band in the ALSEP

[d]The lower concentration of metal was necessary in these solutions in order to prevent third-phase formation of the organic phase.

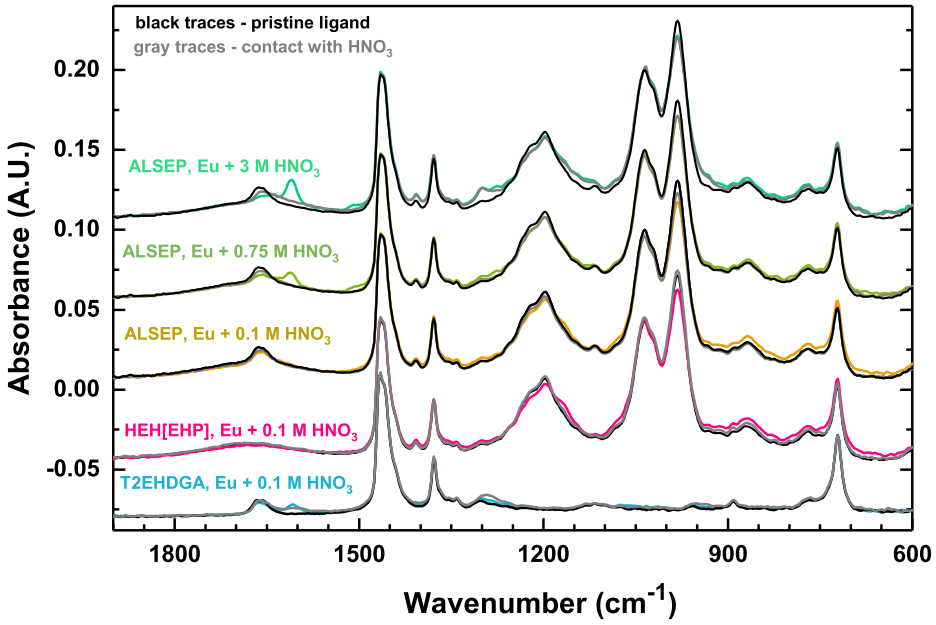

Figure 5.9: IR spectra of ALSEP solvent (in *n*-dodecane) before (pristine, black traces) and after equilibration with solutions of 15 mM Eu(III) in (green, top) 3 M HNO_3, (yellow-green) 0.75 M HNO_3, (yellow) 0.1 M HNO_3; 0.75 M HEH[EHP] before (pristine, black trace) and after equilibration (pink trace) with 15 mM Eu(III) in 0.1 M HNO_3; and 0.05 M T2EHDGA before (pristine, black trace) and after equilibration (blue trace) with 3 mM Eu(III) in 3 M HNO_3. The gray traces at each offset show the IR spectra of the ligand solution after equilibration with 0.1, 0.75, or 3 M HNO_3, corresponding to the acid concentration of the metal solution.

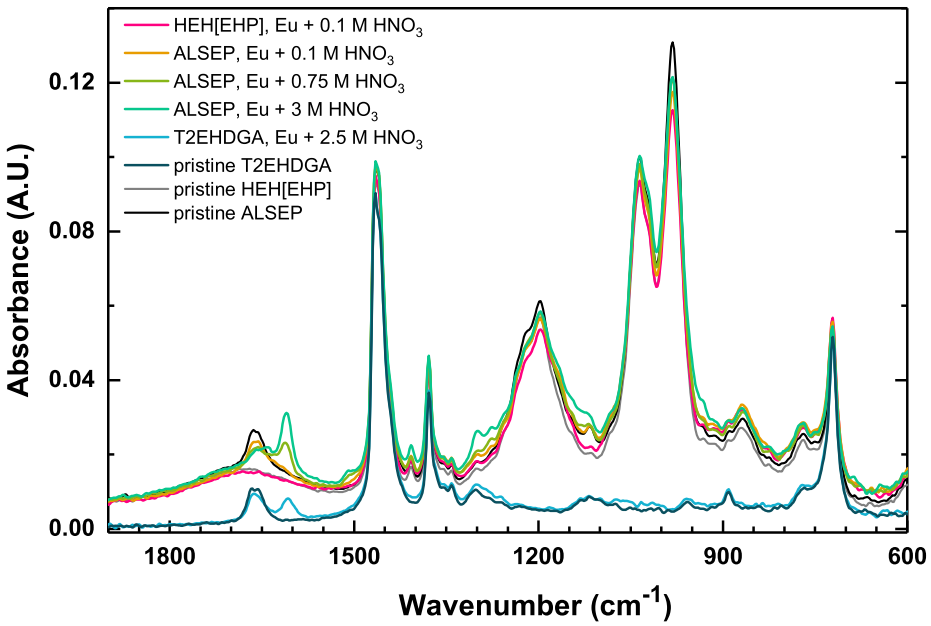

Figure 5.10: IR spectra of ALSEP solvent (in *n*-dodecane) before (pristine, black) and after equilibration with solutions of 15 mM Eu(III) in (green) 3 M HNO_3, (yellow-green) 0.75 M HNO_3, (yellow) 0.1 M HNO_3; 0.75 M HEH[EHP] before (gray) and after equilibration (pink) with 15 mM Eu(III) in 0.1 M HNO_3; and 0.05 M T2EHDGA before (dark blue) and after equilibration (light blue) with 3 mM Eu(III) in 3 M HNO_3.

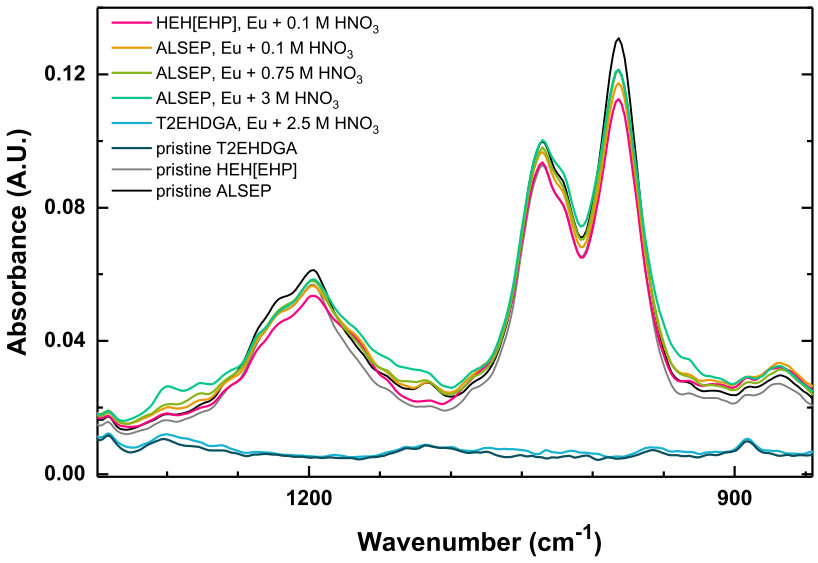

Figure 5.11: P=O, P-O-C and P-O-H band region of the IR spectra of ALSEP solvent (in *n*-dodecane) before (pristine, black) and after equilibration with solutions of 15 mM Eu(III) in (green) 3 M HNO_3, (yellow-green) 0.75 M HNO_3, (yellow) 0.1 M HNO_3; 0.75 M HEH[EHP] before (gray) and after equilibration (pink) with 15 mM Eu(III) in 0.1 M HNO_3; and 0.05 M T2EHDGA before (dark blue) and after equilibration (light blue) with 3 mM Eu(III) in 3 M HNO_3.

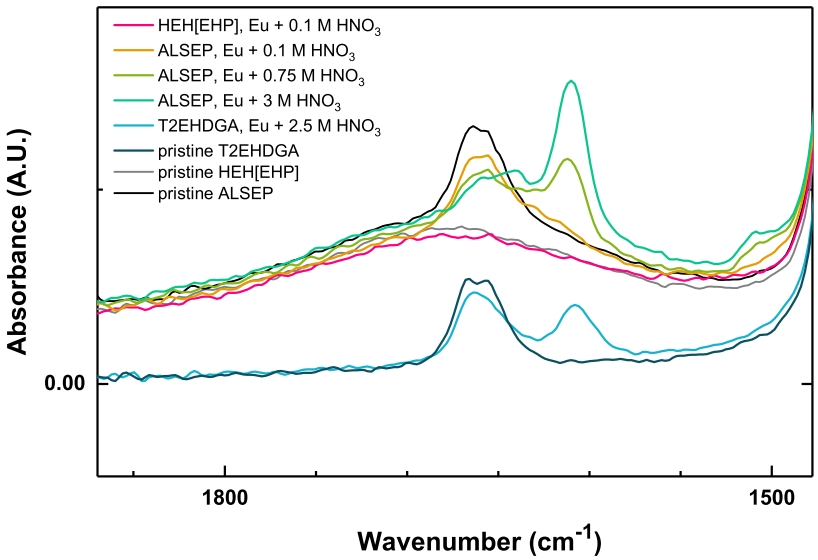

Figure 5.12: C=O band region of the IR spectra of ALSEP solvent (in *n*-dodecane) before (pristine, black) and after equilibration with solutions of 15 mM Eu(III) in (green) 3 M HNO_3, (yellow-green) 0.75 M HNO_3, (yellow) 0.1 M HNO_3; 0.75 M HEH[EHP] before (gray) and after equilibration (pink) with 15 mM Eu(III) in 0.1 M HNO_3; and 0.05 M T2EHDGA before (dark blue) and after equilibration (light blue) with 3 mM Eu(III) in 3 M HNO_3.

solvent, is greatest on extraction of Eu(III) from 0.1 M HNO_3, slight after on extraction of Eu(III) from 0.75 M HNO_3, and shows an slight increase on extraction of Eu(III) from 3 M HNO_3 (Figure 5.10).

Metal will necessarily compete with HNO_3 for ligand coordination sites. The difference in the behavior of the P-O-H stretch in the ALSEP solvent after Eu(III) extraction from 0.1 M HNO_3 (where minimal change in the C=O stretch confirms minimal metal coordination by T2EHDGA under these extraction conditions) compared to Eu(III) extraction from 0.75 or 3 M HNO_3 provides an indication of the degree to which HEH[EHP] coordination in the ALSEP solvent is acid-dependent (Figure 5.11). Given the similarity in changes to the P-O-H band after contact with 0.75 or 3 M HNO_3 and after extraction of Eu(III) from the same concentrations of HNO_3, it is difficult to confirm, from this method alone, that HEH[EHP] participates in the metal complex.

Changes in the C=O region of the ALSEP solvent were strongly dependent on the aqueous phase extraction conditions (Figure 5.12). Extraction of Eu(III) from 0.1 M HNO_3 resulted in a decrease in the intensity of the C=O band and in the appearance of a broad shoulder at lower wavenumber (ca. 1620 cm^{-1}), similar to the changes observed after contact with moderate (0.75 M) concentration HNO_3. Extraction of Eu(III) from 0.75 and 3 M HNO_3 resulted in similar decreases in C=O band intensity and in the appearance of new bands at 1611 and 1609 cm^{-1}, respectively, corresponding to the Eu-coordinated C=O, as observed in T2EHDGA.[104,131] In T2EHDGA, the C=O shift upon metal complexation is to a slightly lower wavenumber (1607 cm^{-1}) than in the ALSEP solvent, indicating stronger complexation through the C=O occurs in solutions of the independent T2EHDGA ligand than in the ALSEP solvent. Additionally, in the ALSEP extraction from 3 M HNO_3, a band at 1641 cm^{-1} was present which was not observed on extraction of Eu(III) from the lower HNO_3 concentrations, nor on extraction with T2EHDGA from 3 M HNO_3. This suggests that the metal coordination of T2EHDGA in the ALSEP solvent at 3 M HNO_3 differs from the Eu(III) coordination in the T2EHDGA solution under the same extraction conditions. The difference in the intensity of the coordinated C=O (1607–1611 cm^{-1}) is due, in part, to the varying

concentration of Eu(III) and HNO_3 in the organic phase in these samples.

5.3.1.4 Extraction of Am(III)

Extractions of ^{243}Am(III) into solutions of 0.05 M T2EHDGA, 0.75 M HEH[EHP], or ALSEP solvent were performed from aqueous phases of 0.1 M, 0.75 M, and 3 M HNO_3 containing varying concentrations of Am(III). Aqueous phase Am(III) concentration was varied in order to obtain concentrations of ca. 2 mM Am(III) in the organic phase of each sample. The concentration of Am(III) in the organic phase was determined by gamma spectroscopy (HPGe).

As with extraction of Eu(III), the changes of various spectral features in the ALSEP solvent after Am(III) extraction were found to depend on the extraction conditions (Figure 5.13).

As with Eu(III) extraction, the HEH[EHP] P-O-H band was observed to changed more than the P-O-C band (Figure 5.14). The decrease in P-O-H band was greatest for the extraction from 0.1 M HNO_3 by HEH[EHP], followed by the 3 M HNO_3 / ALSEP solution, indicating the greatest change in P-O-H environment in these samples. This change is consistent with either deprotonation of the ligand or with disruption of HEH[EHP] dimers, both consistent with metal binding. The ALSEP organic phases after extraction from 0.1 and 0.75 M HNO_3 showed little difference in this band, indicating that the P-O-H bonding and coordination under these extraction conditions is similar.

The broadening and shift of the P=O band toward lower energy indicate the participation of this group in Am(III) complexation in the ALSEP solvent upon extraction from 3 M HNO_3 (Figure 5.14). This shift is most significant for Am(III) extraction from 3 M HNO_3, with smaller shifts observed in the ALSEP solvent after Am(III) extraction from 0.1 M and 0.75 M HNO_3. Broadening of the P=O band in the ALSEP solvent was found to be greater in organic phases containing Am(III) compared to those equilibrated with only HNO_3, indicating, as in the extraction of Eu(III), participation of

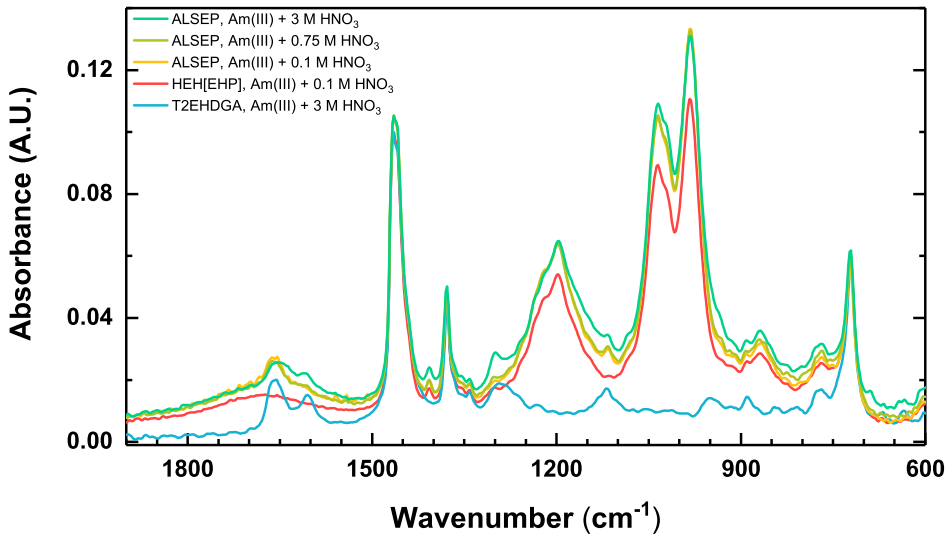

Figure 5.13: IR spectra of ALSEP solvent (in *n*-dodecane) after extraction of Am(III) from 2 mM Am + 3 M HNO_3 (green), 3 mM Am + 0.75 M HNO_3 (yellow-green), 2.5 mM Am + 0.1 M HNO_3 (yellow); 0.75 M HEH[EHP] after extraction from 4 mM Am + 0.1 M HNO_3 (pink); and 0.05 M T2EHDGA after extraction from 2 mM Am + 3 M HNO_3 (blue). Concentration of Am(III) in analyzed organic phase of all samples ca. 2 mM.

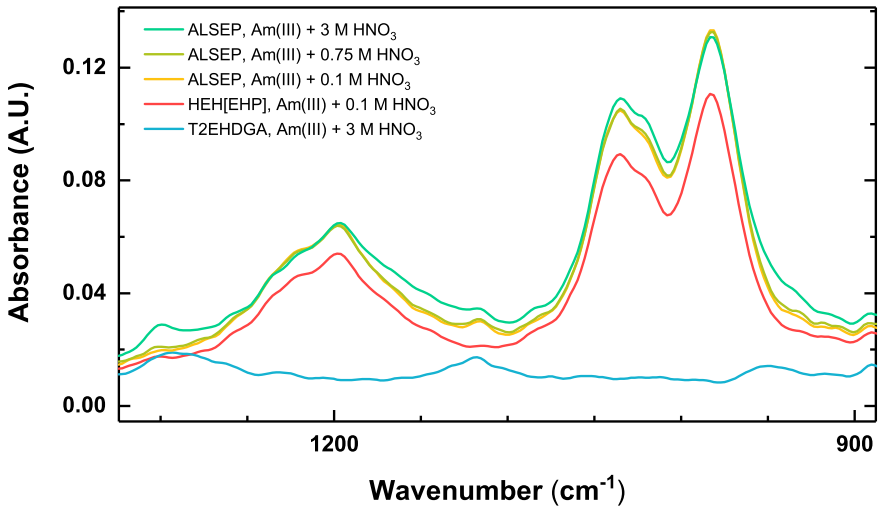

Figure 5.14: P=O, P-O-C and P-O-H band region of IR spectra of ALSEP solvent (in *n*-dodecane) after extraction of Am(III) from 2 mM Am + 3 M HNO_3 (green), 3 mM Am + 0.75 M HNO_3 (yellow-green), 2.5 mM Am + 0.1 M HNO_3 (yellow); 0.75 M HEH[EHP] after extraction from 4 mM Am + 0.1 M HNO_3 (pink); and 0.05 M T2EHDGA after extraction from 2 mM Am + 3 M HNO_3 (blue). Concentration of Am(III) in analyzed organic phase of all samples ca. 2 mM.

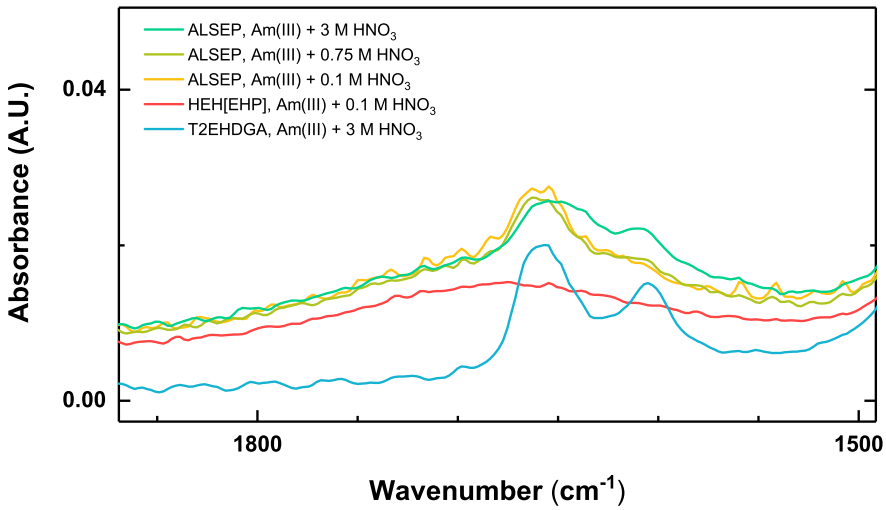

Figure 5.15: C=O band region of IR spectra of ALSEP solvent (in *n*-dodecane) after extraction of Am(III) from 2 mM Am + 3 M HNO_3 (green), 3 mM Am + 0.75 M HNO_3 (yellow-green), 2.5 mM Am + 0.1 M HNO_3 (yellow); 0.75 M HEH[EHP] after extraction from 4 mM Am + 0.1 M HNO_3 (pink); and 0.05 M T2EHDGA after extraction from 2 mM Am + 3 M HNO_3 (blue). Concentration of Am(III) in analyzed organic phase of all samples ca. 2 mM.

the P=O in metal complexation at all three acid concentrations. This corresponds well with the distribution ratio data (Figure 4.7), which shows a synergic effect over this acid range.

The free C=O was observed at 1660 cm^{-1} in the ALSEP solvent after extraction of Am(III) from 0.1 and 0.75 M HNO_3, and at the same position in the T2EHDGA organic phase after extraction of Am(III) from 3 M HNO_3 (Figure 5.15). In the ALSEP organic phase after extraction of Am(III) from 3 M HNO_3, the C=O band was shifted slightly to 1651 cm^{-1}, and substantially broadened. In extractions of Am(III) from 0.1 and 0.75 M HNO_3 in ALSEP solvent, the complexed C=O vibration appears as a broad shoulder above the O-H stretch of HEH[EHP], around 1610 cm^{-1}. On extraction from Am(III) in 3 M HNO_3, the C=O band appears at 1608 cm^{-1} in the ALSEP solvent. Under the same extraction conditions, in the T2EHDGA solution the same band is shifted to 4 cm^{-1} lower energy, as was observed with Eu(III). This suggests that the Am(III)·carbonyl bond in the ALSEP solvent is slightly weaker than the same bond in the T2EHDGA solution. This may be due to the influence and/or participation of HEH[EHP] in the complex.

5.3.2 Electronic Spectroscopy

In order to further elucidate the mechanism of metal complexation and effect of extractant conditions on organic phase speciation in the ALSEP system, electronic spectroscopy was used to probe the metal center. The sharp absorption band at 503 nm, arising from the $^7F_{0'} \rightarrow {}^5L_{6'}$ transition, is sensitive to changes in coordination of the metal, and has been used to determine the coordination of nitrate to Am(III) in aqueous solutions.[132,133] UV-visible spectra of Am(III) extracted by HEH[EHP], T2EHDGA, and ALSEP solutions (all in *n*-dodecane diluent) from aqueous phases of varying composition (HNO_3, $NaNO_3$, or citrate) revealed distinct changes in the organic phase metal environment. The influence of the aqueous phase extraction conditions on the coordination of the extracted organic phase Am(III) complex was found to be significant, and is discussed below.

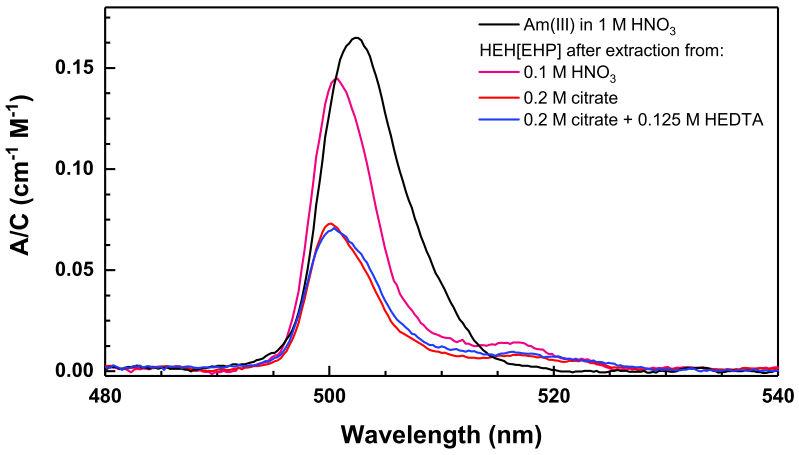

Figure 5.16: Dependence of Am-extraction organic phase Am-HEH[EHP] spectra on aqueous extraction phase composition. UV-vis spectra of organic phase after extraction by HEH[EHP] from 0.1 M HNO_3 (pink); 0.2 M citrate, pH 3 (red); and 0.2 M citrate + 0.125 M HEDTA, pH 3 (blue). Shown in black is a solution of Am(III) in 1 M HNO_3. Note that spectra are normalized by concentration of Am(III).

Extraction of Am(III) from solutions of 0.1 M HNO_3, 0.2 M citrate (pH 3), or 0.2 M citrate + 0.125 M HEDTA (pH 3) by 0.75 M HEH[EHP] yielded organic phase Am(III) spectra that were similar in shape (but of different intensity), with the same shape and relative intensity at the 503 nm band (Figure 5.16). This indicates the coordination of Am(III) to HEH[EHP] is not strongly dependent on the extracting aqueous phase. The slight shoulder arising around 516 nm may be indicative of a second species in solution, either lower in concentration or weakly absorbing. A substantial difference between the spectra of the extracted Am(III) (i.e, the organic phase HEH[EHP] complex) and the various initial (pre-extraction) aqueous Am(III) solutions in HNO_3, citric acid, and HEDTA/citric acid indicates that the coordination of Am(III) in the organic phase HEH[EHP] complex differs from the aqueous phase coordination.

Extractions with the ALSEP solvent were performed from 0.1, 0.75 and 3 M HNO_3 containing Am(III) (Figure 5.17). In the extracted organic phases, a bathochromic shift and increase in the relative intensity of the Am(III) 503 nm band was observed as aqueous phase HNO_3 increased. This suggests a change in the coordination of the Am(III) due to the change in HNO_3 concentration of the contacting aqueous phase.

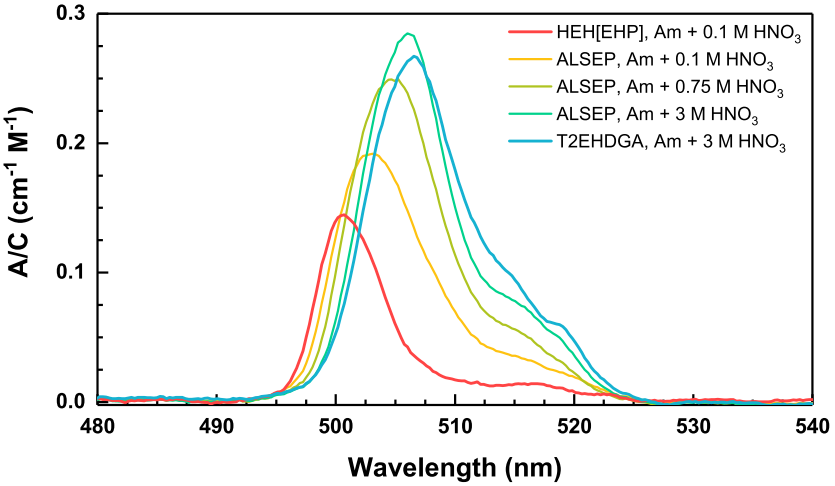

Figure 5.17: Dependence of Am-extraction organic phase spectra of HEH[EHP], T2EHDGA, and ALSEP on HNO_3. UV-vis spectra of organic phase after extraction of Am(III) by HEH[EHP] from 0.1 M HNO_3 (pink); T2EHDgA from 3 M HNO_3 (blue); and ALSEP from 0.1 M HNO_3 (yellow), 0.75 M HNO_3 (yellow-green) and 3 M HNO_3 (blue-green). Note that spectra have been normalized by organic phase concentration of Am(III).

The ALSEP organic phase spectra of Am(III) extracted from 3 M HNO_3 shows a strong similarity to the T2EHDGA spectra extracted under the same conditions, suggesting that the metal coordination in the ALSEP solvent is primarily through T2EHDGA under these extraction conditions.

After extraction of Am(III) from 0.1 M HNO_3 the ALSEP organic phase has intensity and λ_{max} intermediate between that of the post-extraction HEH[EHP] from 0.1 M HNO_3 and the ALSEP organic phase after extraction of Am(III) from 0.75 M HNO_3. The organic phase ALSEP extraction from 0.75 M HNO_3 had intensity and λ_{max} intermediate between the spectra of ALSEP extractions from 0.1 M and 3 M HNO_3. This behavior indicates that the speciation of the metal in the organic phase changes as the concentration of HNO_3 in the aqueous phase increases. It is consistent with the formation of a mixed-ligand species, with replacement of HEH[EHP] by T2EHDGA as HNO_3 concentration increases. However, the spectra may also be explained by the presence of multiple homoleptic species in solution, with the observed spectra corresponding

to the convolution of the (unobservable) homoleptic component spectra.

The changes in relative intensity of the HEH[EHP], T2EHDGA, and ALSEP spectra indicate changes in the symmetry of the Am(III) complexes formed under the various extraction conditions. Increased symmetry is indicated by the lower relative intensity for extraction by ALSEP from lower concentrations of HNO_3 and in the HEH[EHP] solutions.

Extraction by the T2EHDGA solvent from 3 M HNO_3 resulted in the largest bathochromic shift observed in any of the organic phase Am(III) spectra. This spectrum exhibits two shoulders, at 514 and 519 nm, which may indicate contributions of minor species. As was observed with extraction by HEH[EHP], the Am-T2EHDGA spectra showed substantial difference from spectra of Am(III) in the initial aqueous phase, indicating the coordination of the extracted Am(III) differs substantially from the aqueous Am(III).

To evaluate the role of the nitrate source in the ALSEP system, an extraction was performed from a solution of Am(III) in 0.1 M HNO_3 with supporting 2.9 M $NaNO_3$. If metal extraction in the ALSEP system at high HNO_3 concentration occurs solely *via* the neutral extractant, T2EHDGA, increasing the counter-ion concentration while holding the acid concentration constant at 0.1 M is expected to push metal complexation from HEH[EHP] (the dominant complexant at 0.1 M HNO_3) to the neutral extractant, T2EHDGA (the dominant complexant at 3 M HNO_3). Extraction of Am(III) from a 0.1 M HNO_3 + 2.9 M $NaNO_3$ aqueous phase by the ALSEP solvent yielded an organic phase Am(III) spectra very similar to the spectra of ALSEP extraction from 0.1 M HNO_3 (Figure 5.18). This suggests that HEH[EHP] still significantly contributes to metal complexation under conditions of low HNO_3 concentration and high $NaNO_3$ concentration, and that the source of nitrate, i.e., as $NaNO_3$ or HNO_3, plays a significant role toward determining the extraction mechanism.

Complexes of the dialkyl phosphoric acid, HDEHP, with Nd(III) have been previously found to have pseudo-octahedral coordination,[120] and it is likely that HEH[EHP]

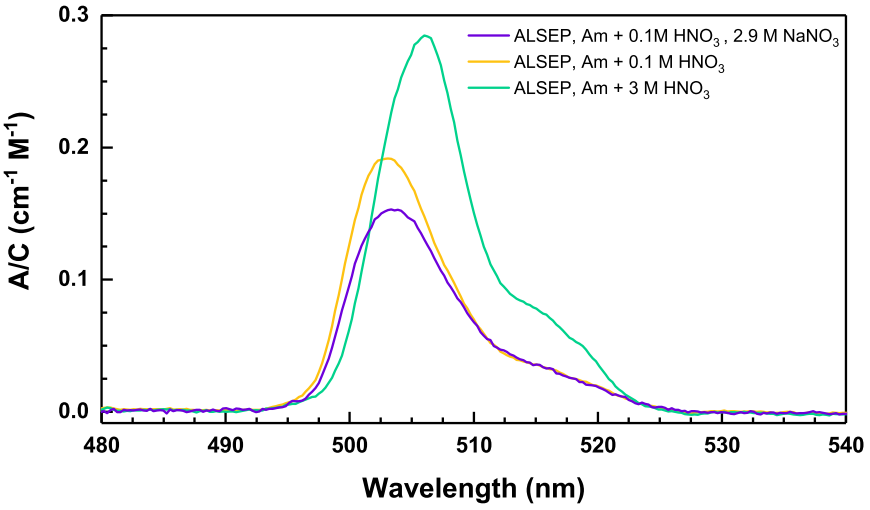

Figure 5.18: Organic phase spectra of ALSEP solvent after extraction from 0.1 M HNO_3 (yellow), 3 M HNO_3 (green), and 0.1 M HNO_3 + 2.9 M $NaNO_3$ (purple). Note that spectra have been normalized by organic phase concentration of Am.

adopts a similar coordination geometry. A hyperchromic effect has been reported when T2EHDGA was added to organic phases containing Am complexed by HEH[EHP] or HDEHP, suggesting that addition of the DGA to the complex decreases the overall symmetry.[106] In the current system, the hyperchromic effect with increasing concentration of nitric acid in the aqueous phase indicates decreasing symmetry and change in metal coordination, either due to the (stepwise) disruption of the tris-dimer HEH[EHP] complexation by inclusion of T2EHDGA, and/or by the inclusion of nitric acid and/or nitrate in the complex. The similarity of the ALSEP and T2EHDGA spectra after extraction from 3 M HNO_3 indicate the inclusion of T2EHDGA in both complexes.

Overall, the results of the electronic spectroscopy indicate that the HEH[EHP] complexes possess a higher degree of symmetry, and that aqueous phase HNO_3 concentration drives speciation of the extracted organic phase in the ALSEP system, with indication of a mixed-ligand system from moderate acid conditions.

5.3.3 Nuclear Magnetic Resonance Spectroscopy

^{13}C and ^{31}P NMR was performed on solutions of ALSEP solvent and on solutions of the individual extractants (0.05 M T2EHDGA and 0.75 M HEH[EHP]) prepared in the four diluents (*n*-dodecane, branched dodecane, 1,4-DIPB, and *p*-xylene), under pristine conditions (i.e., the solvent as prepared), after equilibration with water, and after equilibration with 3 M HNO_3.

5.3.3.1 ^{13}C NMR

^{13}C NMR spectra were collected on solutions of 0.05 M T2EHDGA and ALSEP (0.05 M T2EHDGA+ 0.75 M HEH[EHP]) in the four studied diluents, under pristine conditions, after equilibration with water, and after equilibration with 3 M HNO_3. ^{13}C spectra of HEH[EHP] solutions were not collected.

In the ^{13}C spectra of the pristine solutions, in each diluent, a downfield shift of the T2EHDGA C=O resonance was observed in the ALSEP solvent relative to the shift in the individual T2EHDGA solution (Table 5.2). This change in the shielding of the C=O upon the addition of HEH[EHP] is consistent with the formation of an adduct between the two ligands. The shift could also be due to the change in the polarity of the bulk solvent resulting from the addition of HEH[EHP]; C=O are known to be sensitive to changes in solvent polarity.[134] This matter is investigated in greater detail for the *n*-dodecane system in Chapters 6 and 7. The magnitude of the C=O shift (between ALSEP and T2EHDGA in pristine solutions) is nearly identical in the two aliphatic diluents, decreases in 1,4-DIPB, and is significantly less in *p*-xylene. The aromatic diluent may inhibit adduct formation between the ligands, resulting in a smaller chemical shift difference. Alternatively, the shift could be diminished by the effects of the solvent, i.e., the aromatic solvent induced shift (ASIS). An upfield shift of the ethereal carbon (denoted C-O) is observed in each diluent (Table 5.3). The upfield shift is attributed to the gamma effect. The upfield shifts of the C-O follow a similar trend to that observed in the C=O, with the difference that the $\Delta\delta$ of the C-O in the

aromatic solvents are more similar (-0.12 and -0.10 ppm) than the C=O in the aliphatic solvents (-0.26 and -0.21 ppm).

After equilibration with water, there was little change in the ^{13}C spectra of solutions of T2EHDGA or ALSEP in each of the diluents (less than 0.05 ppm shift), consistent with the IR results, which showed very little change after water equilibration. After equilibration with 3 M HNO_3, there was a significant downfield shift of the C=O resonance in solutions of T2EHDGA and ALSEP in all diluents, suggesting association with HNO_3 occurs primarily through the C=O, again consistent with IR data (Table 5.2). The magnitude of the C=O shift in the acid-equilibrated solutions is greater in the ALSEP solvent than in T2EHDGA solutions, and is greater in the aliphatic diluents than in the aromatic diluents. This may indicate that less acid is partitioned into the aromatic diluents, which may contribute to their suppressed D_M values relative to the aliphatic diluents. Assuming fast exchange between acid-coordinated and free T2EHDGA species in the ALSEP and T2EHDGA-only solutions, the greater chemical shift in the ALSEP solvent indicates more acid is extracted by the ALSEP solvent than by the independent T2EHDGA ligand, which is consistent with results of the acid distribution study presented in Chapter 4. The ether carbon was observed to shift upfield, both in T2EHDGA solutions and ALSEP solvent in all diluents after equilibration with H_2O and HNO_3 (Table 5.3); the upfield shift is again attributed to the gamma effect. The carbons on the ethylhexyl substituents shifted downfield in all diluents. The magnitude of all of these shifts were much less than the C=O shift (or the C-O shift), as expected, given their increased distance from the site of association.

5.3.3.2 ^{31}P NMR

^{31}P NMR spectra were collected on solutions of 0.75 M HEH[EHP] and ALSEP (0.05 M T2EHDGA+ 0.75 M HEH[EHP]) in the four studied diluents, under pristine conditions, after equilibration with water, and after equilibration with 3 M HNO_3. ^{31}P spectra of T2EHDGA solutions were not collected.

Table 5.2: Effect of water and acid equilibration, and HEH[EHP] addition, on δ C=O of T2EHDGA. Relative difference in observed chemical shift ($\Delta\delta$, in ppm) of the T2EHDGA C=O in pristine solution of ALSEP solvent vs. pristine 0.05 M T2EHDGA solution, and after equilibration with H_2O and HNO_3, in the four diluents studied.

Diluent	pristine $\Delta\delta$ (ppm)	H_2O $\Delta\delta$ (ppm)	3 M HNO_3 $\Delta\delta$ (ppm)
n-dodecane	0.46	0.48	0.82
branched dodecane	0.48	0.5	0.83
1,4-DIPB	0.29	0.33	0.77
p-xylene	0.12	0.19	0.51

Table 5.3: Effect of water and acid equilibration, and HEH[EHP] addition, on δ C-O of T2EHDGA. Relative difference in observed chemical shift ($\Delta\delta$, in ppm) of the T2EHDGA C-O carbon in pristine solution of ALSEP solvent vs. pristine 0.05 M T2EHDGA solution, and after equilibration with H_2O and HNO_3, in the four diluents studied.

Diluent	pristine $\Delta\delta$ (ppm)	H_2O $\Delta\delta$ (ppm)	3 M HNO_3 $\Delta\delta$ (ppm)
n-dodecane	-0.26	-0.27	-0.42
branched dodecane	-0.21	-0.20	-0.39
1,4-DIPB	-0.12	-0.13	-0.33
p-xylene	-0.10	-0.13	-0.26

In the ^{31}P NMR, slight shifts in the phosphorus resonance were observed between the HEH[EHP] individual ligand and ALSEP solvent in all diluents ("pristine" Table 5.4). Due to the excess concentration of HEH[EHP] relative to T2EHDGA, association between the two ligands is not expected to result in a large shift, as the change in chemical shift is weighted by the mole fraction of each species. While the phosphorus shift may be due to a change in the bulk solvent properties, due to the addition of 50 mM T2EHDGA to the 0.75 M HEH[EHP] solution. However, it seems more likely that the change is a result of the interaction between the ligands, consistent with the interpretation of the ^{13}C C=O shift due to ligand association. This matter is investigated in greater detail for the *n*-dodecane system in Chapters 6 and 7.

Water equilibration caused an upfield shift of the phosphorus resonance in the HEH[EHP] and ALSEP systems, in all diluents, with a greater magnitude shift change observed in the aromatic diluents (Table 5.4). The shift had a greater magnitude in the ALSEP solvent, indicating additional water is coordinated to HEH[EHP] in the ALSEP solvent. The chemical shifts of ^{31}P nuclei have been shown to be very sensitive to the bond angle about the phosphorus.[94,135,136] Coordination of water to the HEH[EHP] dimer may cause a change in bond angle and corresponding change in chemical shift. While the IR spectra of HEH[EHP] solutions showed only slight changes upon water contact, results of Karl Fischer titration indicate 0.06 M water, corresponding to approximately 15% of HEH[EHP] dimers containing an associated water molecule. The observation of a chemical shift in both HEH[EHP] and ALSEP solutions after water equilibration are consistent with the Karl Fischer results.

After equilibration with 3 M HNO_3, the phosphorus resonance shifted downfield, in both HEH[EHP] and ALSEP solutions in all diluents studied (Table 5.4). The downfield shift upon equilibration with HNO_3 indicates the association of HNO_3 to HEH[EHP] in the individual ligand solution and in the ALSEP solvent, again consistent with the results of IR spectroscopy. The magnitude of the shift is greater in the HEH[EHP] solution than in the ALSEP solvent, indicating different chemical environments about the P atom in these two solvents. This does not necessarily correspond to less coordinated

Table 5.4: Effect of water and acid equilibration on δ of HEH[EHP]. Relative difference in observed chemical shift ($\Delta\delta$, in ppm) of the HEH[EHP] P=O carbon in pristine solution of ALSEP solvent vs. pristine 0.75 M HEH[EHP] solution, and after equilibration with H_2O and HNO_3, in the four diluents studied.

Diluent	pristine $\Delta\delta$ (ppm)	H_2O $\Delta\delta$ (ppm)	3 M HNO_3 $\Delta\delta$ (ppm)
n-dodecane	0.05	0.04	0.11
branched dodecane	0.01	0.05	0.15
1,4-DIPB	0.03	0.01	0.13
p-xylene	0.06	0.1	0.19

HNO_3 in the ALSEP system.

Overall, there is evidence for the association between the ligands T2EHDGA and HEH[EHP] in aliphatic and aromatic diluents, before contact with any solution (pristine solutions). This association appears to persist after equilibration with water and HNO_3.

5.4 Conclusions

Water, acid, and metal extraction significantly affect the ALSEP system. IR investigations reveal the association of acid to the C=O and P=O groups in the individual components and in the mixed-ligand system. Decrease in intensity of the P-O-H stretch indicates HEH[EHP] dimers dissociate after equilibration with HNO_3 and metal solutions in HEH[EHP] and ALSEP solvents. ^{13}C and ^{31}P NMR spectroscopy provide evidence for the formation of an adduct between T2EHDGA and HEH[EHP] in the four diluents studied. The adduct appears to be stable toward water, HNO_3 and metal extraction, and will be the subject of the subsequent chapters. In UV-vis spectra, an increase in the extinction coefficient of Am(III) complexes in the ALSEP solvent upon extraction from increasing concentration of HNO_3 is consistent with the formation of a less symmetric organic metal species. Extraction performed with ALSEP solvent from moderate aqueous phase HNO_3 concentration are consistent with the formation of a

ternary complex, with both ligands participating in metal extraction. This ternary complex may be responsible for the synergistic extraction from moderate-concentration HNO_3 (with synergism maximal from 0.5 to 2 M) which is observed in all four diluents.

5.5 Contribution of Authors

Collection of the ^{243}Am UV-vis and IR spectra was performed jointly with Emily L. Campbell. ^{243}Am solutions were prepared by Emily L. Campbell.

Handling of ^{243}Am stock in glovebox facility and evaporation of ^{243}Am stock to dryness was performed by Gabriel B. Hall.

Robert P. Young assisted in collection of *n*-dodecane and branched dodecane NMR spectra.

6 Study of Ligand Association Constants by Chemical Shift Analysis

6.1 Introduction

Evidence consistent with the formation of a ternary metal complex, containing HEH[EHP] and T2EHDGA, has been found by distribution ratio studies, IR spectroscopy, and UV-vis spectroscopy. Preliminary NMR studies, presented in Chapter 5, were consistent with the formation of a T2EHDGA·HEH[EHP] adduct in the four studied diluents, under pristine conditions, and after equilibration with H_2O and HNO_3. The formation of such an adduct, or a *preassembly* of the ligands, may aid in explaining the synergistic metal extraction observed in the ALSEP system. Additionally, the stability constant of the T2EHDGA·HEH[EHP] adduct is necessary to accurately model metal transfer in the complete thermodynamic model, which is necessary for scale up of the process.

Given the indication of adduct formation in the scoping NMR study presented in Chapter 5, a thorough NMR investigation of each ligand, and of the combined system, was undertaken. The objective of these experiments was to determine the dimerization constant of each ligand (HEH[EHP] and T2EHDGA), and to determine the association constant of the T2EHDGA·HEH[EHP] adduct in *n*-dodecane. This chapter focuses on the determination of these constants using chemical shift analysis (CSA, or chemical shift titration).

In chemical shift analysis, the binding of two analytes (typically a metal and ligand, protein and ligand, or ligand and other substrate) is determined by monitoring the chemical shift, which is induced by complexation, of either analyte. This method has been successfully employed to study a wide range of binding events, and a number of nuclei have been routinely probed (e.g., ^{1}H, ^{13}C, ^{15}N, ^{31}P, ^{6}Li,^{23}Na).[137] As a con-

sequence of the sensitivity of NMR spectroscopy and the concentrations of each analyte that are usually necessary, the range of measurable binding constants is typically considered to be from 10 to 10^5 M^{-1}, although K < 2 and K > 10^6 have been measured successfully by this method.[138,139] The chemical shift (δ) arises from changes in electronic shielding (σ) of the nucleus, which may be perturbed by the complexation event. The changes occurring upon complexation affect the chemical shift in a variety of ways, which will be, to a degree, nuclei-dependent. For example, ^{1}H nuclei involved in hydrogen bonds are usually very sensitive to polar and ionic interactions,[140] and through-space and through-bond interactions have different effects on ^{1}H and ^{13}C nuclei.[141] Additionally, due to the presence of *p* orbitals, ^{13}C shifts are more sensitive to changes in bond geometry (and, consequently, changes in orbital hybridization, overlap, and mixing) than ^{1}H shifts.[141] The presence of *d* and *p* orbitals in phosphorus, in combination with the wider range of geometry available to phosphorus relative to carbon, contributes to the additional sensitivity of chemical shift observed with change in bond angle in this nuclei relative to ^{1}H or ^{13}C.[135,136,142]

If the two analyte species in solution (i.e., monomer and dimer, or free and bound ligand) are in fast exchange (on the NMR time scale), a single resonance will be observed. The observed position of the single resonance will be a weighted average of the resonances from each component species:[140]

$$\delta_{obs} = \delta_1 f_1 + \delta_2 f_2 \tag{6.1}$$

where δ_i is the chemical shift of species *i* and f_i is the mole fraction of species *i*. The *equilibrium* or *association constant*, K, between two species L_i and L_j is defined as

$$K = \frac{\gamma_{i,j}[L_i L_j]}{\gamma_i \gamma_j [L_i][L_j]} \tag{6.2}$$

where L_i and L_j are the free ligands, $L_i L_j$ is the 1:1 ligand adduct, and γ_i, γ_j and $\gamma_{i,j}$ are the activity coefficients of L_i, L_j and $L_i L_j$, respectively. *K* for this equilibrium reaction may also be referred to as K_{11}, to reflect that the product is the 1:1 species; in

general, K_{mn} refers to the the m:n product. Throughout the rest of this chapter, activity coefficients will be assumed to be unity, and are omitted from subsequent equations. The following expression for the observed chemical shift, δ_{obs}, can be written:[140]

$$\delta_{obs} = \delta_f + \frac{(\delta_b - \delta_f)K[L_i]}{1 + K[L_i]} \tag{6.3}$$

where the subscripts b and f refer to the free and bound species, respectively. L_i is the ligand concentration of the species of which the chemical shift is being monitored (i.e., the ligand with resonance at δ_{obs}). In the case of dimerization of ligand L, the relevant equations are[140]

$$K_2 = \frac{[L_2]}{[L]^2} \tag{6.4}$$

and

$$\delta_{obs} = \delta_m + \frac{2K_2(\delta_d - \delta_m)[L]^2}{L_t} \tag{6.5}$$

where δ_m and δ_d are the chemical shifts of the monomer and dimer, respectively, and L_t is the total ligand concentration. This equation can be written in terms of L_t as

$$\delta_{obs} = \delta_m + (\delta_d - \delta_m)\frac{1 + 4K_2L_t - (1 + 8K_2L_t)^{1/2}}{4K_2L_t} \tag{6.6}$$

The parameters of Equations 6.3 and 6.6 (δ_f, δ_b, K, and δ_m, δ_d, K_2, respectively) are obtained by either linearizing the equation and using graphical methods (i.e., Scatchard or Benesi-Hildebrand plots), or can be solved using non-linear least squares methods. Many of the linearizations rely on particular mathematical assumptions or approximations, and only yield accurate results when the chemical system under examination fits the assumptions of the linearization (e.g., one ligand in large excess or $K[L] << 1$).[138–140,143,144] A number of reviews have explored particular experimental conditions under which various linearizations yield reliable and accurate parameter estimates.[143,144] However, the optimal experimental conditions may not be accessible due, for example, to the solubility or detection limits of one or both analytes.

The advent of non-linear fitting methods largely eliminates the need to linearize the equations, and thus allows a wider range of experimental conditions. In this work, non-linear least squares methods are applied to fit Equations 6.3 and 6.6.

6.2 Methods

6.2.1 Sample Preparation

Four titration sets of samples were prepared in *n*-dodecane, with each set containing at least 15 independent samples. The first titration set contained T2EHDGA, varying in concentration from 5 – 244 mM. The second titration set contained HEH[EHP], with concentration ranging from 0.5 – 1000 mM. Two titration sets containing T2EHDGA and HEH[EHP] were prepared, with the concentration of one ligand kept constant in each. One set contained 10 mM HEH[EHP] with T2EHDGA varied from 5 – 300 mM, and the other set contained 50 mM T2EHDGA with HEH[EHP] varied from 1 – 750 mM. HEH[EHP] was obtained from BOC Sciences (Shirley, NY) and purified[71] before use; T2EHDGA was obtained from Eichrom (Lisle, IL) as used as received; *n*-dodecane (99+%) was obtained from Alfa Aesar and used as received. All NMR spectra were recorded on samples as prepared, i.e., "pristine," without equilibration with water or acid.

6.2.2 NMR Measurements

NMR measurements were performed on a Varian VNMRS spectrometer operating at a field strength of 17.6 T (^{1}H ν_0 = 748.4 MHz, ^{13}C ν_0 = 188.2 MHz, ^{31}P ν_0 = 303.0 MHz) with a Varian 5mm direct, broadband tuneable, pulsed-field gradient (PFG) probe. The temperature was regulated at 25 °C for all experiments. The 90° pulse width was calibrated for each nucleus. The number of transients collected varied from 16 to 2048. Broadband ^{1}H decoupling employing the WALTZ-16 composite pulse scheme was applied only during acquisition of ^{13}C and ^{31}P spectra. The resulting

free induction decays were zero-filled to 64k points and multiplied by an exponential decay function to give 0.5 or 1 Hz line broadening for ^{13}C and ^{31}P spectra, respectively. No line broadening was applied to ^{1}H spectra. A coaxial insert containing 50 mM tetraphenylphosphonium chloride in D_2O was used to lock the samples and as a chemical shift reference (^{1}H, ^{13}C and ^{31}P). Processing was performed using VNMRJ 4.0 and Mestrenova 10.0.

6.2.3 Data analysis

The data were fit using three different software packages, each of which implements non-linear least squares routines. The purpose-built NMR fitting software, HypNMR2008[145] (referred to in the text as HypNMR) and WinEQNMR2,[146] was used, as well as the statistical software *R*.[147] Each program offered different functionality and utility. HypNMR has the ability to add additional species (e.g., 1:2, 1:3 complexes) easily. WinEQNMR2 allows only modeling of dimer, 1:1 and 1:2 complexes. *R*, which is not purpose built, requires the user to set up the appropriate model equations. Each resonance was treated independently (i.e., resonances were not fit simultaneously). In each of the three methods, initial guesses of the parameters are supplied as inputs, which are then refined to achieve the best fit between the observed and calculated δ_i. In each method, after convergence was attained, input parameter estimates were varied and then re-run, to determine the effect of the starting parameter values on the refined parameter estimates. Significant dependence or sensitivity of the refined parameter estimates on the starting estimates was interpreted as evidence of a poor model fit, and such results were not reported.

Each observable resonance of the ligands showed a gradual chemical shift upon titration, consistent with association. However, for many of the resonances, the total shift ($\Delta\delta$) over the concentration range of the experiment was very small (less than 0.1 ppm). Fitting data with a small range of chemical shift is challenging, and typically results in large error in the fitted stability constants.[137,138,148] Efforts were initially made to fit all observed resonances; however, it was determined that only resonances with significant

chemical shift differences (>0.2 ppm $\Delta\delta$ over the titration range) could be successfully fit.

Before fitting the line width data for HEH[EHP] (Section 6.3.2.1), data were normalized by the linewidth of the ^{31}P reference (tetraphenylphosphonium chloride in coaxial insert). This normalization accounts for any sample-to-sample differences in line width that are due to instrumental variances (e.g., differences in shimming between samples).

6.3 Results and Discussion

Chemical shift analysis was used to investigate the association behavior of the ligands used in the ALSEP concept. Each ligand was first investigated independently, to determine the dimerization constants. Then, the ALSEP solvent (0.05 M T2EHDGA + 0.75 M HEH[EHP]) was studied, in order to determine the association constant between HEH[EHP] and T2EHDGA.

6.3.1 Dimerization of T2EHDGA

A set of 14 solutions of T2EHDGA, varying in concentration from 4 – 244 mM, was measured by ^{1}H and ^{13}C NMR. The chemical shift of various resonances vs. ligand concentration was observed to follow a smooth, monotonic curve with a shape typical of association. However, not all resonances exhibited sufficient chemical shifts ($\Delta\delta$) to be accurately fit by Equation 6.3. In the T2EHDGA data, only the ^{13}C carbonyl resonance was able to be successfully fit; fits of other resonances resulted in unacceptably large parameter error estimates. This reflects the sensitivity of particular nuclei within the T2EHDGA molecule to the changes induced by in complexation. It is expected that nuclei closest to the site of the interaction will experience the greatest change in electronic shielding, and therefore undergo the greatest chemical shift; nuclei far from the bonding site may exhibit very little chemical shift.

Table 6.1: Dimerization constants of T2EHDGA in *n*-dodecane diluent. Shown are the parameter values found fitting the ^{13}C carbonyl using each fitting method.

Method	K_2 (M^{-1}) $(\pm\sigma)$	δ_m $(\pm\sigma)$	δ_d $(\pm\sigma)$
R	4.3 (0.8)	169.19 (0.02)	170.23 (0.06)
WinEQNMR2	5.9 (0.5)	169.15 (0.01)	170.12 (0.03)
HypNMR	4.3 (1.2)	169.19 (0.02)	170.23 (0.02)

Values for the dimerization constant of T2EHDGA were found using HypNMR, WinEQNMR2, and non-linear least squares fitting in *R*. The parameter estimates (K_2, δ_m and δ_d) resulting from fitting the observed δ of the ^{13}C carbonyl resonance to Equation 6.6 by the three fitting routines are shown in Table 6.1

The observed T2EHDGA ^{13}C carbonyl data, together with one set of predicted values (obtained in *R*), are shown in Figure 6.1. Fits obtained in other programs are similar.

The parameter estimates obtained by the three methods are observed to be in good agreement. The predicted chemical shift value of the free monomer, δ_m, is up to 0.1 ppm lower than δ_{obs}, and the predicted dimer shift, δ_d, is up to 0.5 ppm higher than δ_{obs}. This reflects the experimental constraints, and the weighting inherent in δ_{obs} (Equation 6.1). The true monomer shift, δ_m, will be observed only at infinite dilution (samples of concentration lower than 5 mM were prepared but did not have observable ^{13}C signal in reasonable acquisition times). Similarly, the predicted dimer shift, δ_d, is at higher field than the maximum observed δ, indicating the ligand is not fully dimerized at the highest experimental concentration. Given the value found for the dimerization constant, K_2, a high concentration of ligand would be necessary to drive complete formation of the dimer (and hence to directly observe δ_d). The maximum experimental concentration was limited by the solubility of the ligand. The difference between δ_{obs} and δ_d at teh maximal T2EHDGA concentration is explained by the presence of a significant mole fraction of T2EHDGA monomer in solution (Figure 6.2). Few dimerization constants of similar molecules are known to be published. The most reasonable analog for the DGAs may be the malonamide group of extractants, which have been studied extensively for many of the MA/Ln separation schemes pursued in Europe.

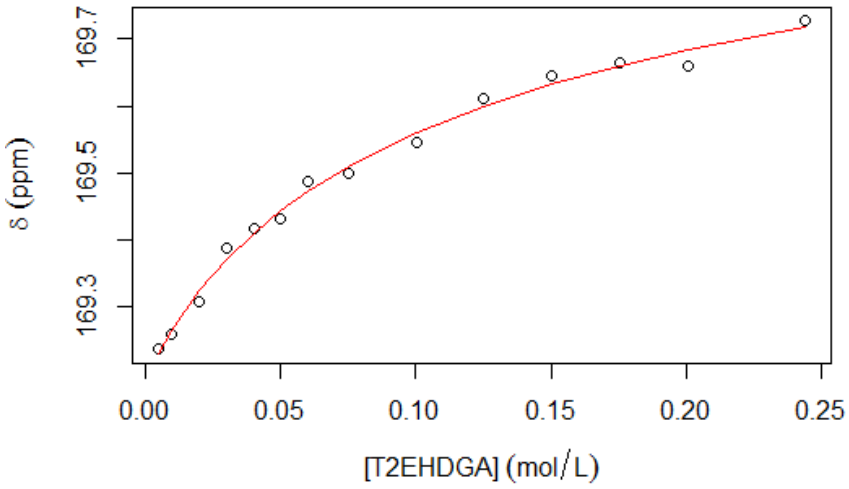

Figure 6.1: T2EHDGA (^{13}C, carbonyl) observed (circles) and predicted (line) chemical shift values as a function of concentration. Predicted values found by fitting Equation 6.6 using NLLS in *R*.

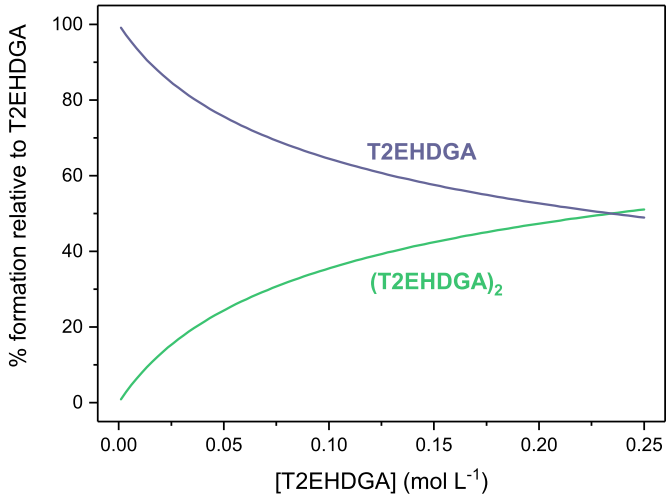

Figure 6.2: Speciation diagram of T2EHDGA in *n*-dodecane (K_2 = 4.3, determined in this work) over the concentration range of the NMR experiment.

Dimerization constants for two malonamides, DMDBTDMA and DMDBODMA (in d_6-benzene) are reported to be 4.78 and 5.02, respectively,[149] which are on the same order as the dimerization constant obtained in this work for T2EHDGA.

6.3.2 Dimerization of HEH[EHP]

A set of 21 solutions of HEH[EHP], varying in concentration from 0.5 mM – 1 M, was measured by ^{1}H and ^{31}P NMR. In the HEH[EHP] titration series, two resonances showed significant changes in chemical shift: the phosphorus resonance (^{31}P) and the acidic proton (^{1}H), having a total shift of ca. 1.7 ppm and 4 ppm, respectively. Each of these resonances was fit independently.

The ^{31}P chemical shift data for HEH[EHP] was fit by *R*, HypNMR, and WinEQNMR, each yielding a value for K_2, δ_m and δ_D (Table 6.2). However, the value obtained for K_2, ca. 2, is several orders of magnitude lower than the published values[35] of K_2 in aliphatic diluents (which range from log K_2 = 4 – 7.23). In a critical review[35] of formation constants of organophosphorus extractants, Kolarik determined that none of the eight HEH[EHP] dimerization constants reviewed could be determined to be of "acceptable quality," which together with the wide range of reported values raises questions regarding the true value of the HEH[EHP] K_2. There may be several contributing factors for the low value of K_2 obtained by chemical shift titration in the present work, which is discussed below.

It was also observed that the dimer equilibria (Equation 6.5) does not adequately describe the shift of the acidic OH proton of HEH[EHP]; no convergent fits were attained in any of the modeling programs. Unlike the ^{31}P data, the shape of the curve of the acidic OH ^{1}H δ vs. concentration is characteristic of a very large binding constant,[138,141] rising nearly linearly before reaching a plateau. Attempts to fit the data using models more complex than Equation 6.5 were unsuccessful. Models created in HypNMR that included the trimeric, tetrameric, and/or hexameric species failed to fit the data. The difference in the shape of the ^{31}P and acidic OH titration curves, with one suggesting

Table 6.2: Dimerization constant of HEH[EHP] in *n*-dodecane diluent found by chemical shift analysis of ^{31}P resonance. Shown are the constants as determined by each of the three fitting methods described in the text. Other resonances either did not result in convergent fits or yielded very spurious results.

Method	K_2 (M^{-1}) $(\pm\sigma)$	δ_m $(\pm\sigma)$	δ_d $(\pm\sigma)$
R	1.64 (0.34)	34.44 (0.03)	31.7 (0.2)
WinEQNMR2	1.64 (0.32)	34.43 (0.03)	31.7 (0.2)
HypNMR	2.0 (1.2)	34.42 (0.02)	32.02 (0.02)

a weak K_2, and the other a strong K_2, may be indicative of an interfering species (i.e., an impurity, *vide infra*) in the chemical system which perturbs the shift of at least one of the resonances.

Inherent in this modeling approach is the assumption that the system behaves as an ideal solution (i.e., that concentrations of the ligand can be used). Given the concentration range of the experiment (5 mM – 1 M), and the known propensity for this class of ligands to deviate from ideality,[73,117,150] this assumption is almost certainly not valid over the entire concentration range. Accurate determination of the activity coefficients of HEH[EHP] have not been made nor published. However, Gray et al. show[117] that in *n*-dodecane diluent, the activity coefficients of the phosphoric acid analogue of HEH[EHP], HDEHP, diverge from unity as the mole fraction of HDEHP dimer increases (e.g., γ = 0.4 for f_{dimer} = 0.05).[151] To account for the non-ideality, activities, instead of concentrations, of HEH[EHP] should be used. However, without known activity coefficients, (at least) two approaches are possible. One is to use the activity coefficients of a chemical analogue (i.e., HDEHP). A second approach is to let the ligand concentration vary as a semi-free parameter. It is not uncommon in chemical shift analysis titrations to fit the concentration as a free or semi-free parameter.[141,152]

In addition to the non-ideality of the solution, impurities in the HEH[EHP] solution may account for some of the discrepancy between the modeled and observed behavior. The non-monotonic behavior present in the plot of δ versus ligand concentration for the RCH_2O- protons (which overall, have a small total chemical shift) suggests

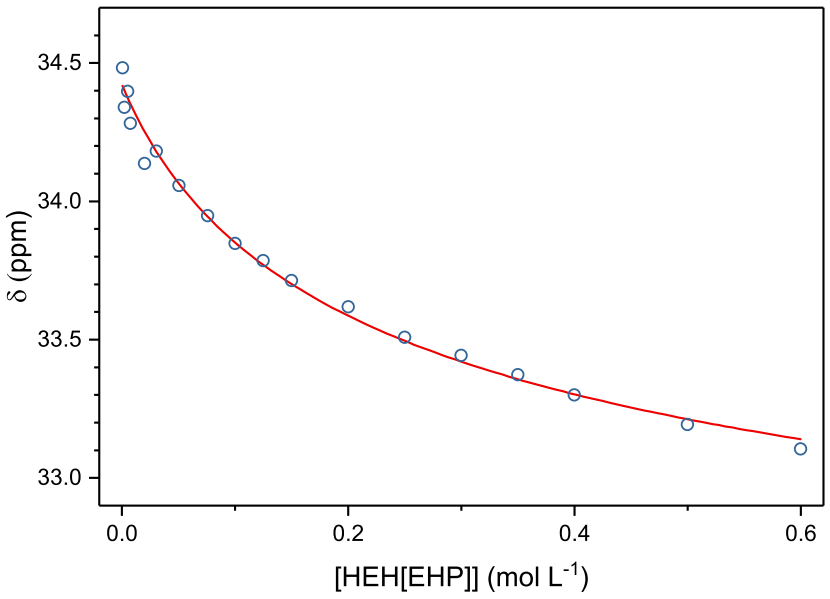

Figure 6.3: Predicted values of δ (red line) and observed values (circles) of the HEH[EHP] ^{31}P resonance, fit by HypNMR. *Note: two data points at low concentration were omitted from the data set, to attain convergent fit in HypNMR.*

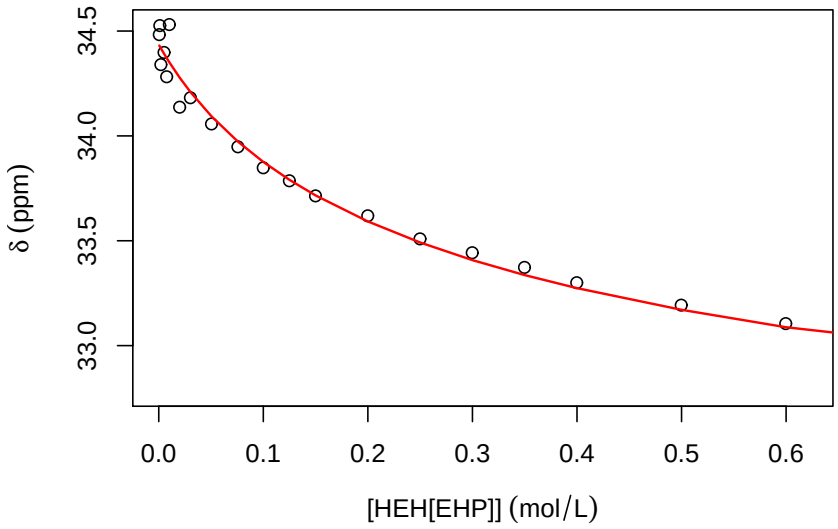

Figure 6.4: Predicted values of δ (red line) and observed values (circles) of the HEH[EHP] ^{31}P resonance, fit in *R*.

the presence of higher order species.[137] It has been demonstrated[105] that commercially available HEH[EHP] contains numerous impurities, phosphorus-bearing and not, some which may persist after typical purification methods. There is also evidence to suggest that some of the impurities coordinate with HEH[EHP],[105] particularly 2-ethylhexanol. Such associations are not taken into account in the dimerization model, and would contribute to the observed chemical shift.[105] 2-Ethylhexanol has been found to significantly affect the shift the ^{31}P resonance of HEH[EHP][105] and the acidic proton (Figure 6.5). Depending on the impurity concentration and the association constant of the impurity with HEH[EHP], and assuming fast exchange, impurities could affect the reliability of the chemical shift titration data. The concentration of P-bearing impurities in the purified material used in these experiments was less than 1.5 P-atom-% relative to HEH[EHP] concentration, and thus is expected to contribute minimally to δ_{obs}. The presence of 2-ethylhexanol in samples of purified HEH[EHP] from various sources has been determined by GC/MS.[105] For these experiments, purified HEH[EHP] with the lowest concentration of 2-ethylhexanol was used, to limit its impact.

Another contributor to the disagreement between the fitted results and the literature values of K_2 may stem from the choice of nucleus probed by NMR. The phosphorus nucleus may not be an ideal probe for this measurement, for a variety of factors. It is well established that the chemical shift of ^{31}P is sensitive to changes in the bond angle and orbital overlap, changes in atomic charges, and to changes in hybridization.[94,135,153] As a result of the asymmetry of the charge distribution in the phosphorus nucleus, the paramagnetic shielding term is found to contribute significantly to the chemical shift.[154] An ab initio study[154] predicted a significant chemical shift difference (6 ppm) between the gauche-gauche and gauche-trans conformers of dimethyl phosphate, demonstrating that the molecular geometry contributes significantly to the chemical shift. Considering the dimerization of HEH[EHP], the chemical shift of ^{31}P is results not only from the electronic shielding effects that occur upon coordination, but also from changes in molecular geometry as bond angle varies. In consideration of the Prado study[154] of dimethyl phosphate conformers, the ethylhexyl substituents of HEH[EHP] present many opportunities for conformal changes, potentially induced

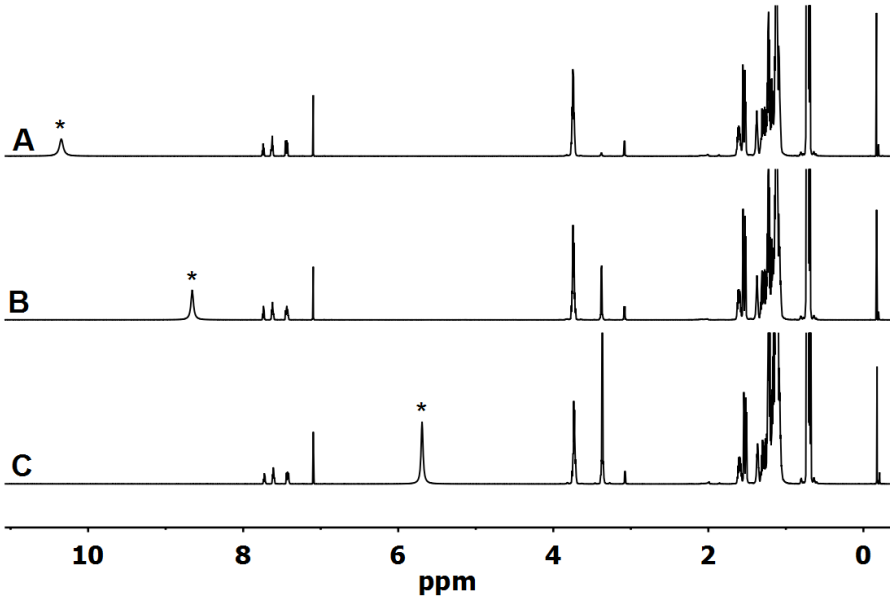

Figure 6.5: Increasing concentration of 2-ethylhexanol causes a significant shift of the HEH[EHP] acidic proton (marked by *). Shown are ^{1}H spectra of (A) unpurified 0.17 M HEH[EHP], (B) the same with 0.05 M 2-ethylhexanol added, and (C) with 0.26 M 2-ethylhexanol added. All spectra recorded in $CDCl_3$.

upon dimerization due to steric crowding, which may affect the chemical shift. Given the unverified relationship between this chemical-shift induced change and concentration, coupled with the fact that electronic effects still contribute to the chemical shift, it may be difficult to obtain accurate values for the dimerization constant. These effects contribute to make ^{31}P a complicated nucleus to monitor for induced chemical shift in these experiments.

It is also possible that the inadequate fit of the dimerization model (reflected by the parameter estimates obtained for K_2) is a consequence of fitting a model that does not sufficiently describe the underlying data. By fitting the HEH[EHP] data by a model which considers only the dimer species, there is no mechanism to account for the presence of higher order species – trimers, tetramers, or hexamers, should they exist in solution. Results presented in Chapter 7 indicate the presence of higher order n-mers in HEH[EHP] solutions. The omission of these species from the models of this section, together with other reasons discussed, may explain the deviation of the obtained K_2

from literature values.

6.3.2.1 Fitting by Line Width

Significant change in the line width of the ^{31}P resonance is observed in the HEH[EHP] titration experiment, indicating a change in the relaxation time of the phosphorus atom. The lineshape as well as the line width at half height, $\Delta\nu_{1/2}$, have been used for the determination of association constants.[155–159]

The non-monotonic behavior of the line width with concentration, shown in Figure 6.6, is suggestive of the presence of higher order species.[137] Non-monotonic behavior was also observed in the ^{1}H RCH_2O- resonance. To avoid the mathematical complexity and potential over-parameterization that would result from accounting for all of the relevant species, the concentration range was split into two domains and each modeled separately. Constraining the concentration range from 0.5 – 5 mM reveals a curve that is monotonic and has the profile characteristic of a 1:1 complexation with high K value.[138,141] The results of fitting this concentration domain are presented in Table 6.3, and are found to yield values for the dimerization constant on the order of log 4, which is in agreement with many of the published values.[35] However, while the three fitting methods produced consistent and reasonable parameter estimates (K_2 and $\Delta\nu_{1/2}$), the error estimate for K_2 is quite large in all three methods. This is likely a consequence of using the restricted dataset, which leaves only four degrees of freedom in the model. This will necessarily result in large errors of the parameter estimates.

In this system, the maximum line width is observed at 50 mM HEH[EHP] concentration, after which line width decreases. It is plausible that in addition to dimers, higher-order species also form in solution (e.g., trimer, tetramer, hexamer, or other n-mer) as HEH[EHP] concentration increases. It is possible that some of these n-meric species contribute to the narrowing of the linewidth, which may result from changes to the chemical shift anisotropy (related to symmetry) of these species compared to the dimer, despite the expected increase in linewidth as a consequence of the expected

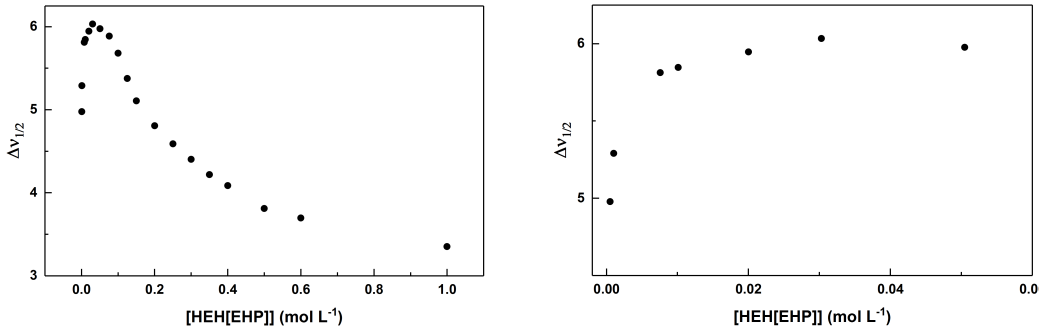

(a) 5 mM – 1 M

(b) 5 mM – 50 mM

Figure 6.6: Linewidth at half height $\Delta\nu_{1/2}$ of variable concentration HEH[EHP].

Table 6.3: Dimerization constants of HEH[EHP] in *n*-dodecane, determined by line width analysis. NR: not reported by software program.

Data set	$\log K_2\ (M^{-1})\ (\pm\sigma)$	$\Delta\nu_{1/2,\mathrm{mon}}\ (\pm\sigma)$	$\Delta\nu_{1/2,\mathrm{dim}}\ (\pm\sigma)$
5 – 50 mM, R	4.2 (4.6)	1 (6)	6.15 (0.04)
5 – 50 mM, WinEQNMR2	4.1 (4.4)	2 (4)	6.2 (0.05)
5 – 50 mM, HypNMR	4.2 (NR)	1.0 (0.1)	6.2 (0.1)
50 mM – 1 M, R	0.9 (0.3)	1.7 (0.1)	9.0 (0.5)

increase in correlation time, τ_c, expected with a larger complex.

6.3.3 Association between HEH[EHP] and T2EHDGA

The data from distribution studies (Chapter 4) indicates possible association between the ligands and demonstrates the synergistic extraction of Am(III) and Eu(III) by HEH[EHP] and T2EHDGA from varying concentrations of HNO_3. The spectroscopic studies presented in Chapter 5 further indicate the participation of both ligands in the extracted metal complex under varying aqueous phase conditions. What remains to be observed is association between the ligands themselves, both in "pristine" solvent (solvent prior to equilibration with any aqueous phase) and after metal extraction. The existence of an adduct between the two ligands may have several consequences for the solvent extraction system, the effect of which may be difficult to precisely quantify.

The presence of an adduct may have a negative effect on the ALSEP system, *via* an impairment of the metal extraction or stripping step. Under the assumption that metal extraction is accomplished solely by the DGA,[2] formation of T2EHDGA·HEH[EHP] adduct will decrease the concentration of free T2EHDGA, thus limiting the metal loading capacity of the solvent. This was found to be problematic in the TRUSPEAK solvent extraction system, where the CMPO·HDEHP adduct severely decreased the concentration of free CMPO.[160] In the TRUSPEAK system, HDEHP dimers dissociated to form adducts with CMPO (adduct log β = 3.4), and, on extraction with metal, various mixed-ligand species were identified. The existence of a T2EHDGA·HEH[EHP] adduct could potentially impair Am(III) or Ln(III) stripping. If the adduct is capable of forming more thermodynamically stable organic phase metal complexes than either ligand alone, it could result in unfavorable process conditions, such as slower stripping kinetics or increased metal retention in the organic phase.

In some cases, the formation of mixed-ligand adducts has been found to result in synergistic metal extraction.[161,162] The increased stability resulting from metal coordination to the ligand adduct has been termed the "assembly effect."[163] The increase in metal complexation by the (stable) adduct may be due to one or more effects: preorganization of the coordination shell, an increase in lipophilicity of the complex, or favorable entropy or enthalpy effects.[161,163]

Ligand preorganization has been demonstrated to facilitate metal binding (and hence increases in extraction).[164–166] This is of particular relevance to the diglycolamide (DGA) ligand, T2EHDGA. It has been established *via* DFT calculations that the carbonyl and ether oxygen of DGA ligands are not always co-planar in their lowest energy states,[167] and that their conformation can vary with the length and branching of the substituent alkyl groups. The lowest energy conformation of free TODGA was found to occur when the ether oxygen and one carbonyl oxygen were coplanar, and the second carbonyl oxygen was rotated 90° out of this plane.[167] This conformation is not conducive to tridentate metal coordination, which will be favored when the three oxygens are nearly co-planar. Multiple studies (XRD, XAS, and DFT) have found DGAs

bind in a tridentate manner through the oxygens,[109–114] and crystal structures and DFT studies show that the DGA oxygens are nearly coplanar in these structures.[109,168] It is possible that the association of HEH[EHP] to T2EHDGA causes a conformational change, resulting in a preorganization of the T2EHDGA binding pocket making it it more favorable for metal complexation. The formation of a T2EHDGA·HEH[EHP] adduct might also be described by the "assembly effect,"[161,163] in which both ligands are preorganized for cooperative metal complexation.

To determine the association constant between T2EHDGA and HEH[EHP] *via* chemical shift analysis (^{1}H, ^{13}C and ^{31}P NMR), two independent titration experiments were performed. In one, the concentration of HEH[EHP] was held constant (10 mM) and T2EHDGA was varied (5 mM – 300 mM). In the other, the concentration of T2EHDGA was held constant (50 mM) with HEH[EHP] varied (1 mM – 750 mM). In the titration with variable T2EHDGA concentration, HEH[EHP] concentration was held at 10 mM to maximize concentration of the monomer while still having an (NMR) observable concentration of HEH[EHP]. Using a literature value of the HEH[EHP] dimerization constant,[169] and ignoring any other complexation, the concentration of the HEH[EHP] monomer in the 10 mM solution is 7% of the total HEH[EHP] concentration in these solutions. Using the dimerization constant of T2EHDGA established in this work, 76% of T2EHDGA is in the monomeric form at 50 mM total (analytic) T2EHDGA concentration. The presence of the dimeric species of the non-varied ligand was not explicitly accounted for in the 1:1 association model.

The resonances most affected by the change in ligand concentration are the carbonyl carbon (^{13}C), the phosphoryl phosphorus (^{31}P), and the HEH[EHP] acidic proton (^{1}H). The nuclei of these resonances are expected to experience the largest chemical shift upon association of the ligands. They are the observable nuclei[e] that are closest to the functional groups where association is likely to occur (i.e., the carbonyl and phosphoryl groups), and therefore these nuclei would experience the greatest change in

[e]While ^{17}O is NMR active, the low natural abundance (0.037%) of this quadrupolar (spin 5/2) isotope contribute to make it, unfortunately, quite challenging to probe.

chemical environment upon association of the ligands.

The results of fitting the two sets of titration data (Table 6.4) show that the parameter estimates for K_{11}, δ_{free}, and δ_{bound} differ significantly depending on which ligand is held constant in the titration. This either highlights the conditional nature of the stability constants derived, or else demonstrates that the 1:1 association model fails to adequately describe the system. Given the differences in ligand concentration ratios spanned by the two titration sets (0.1:15 vs. 0.5:30), the different behavior of the ligand that is in excess in each titration (i.e., K_2 of T2EHDGA relative to K_2 of HEH[EHP]), and the differing bulk solution properties (i.e., viscosity), it is not surprising to observe differences in the parameter estimates between the two systems when none of these factors are taken into account by the 1:1 model.

When [HEH[EHP]] is held constant, the total shift ($\Delta\delta$) of the T2EHGDA carbonyl resonance differs only slightly (<0.05 ppm) from the shift observed in the absence of HEH[EHP]. This is a result of the large excess of T2EHDGA relative to HEH[EHP], and can be expected given Equation 6.1 (that is, the small concentration of HEH[EHP] has only a minimal effect on the chemical shift of δ_{bound}). Thus, it is expected that some of the fitted shift is due not to association between T2EHDGA and HEH[EHP], but due instead to the dimerization of T2EHDGA resulting from the increase in T2EHDGA concentration (Figure 6.2). Fitting the data in HypNMR using a 1:1 model (to describe the associated complex) and including the T2EHDGA_2 species was unsuccessful (no fits converged).

Similarly, when [T2EHDGA] is held constant, a large excess of HEH[EHP] dimer exists in solution, pushing δ_{obs} toward the chemical shift of the HEH[EHP] dimer, δ_{HEH_2}. However, especially at low [HEH[EHP]], there is a substantial difference in δ_{obs} in the ^{31}P NMR: in the presence of T2EHDGA, the phosphoryl resonance shifts in the *opposite* direction (Figure 6.7). As [HEH[EHP]] increases, δ_{obs} begins to parallel the shift observed in the absence of T2EHDGA. Again, this suggests that the dimer of the excess species contributes to δ_{obs}, and obfuscates the fit of the data to Equation 6.3.

Table 6.4: Association constant, K_{11} of the T2EHDA·HEH[EHP] adduct in *n*-dodecane found by chemical shift analysis. Shown are the parameter values found fitting (Equation 6.3) the phosphoryl and carbonyl resonances using WinEQNMR and R. No models in HypNMR achieved convergence for the array of input parameters tested.

Resonance	$K_{11}(M^{-1})$ $(\pm\sigma)$		δ_{free} $(\pm\sigma)$		δ_{bound} $(\pm\sigma)$	
	[T2EHDGA] varied	[HEH[EHP]] varied	[T2EHDGA] varied	[HEH[EHP]] varied	[T2EHDGA] varied	[HEH[EHP]] varied
C=O, WinEQNMR	16 (2)	2.6 (0.2)	165.4 (0.4)	163.7 (0.5)	169.86 (0.14)	170.17 (0.02)
C=O, R	9.9 (0.6)	2.0 (0.2)	169.25 (0.01)	169.4 (0.01)	169.87 (0.01)	170.2 (0.03)
P=O, WinEQNMR	3.7 (0.4)	2.8 (0.6)	103 (11)	45 (3)	31.7 (0.1)	32.3 (0.1)
P=O, R	3.3 (0.4)	2.23 (0.08)	34.33 (0.02)	33.96 (0.01)	31.7 (0.2)	32.3 (0.3)

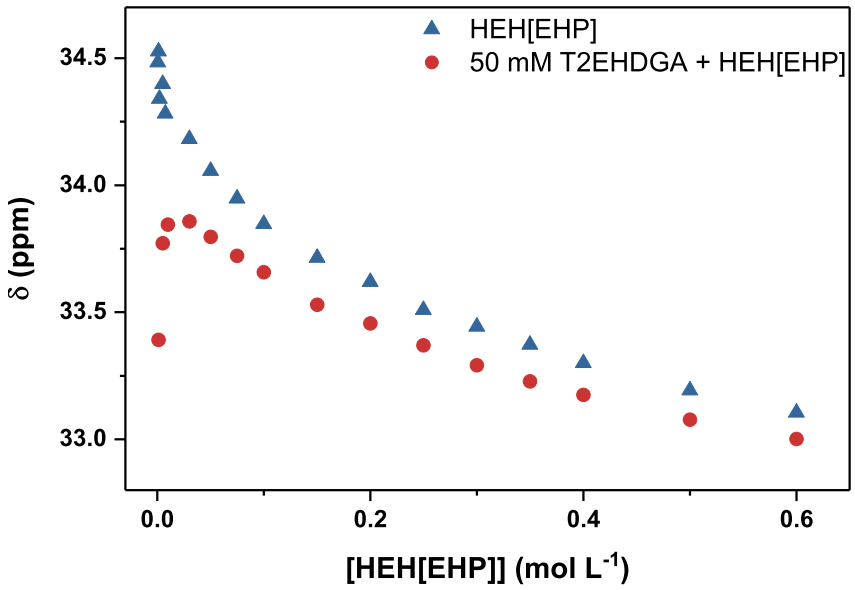

Figure 6.7: ^{31}P phosphoryl resonance of variable concentration HEH[EHP] solutions in *n*-dodecane (blue triangles) and on the addition of 50 mM T2EHDGA (red circles).

In the variable [HEH[EHP]] titration experiment, the parameter estimates obtained for K_{11} are observed to be reasonably consistent, both between methods and between resonances (carbonyl and phosphoryl). In contrast, in the variable [T2EHDGA] titration, the parameter estimates are not self-consistent: the estimates for K_{11} obtained by fitting the carbonyl do not agree with those obtained by fitting the phosphoryl (nor do the carbonyl estimates obtained by two fitting programs agree). In both datasets, the predicted δ_{free} and δ_{bound} are in worse than expected agreement, especially those found by WinEQNMR for the phosphoryl (both datasets). The unrealistic chemical shifts (i.e., δ_{free} = 100 ppm) predicted call into question the validity of this particular model fit. Given these identified problems in fitting the data, the approach of section 6.3.2.1 was used to fit the line width of the phosphoryl resonance.

6.3.3.1 Line Width analysis of the T2EHDGA·HEH[EHP] Adduct

As in the titration of HEH[EHP] alone, significant changes in the line width ($\Delta\nu_{1/2}$) are observed in both titration datasets. The approach of section 6.3.2.1 was applied to

fit the titration data, in hopes to clarify the results of the chemical shift analysis.

The fits obtained from both data sets are shown in Table 6.5. Quite interestingly (but perhaps coincidentally), the value obtained fitting K_{11} for the variable [T2EHDGA] titration by this method is in agreement with the values obtained for variable [HEH[EHP]] by chemical shift analysis. However, the predicted values for $\Delta\nu_{1/2,\text{free}}$ and $\Delta\nu_{1/2,\text{bound}}$ are too large: $\Delta\nu_{1/2,\text{bound}}$ is over twice the observed value, and $\Delta\nu_{1/2,\text{free}}$, while dependent upon concentration, is almost twice the value of $\Delta\nu_{1/2}$ of the "plateau" of the modeled set (which indicates the limit of $\Delta\nu_{1/2,\text{free}}$). The shape of the curve of $\Delta\nu_{1/2}$ vs. [T2EHDGA] lacks curvature, and thus fits to it may be unreliable.[141]

Fitting the line width of the the variable [HEH[EHP]] titration yields parameter estimates that agree with the observed limits of $\Delta\nu_{1/2}$, and a reasonable value, given the observed chemistry of the system, of K_{11}. However, this K_{11} is *not* in agreement with those obtained by chemical shift analysis. Given the reported value of the K_2 of HEH[EHP], and the evidence through the NMR titration that T2EHDGA and HEH[EHP] do associate, it is reasonable to assume that the formation of the adduct results in the cleavage of a dimer of HEH[EHP], similarly to the cleavage of the HDEHP dimer in the formation of the CMPO·HDEHP adduct.[160] For this reaction to occur at high enough yield to produce an NMR-observable species (i.e., the adduct or the decrease in HEH[EHP] dimer), the K_{11} of the adduct is expected to be reasonably large relative to the K_2 of HEH[EHP], especially given the disparity in concentration between T2EHDGA and HEH[EHP] in the ALSEP solvent.

Given the lack of agreement between the K_{11} obtained by the different methods described in this chapter, another method was attempted. The next chapter describes an alternate approach to determine the association constants using DOSY NMR.

Table 6.5: Association constant, K_{11} of the T2EHDA·HEH[EHP] adduct in *n*-dodecane found by line width analysis. Shown are the parameter values found fitting (Equation 6.3) the line width at half height $\Delta\nu_{1/2}$ of the phosphoryl resonance using R.

Data set	$K_{11}(M^{-1})$ $(\pm\sigma)$	$\Delta\nu_{1/2,\text{free}}$ $(\pm\sigma)$	$\Delta\nu_{1/2,\text{bound}}$ $(\pm\sigma)$
[T2EHDGA] varied	2.0 (0.8)	6.0 (0.5)	57 (14)
[HEH[EHP]] varied	112 (24)	3.4 (0.1)	22 (2.3)

6.4 Conclusions

The dimerization and association of the ligands used in the ALSEP solvent, T2EHDGA and HEH[EHP], were investigated using traditional NMR methods, *via* chemical shift analysis and line width analysis. The dimerization constant of T2EHDGA in *n*-dodecane was found to be 4.3 (log K_2 = 0.63), which is previously unreported in the literature. Inconsistent, and ultimately, inconclusive results were obtained via this method regarding the dimerization constant, K_2 of HEH[EHP], and association constant, K_{11} of the ligands in *n*-dodecane. This is due to a failure of the available methods to fit the data, and their inability to accurately take into account all of the chemical equilibria. Nonetheless, the data support the association of each ligand with itself (i.e., dimerization), as well as formation of a T2EHDGA·HEH[EHP] adduct. Fitting the data using a more sophisticated model, which will account for all of the major species, is left as future work.

6.5 Contribution of Authors

Robert P. Young assisted in set up of NMR instrument and in collection of some spectra.

7 Study of the ALSEP System via DOSY NMR

7.1 Introduction

The diffusion ordered spectroscopy (DOSY) NMR method has been likened to "NMR chromatography" for its ability to separate molecules in solution by their self-diffusion coefficient, D. The self-diffusion coefficient of a molecule in solution can be described by the Stokes-Einstein equation:[170]

$$D = \frac{kT}{6\pi\eta r_H} \tag{7.1}$$

where k is the Boltzmann constant, T is temperature, η is solution viscosity and r_H is the hydrodynamic radius of the molecule. DOSY is an extension of the pulsed field gradient (PFG) NMR methods, which can also be used to measure diffusion. The PFG pulse sequences were pioneered by Stejskel and Tanner,[171] who built upon the constant-gradient spin-echo methods of Hahn, Carr and Purcell.[170] The basis of the PFG experiment is a spin-echo pulse sequence (90° pulse followed by 180° pulse) in which pulsed field gradients follow each pulse of the spin-echo, as show in Figure 7.1.

In this pulse sequence, the gradient is applied along the z-axis. As a result, each nucleus experiences a position-dependent magnetic field (with nuclei in the x-y plane

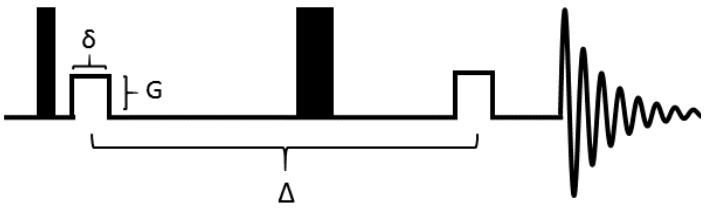

Figure 7.1: Schematic of the pulse sequence of a typical pulsed field gradient spin-echo experiment. Pulses are shown by black bars, with pulsed field gradients shown as open bars. G represents the magnitude of the pulsed field gradient, δ is the length of the gradient pulse, and Δ is the diffusion delay.

of a given z-coordinate experiencing the same field). Consequently, at time τ after the 90° pulse, nuclei at different z-coordinates have now precessed through different angles (i.e., there is spatially dependent phase), and the net x-y magnetization signal has been defocused. Refocusing of the magnetization is achieved by a second, equal, gradient pulse; the 180° pulse is necessary for proper recovery of the signal. However, complete refocusing of the signal is achieved only if each nucleus experiences the same magnetic field gradient during both pulses. Thus, if a nucleus has changed its z-coordinate during the diffusion delay Δ, some magnetization is lost and causes the total signal to be attenuated. The total attenuation is given by the Stejskel-Tanner equation:

$$I = I_0 e^{-\gamma^2 \delta^2 G^2 (\Delta - \frac{\delta}{3}) D} \tag{7.2}$$

where γ is the gyromagnetic ratio, G is the gradient strength, δ is the gradient pulse length, Δ is the diffusion delay, D is the diffusion coefficient, and I_0 is unattenuated signal (signal at zero gradient strength). The parameters G, Δ and δ can all be varied to change the attenuation of the NMR signal in order to determine the diffusion. D is usually obtained after collecting a set of spectra (often 16 to 32), each measured at a different value of gradient strength G. A representative set of spectra showing 16 gradient steps is provided in Figure 7.2. Many improvements have been made to this simplest PFG experiment, e.g., pulse sequences that can compensate for convection.

DOSY is considered to be a pseudo-2D NMR method, as it has one frequency dimension (instead of the usual two), wtih the second dimension being the diffusion coefficient. Fundamentally, it is not different from the advanced PFG spin echo methods, but differs primarily in presentation of the data.

In order to obtain high quality PFG data, the magnetic field must have optimum homogeneity and temperature should be very stable. Any heating of the sample that results in a convection current causes additional movement which is not due to self diffusion, and hence skew the results. The use of an internal molecular weight standard is also common in DOSY experiments; TMS (tetramethylsilane) and ter-

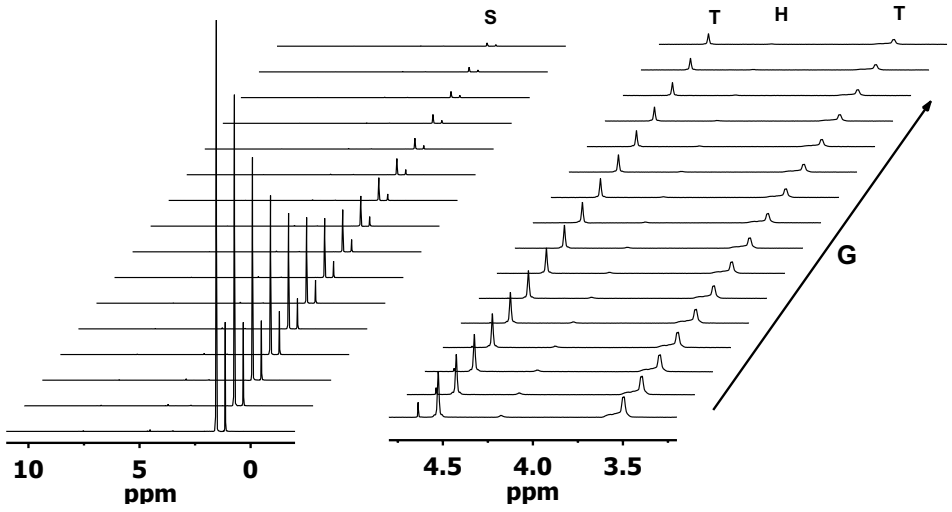

Figure 7.2: PFG ^{1}H NMR spectra of the ALSEP solvent, showing (left) the decay of the solvent peak (S) with increasing gradient strength (G) and (right) the resonances of T2EHDGA (T) (4.4 and 3.5 ppm) and HEH[EHP] (H) (4.1 ppm) in the ALSEP solvent.

akis(trimethylsily)silane (TMSS) have been used.[90] This allows for the correction of any changes in bulk solution viscosity between samples (i.e., due to varying sample composition), which would affect the measured diffusion coefficients. The internal standard is chosen to not interact chemically with the species of interest and to have chemical shift far downfield (or far upfield) of the main components.

The diffusion coefficients of different components of mixtures can be obtained from DOSY spectra. This method works best when the components have reasonably different molecular mass. DOSY has been applied to obtain the critical micelle concentration,[172] determine the size of aggregates in solution,[173] determine self-aggregation of organic molecules,[174–176] and to determine the association constants in host-guest complexes.[138,177–179] NMR-based diffusion methods have the advantage of providing chemical information, and thus providing specificity, over other diffusion methods (e.g., dynamic light scattering).[180]

Similarly to chemical shift analysis of Chapter 6, the diffusion coefficients observable by DOSY can be expressed as a weighted average

$$D_{obs} = \sum D_i f_i \tag{7.3}$$

where D_{obs} is the observed diffusion coefficient and D_i is the diffusion coefficient of species i and f_i is the mole fraction of species i. Fast exchange is not necessarily a requirement for 7.3 to hold; in DOSY, D_{obs} will be a weighted average as long as the exchanging species is faster than the diffusion delay, an experimental parameter.

For a particular resonance in the NMR spectrum corresponding to the exchange between two species, the observed diffusion coefficient is

$$D_{obs} = D_f f_f + D_a f_a \tag{7.4}$$

where D_f and f_f are the diffusion coefficient of and mole fraction of the free species, respectively, and D_a and f_a are the diffusion coefficient of and mole fraction of the

associated (typically, an adduct) species, respectively. Equation 7.4 can be combined with the equilibrium expression for K, and solved analogously to Equation 6.1 for the parameters K, D_f, and D_a.

A useful relationship between the mass of a molecule and its diffusion coefficient is easily derived. Given a spherical molecule with molar mass M_w and partial specific volume v, its hydrodynamic radius, r_H, is given by[139]

$$r_H = \left(\frac{3vM_w}{4\pi N_A}\right)^{1/3} \tag{7.5}$$

Combining this relationship with the Stokes-Einstein equation, yields a relationship between the mass of two molecules and their diffusion coefficients:[139]

$$\frac{D_1}{D_2} = \left(\frac{M_2}{M_1}\right)^{1/3} \tag{7.6}$$

Changes in solution conditions, such as viscosity change, or aggregation of a solute, can affect the the diffusion coefficient of an analyte.[181] In order to eliminate the effect of differing sample viscosity on diffusion, in this work, the ratio D_{obs}/D_{sol} (where D_{sol} is the diffusion coefficient of the solvent) is used instead of D_{obs} directly.[182] From the Stokes-Einstein equation, we obtain:

$$\frac{D_{obs}}{D_{sol}} = \frac{r_{obs}}{r_{sol}} \tag{7.7}$$

where r_{obs} and r_{sol} are the hydrodynamic radii of the solute and solvent, respectively. Since r_{sol} is constant within a series of samples, as the aliphatic solvent is non-interacting, the ratio D_{obs}/D_{sol} provides a measure of the change in hydrodynamic radius of the solute, i.e., the change in particle or aggregate size.

Diffusion data have been successfully fit by methods similar used to fit 1D-titration data, and DOSY can yield results for association constants that agree with those obtained by the classical chemical shift titration method.[178] The DOSY titration does offer some advantages over chemical shift analysis method. As the observed parameter in

the DOSY experiment is affected by changes in the molecular size of the analyte, it is relatively insensitive to low concentrations of impurities, which can be problematic in chemical shift analysis titrations. Additionally, better boundary conditions can be defined for the fitted parameters D_f and D_a of Equation 7.4 than for the δ_i of Equation 6.1, the equivalent chemical shifts of free and bound species. The ability to reasonably and confidently fix one (or more) parameter can ease fitting. The same methodology, non-linear least squares, used to fit the chemical shift titration data is applied to fit the results of the DOSY experiments.

7.2 Methods

Ligand solutions were prepared using the purified reagents, T2EHDGA (Eichrom) and HEH[EHP] (BOC Sciences) in *n*-dodecane (99+%, Alfa Aesar). All aqueous solutions were prepared using distilled water deionized to $\geq$18.2 MΩ resistivity. Acidic solutions were prepared from TraceSELECT HNO_3 (Fluka) and standardized by titration against NaOH using a Titrando Metrohm 905 titrator. $Eu(NO_3)_3{\cdot}6H_2O$ (99.9%, Alfa Aesar) was used to prepare Eu(III) solutions in HNO_3.

Equilibration of ligand solutions with HNO_3 and Eu(III) followed the procedure of Chapter 5. Equal volumes of organic and aqueous phases were contacted for 60 minutes by orbital shaker at 19 °C $\pm$ 1 °C. Phases were disengaged by centrifugation, and the organic phase was removed to a fresh vial for NMR analysis.

^{1}H PFG-NMR measurements were performed on a Varian VNMRS spectrometer operating at a field strength of 17.6 T (^{1}H ν_0 = 748.4 MHz) with a Varian 5mm direct, broadband tuneable, pulsed-field gradient (PFG) probe. The temperature was regulated at 25 °C for all experiments. Diffusion measurements were made using the resonances at δ 4.42 ppm and δ 3.51 ppm for T2EHDGA, the resonance at δ 4.14 ppm for HEH[EHP], and the resonance at δ 1.55 for the solvent (*n*-dodecane). A convection compensation PFG sequence (Dbppste_cc in VNMRJ 3.2) was used to minimize the effect of convection on the diffusion measurements. Samples containing paramagnetic Eu(III) were

measured using a pulse sequence with gradient stimulated echo (DgcsteSL in VNMRJ 3.2), which was necessary to preserve signal sensitivity for fast-relaxing species in the presence of Eu(III). No significant difference in diffusion coefficients was detected by using the two different pulse sequences, as convection was found to be minimal under the experimental conditions. The diffusion gradient length was set at 2.0 ms with a gradient stabilization delay of 3.0 ms, and the diffusion delay ranged from 150 ms to 300 ms. The 90° pulse was calibrated for each sample. 16 – 24 gradient increments were used, with a maximum gradient strength of 56 Gauss/cm, to achieve a total signal decay of at least 90%. Typically 8 transients were collected at each gradient increment, with 8 steady state scans. For samples with low concentration ($\leq$ 1 mM), 32 – 256 transients were used at each gradient increment. Spectra were referenced to the signal of D_2O contained in a coaxial insert, which was also used for lock signal. Processing was performed using VNMRJ 3.2.

7.3 Results and Discussion

DOSY NMR was used to probe the association tendencies of the ligands used in the ALSEP system. First, each ligand was investigated independently. Then, the ALSEP solvent system (containing both ligands) was studied. Please note that, in this chapter only, D refers to the diffusion coefficient, and not to the distribution ratio.

7.3.1 Association of HEH[EHP]

DOSY measurements of varying concentration HEH[EHP] (5 mM – 1 M) (pristine, acid equilibrated, and Eu-equilibrated) were made and the diffusion coefficients, D, determined (Figure 7.3). The observed dependence of D_{obs}/D_{sol} on ligand concentration in the pristine solution is characteristic of dimerization or aggregation,[183] and also similar to the dependence observed in micellization.[148,172,184] The sharp decrease in D_{obs}/D_{sol} with increasing ligand concentration indicates a strong interaction between HEH[EHP]

molecules. Such association is expected, given the polar HEH[EHP] molecule and the apolar, aliphatic, diluent.

A few qualitative assessments can be made about the HEH[EHP] from the collected DOSY data (Figure 7.3). First, the drastic drop in D_{obs}/D_{sol} as the ligand concentration increases from 1 mM to 30 mM indicates strong association occurring at a low concentration of the ligand. Second, the gradual decrease of D_{obs}/D_{sol} as ligand concentration increases from 0.05 M to 1 M may suggest a gradual growth of larger aggregates as ligand concentration increases. The additional decrease of D_{obs}/D_{sol} observed at 1 M HEH[EHP] may be also caused by invalidity of the assumptions of the Stokes-Einstein equation at this high concentration.

The approaches used in the NMR study (Chapter 6) were applied to fit the HEH[EHP] DOSY data *via* Equation 7.4. While parameter estimates were found that approximate the shape of the curve, convergence of the model was not attained in R. This is likely due to the very sharp "knee" present in the data, which is indicative of strong binding. Such isotherms are notoriously difficult to fit, and typically yield inaccurate binding constants when they are fit.[141] Consequently, qualitative discussion follows.

Equilibration of HEH[EHP] with 0.1 M HNO_3 (Figure 7.3) did not result in a significant change in D_{obs}/D_{sol}. A decrease in D_{obs}/D_{sol} was observed after equilibration with 3 M HNO_3 at the highest concentration of ligand tested. This indicates that the low concentrations of acid (and water) that partition to the organic phase after equilibration under these conditions does not appear to significantly promote the growth of HEH[EHP] aggregates. The data set for 3 M HNO_3 is too small to make a conclusive statement, but may indicate that extracted acid promotes further aggregation as HEH[EHP] concentration increases. To examine the effect of metal extraction on HEH[EHP] aggregation, solutions of 10 mM HEH[EHP] (in *n*-dodecane) were equilibrated with aqueous solutions containing 2 mM Eu(III) in 0.1 or 3 M HNO_3. The D_{obs}/D_{sol} of these solutions and those equilibrated with HNO_3 in absence of Eu(III) are not significantly different, again suggesting that, at low ligand concentration (10 mM), metal extraction has little effect on aggregation of the ligand. Given that the

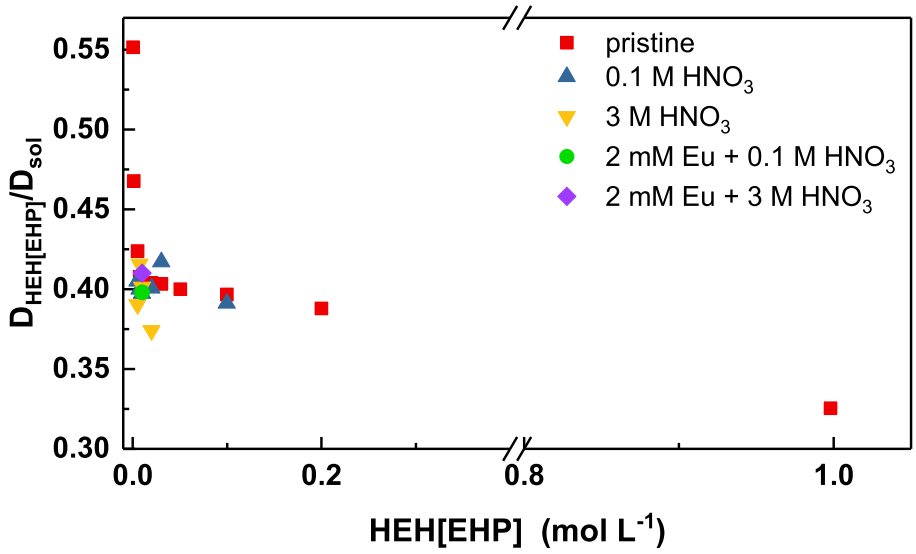

Figure 7.3: Diffusion coefficients of HEH[EHP] (vs. total HEH[EHP] concentration) for pristine HEH[EHP] solvent (red square) or after equilibration with 0.1 M HNO_3 (blue triangle); 3 M HNO_3 (yellow triangle); 2 mM Eu(III)/0.1 M HNO_3 (green circle); 2 mM Eu(III)/3 M HNO_3 (purple diamond). Equilibrations with Eu(III) were performed for 10 mM HEH[EHP] only.

ligand is expected to be primarily dimeric in the pristine solution (FW = 612 g/mol), the addition of an extracted HNO_3 molecule (FW = 64 g/mol) will not significantly change the D_{obs}/D_{sol}.

Under conditions of low metal loading, HEH[EHP] is well established to extract metals by the cation exchange mechanism. In apolar organic diluents, the accepted mechanism of complexation is each complexing dimer exchanges one proton to attain charge balance.[38,99] Thus, in the studied systems, a trivalent metal cation is complexed by three mono-deprotonated HEH[EHP] dimers, which can be written $M(HA_2)_3$ where HA_2 represents the deprotonated dimer of the ligand. Extraction of metal is thus expected to result in the formation of large, hexameric, HEH[EHP] species (FW = 1836 g/mol) containing a metal ion (FW Eu = 152 g/mol), which is expected to produce a measurable decrease in D_{obs}/D_{sol}.

However, this was not observed, and could be due to a combination of reasons. First, it is likely that under the experimental conditions, only a very low concentration of Eu(III) was extracted (initial [Eu(III)] = 2 mM). In this case, D_{obs} will be weighted toward the D of non-complexed HEH[EHP]. The dependence of the distribution ratio on HEH[EHP] concentration has not been established by our laboratory. It is likely that at very low ligand concentrations, such as those used in this experiment (10 mM), that the distribution value is suppressed significantly (this was observed for the neutral extractant, T2EHDGA[62]). Inspection of the ^{31}P and ^{1}H NMR of the metal-equilibrated solutions is consistent with metal extraction (evidenced by ^{31}P peak shift and broadening of ^{31}P and ^{1}H resonances), but does not provide a quantitative measure of metal extraction. As this experiment was part of a set of parallel experiments, the concentrations of HEH[EHP] and Eu(III) were fixed. Future studies to investigate the dependence of diffusion coefficient on metal extraction, as a function of variable HEH[EHP] and Eu(III), may be warranted.

Second, the n-merization state of the "pristine" HEH[EHP] solution (especially as ligand concentration increases) may be higher than dimer. If a significant fraction of trimers, tetramers, or hexamers are already present in a polydisperse solvent, the for-

mation of a small concentration of the hexameric $M(HA_2)_3$ species will have a negligible effect on D_{obs} (per Equation 7.4).

7.3.2 Association of T2EHDGA

Solutions of varying T2EHDGA concentration (3 mM – 175 mM) were measured before contact with any aqueous phase ("pristine" solutions). Portions of the same organic solutions were equilibrated with DI water, 3 M HNO_3, or 2 mM Eu(III) in 3 M HNO_3 and similarly measured, as shown in Figure 7.4.

The change in D_{obs}/D_{sol} with increasing ligand concentration of the pristine solvent is indicative of an associative interaction (e.g., dimerization), evidenced by the rapid drop in D_{obs}/D_{sol} at low concentrations of T2EHDGA (below 25 mM). The continued decrease in D_{obs}/D_{sol} either indicates that dimerization was not complete in the lower concentration range (and hence D_{obs}/D_{sol} at 25 mM is an average of monomer and dimer), or that still larger aggregates form.

Attempts to fit this diffusion data to Equation 6.5, to determine the dimerization constant of T2EHDGA, were unsuccessful. However, as was observed in the HEH[EHP] diffusion data, the dependence of D_{obs}/D_{sol} on ligand concentration is consistent with the behavior of an aggregating solute. In comparison with the HEH[EHP] diffusion data, it appears that the dimerization constant of T2EHDGA is much smaller (a larger dimerization constant, K_2, will result in a sharper "knee" and a greater absolute change in D), which is consistent with the observations of the chemical shift analysis. It is expected that the dimerization constant of T2EHDGA should be less than that of HEH[EHP], as the dimerization of T2EHDGA will be driven by the hydrophobic interaction of the polar carbonyl and ether groups in the apolar solvent. HEH[EHP], on the other hand, can from stronger self associates, as it has both proton acceptor and donor.

Upon equilibration with acid, D_{obs}/D_{sol} decreases as T2EHDGA concentration increases (Figure 7.4, yellow triangles), especially at higher HNO_3 concentration, sug-

gesting the formation of T2EHDGA·$(HNO_3)_n$ adducts. This is consistent with the model of T2EDGA·HNO_3 extraction recently presented by Campbell,[62] and follows the behavior of TODGA, which is believed to form reverse micelle-like tetramers upon HNO_3 extraction.[43]

The ratio D_{obs}/D_{sol} reflects a change in not only the diffusion coefficient of the observed species, but also a change in its hydrodynamic radius relative to that of the solvent (Equation 7.7).

At low concentration ([T2EHDGA] $\leq$ 50 mM), D_{obs}/D_{sol} of the acid-equilibrated solution varies only slightly from the pristine T2EHDGA, but the difference becomes significant as T2EHDGA concentration increases. This indicates the increased tendency toward formation of aggregate species upon equilibration with acid as the concentration of T2EHDGA increases. This is consistent with the vapor pressure osmometry results of a previous study, which found an increase in the average aggregation number of T2EHDGA after equilibration with increasing [T2EHDGA] and [HNO_3].[62] Aggregation, even to the point of phase splitting, upon extraction of acid is a well documented phenomenon for DGA ligands.[43,52,59,62] It is likely that at higher concentrations of the DGA, the extraction of acid promotes the formation of small polar core aggregates, as observed with TODGA,[43] and drives the increase in size and decrease in D_{obs}/D_{sol}. While it is not possible to determine the precise stoichiometry or speciation of the aggregate species from the DOSY results, it is strong evidence that acid uptake promotes aggregation of T2EHDGA.

After equilibration with a solution of 2 mM Eu(III) in 3 M HNO_3 (Figure 7.4, purple diamonds), little difference in D_{obs}/D_{sol} is observed between Eu(III) and the acid-equilibrated solution at high concentrations of T2EHDGA. After equilibration with acid, the predominant speciation of T2EHDGA at this concentration, after equilibration with acid, is expected to be an aggregate (i.e., tetramer or hexamer, FW = 2320 or 3480 g/mol). The resulting change in mass upon extraction of $Eu(NO_3)_3$ (FW = 338 g/mol) will not result in a significant change in mass and therefore not significantly alter the diffusion coefficient. At lower concentrations of T2EHDGA ($\leq$ 50 mM), a

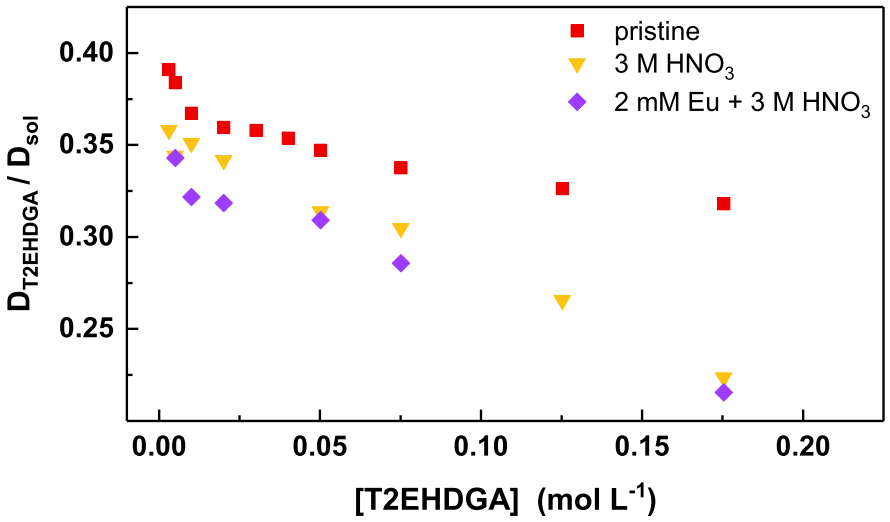

Figure 7.4: Diffusion coefficients of T2EHDGA (vs. total T2EHDGA concentration) for pristine T2EHDGA (red squares) or after equilibration with 3 M HNO_3 (yellow triangles) or 2mM Eu(III)/3 M HNO_3 (purple diamonds).

slight decrease in D_{obs}/D_{sol} of the Eu(III) equilibrated T2EHDGA solution is observed, indicating that under these conditions, a larger, more slowly diffusing species forms after equilibration with Eu(III)/3 M HNO_3 than after equilibration with 3 M HNO_3 alone. This indicates that extraction of $Eu(NO_3)_3$, from these low concentrations of ligands, increases the average aggregate size.

7.3.3 Association of T2EHDGA and HEH[EHP]

DOSY experiments were performed on the mixed ligand solvent, ALSEP, at the ligand concentrations 10 mM HEH[EHP], with variable T2EHDGA concentration (1 – 175 mM). These concentrations differ substantially from the proposed ALSEP process formulation (50 mM T2EHDGA + 750 mM HEH[EHP]), and were chosen for a variety of reasons. Both calculations and initial scoping experiments determined that the large (15 times) excess of HEH[EHP] in the traditional ALSEP formulation would impede the DOSY experiment: the measured diffusion coefficient is heavily biased by the large excess concentration of non-complexed HEH[EHP]. The concentration of HEH[EHP]

used in these experiments was chosen to simplify, as much as possible, the complex solution equilibria. The concentration of HEH[EHP] was chosen to keep a relatively constant ratio of the HEH[EHP] monomer:dimer, as well as to limit the concentration of excess HEH[EHP]. While the results of this section may not be of direct applicability to the ALSEP process due to the concentrations used (e.g., the solution properties may be quite different at the two concentrations, particularly the phase modifier properties of the acidic extractant), new insight was obtained into the fundamental behavior between the two extractants in the system under process-relevant conditions.

In the ALSEP system, the diffusion coefficient of each ligand (T2EHDGA or HEH[EHP]) is found by measuring the decay of its resonance, with normalization by the diffusion coefficient of the solvent, as described in Section 7.2. Thus, the two resonances observed and measured in the ALSEP solvent are of T2EHDGA and HEH[EHP]; comparisons are necessarily made to the diffusion of independent T2EHDGA and independent HEH[EHP]. Discussion of the resonances in the ALSEP solvent will be prefaced as such to avoid the ambiguity.

In the ALSEP solvent, at concentrations of T2EHDGA below 0.1 M, the D_{obs}/D_{sol} of HEH[EHP] is relatively constant, indicating little or no change in the size of the HEH[EHP] species. As the concentration of T2EHDGA increases above 0.1 M in the ALSEP solution, a significant decrease in the D_{obs}/D_{sol} of HEH[EHP] is observed, indicating that HEH[EHP] forms larger, more slowly diffusing species at this concentration. It it reasonable, and consistent with the chemical shift analysis, that the decrease in HEH[EHP] D_{obs}/D_{sol} is due to the formation of an adduct, such as T2EHDGA·HEH[EHP], or more generally, T2EHDGA$_m$·HEH[EHP]$_n$ (for m, n $\geq$ 1) .

For [T2EHDGA] $\leq$ 0.01 M, the D_{obs}/D_{sol} of the T2EHDGA resonance in the ALSEP solvent showed a small decrease relative to the independent T2EHDGA solutions (Figure 7.5, left panel). As the concentration of T2EHDGA increases, the difference between D_{obs}/D_{sol} of the ALSEP system and of the pristine T2EHDGA system becomes insignificant. The molecular weight of T2EHDGA (FW = 580), and of the T2EHDGA

dimer (which forms as the ligand concentration increases), limits the sensitivity of detecting the addition of HEH[EHP] to the complex: the difference in mass between the HEH[EHP] containing species and the baseline, $(T2EHDGA)_n$ species is not sufficient to resolve by this method.

7.3.3.1 Nitric acid and Eu(III) extraction by ALSEP

After equilibration with 3 M HNO_3 and Eu(III) in 3 M HNO_3, the diffusion coefficients of both ligands in the ALSEP solution change considerably relative to the pristine solutions. As discussed in Section 7.3.3, the ratio D_{obs}/D_{sol} reflects the change in size of the analytes with changing solution conditions. The effects on each ligand are discussed separately.

After equilibration with 3 M HNO_3, the $D_{T2EHDGA}/D_{sol}$ of T2EHDGA in the ALSEP solvent (which contains constant 10 mM HEH[EHP]) is very similar to the $D_{T2EHDGA}/D_{sol}$ of the independent T2EHDGA solution. This indicates that the size (and mass) of the T2EHDGA aggregates formed after acid aggregation in both systems is similar.

After equilibration with 2 mM Eu(III) / 3 M HNO_3, the differences between the $D_{T2EHDGA}/D_{sol}$ of T2EHDGA in the ALSEP solvent relative to the independent T2EHDGA system are somewhat subtle, and differ at high and low concentrations of the DGA ligand. Each concentration range is discussed.

At high concentrations of T2EHDGA, the $D_{T2EHDGA}/D_{sol}$ of the ALSEP and T2EHDGA systems tend toward the same value, both in the acid-equilibrated and Eu-equilibrated systems. This provides an indication of the dominant species in solution, which, as T2EHDGA concentration increases, will be a $T2EHDGA_m{\cdot}(HNO_3)_n$ species, in all four solutions (ALSEP and T2EHDGA, acid and Eu(III)/acid equilibrated). At high T2EHDGA concentrations, the dominant species is expected to be the same (or very similar) in the metal- and metal-free solutions, due to the low overall concentration of metal in the system ($\leq$ 2 mM) relative to the ligand concentration. Under conditions

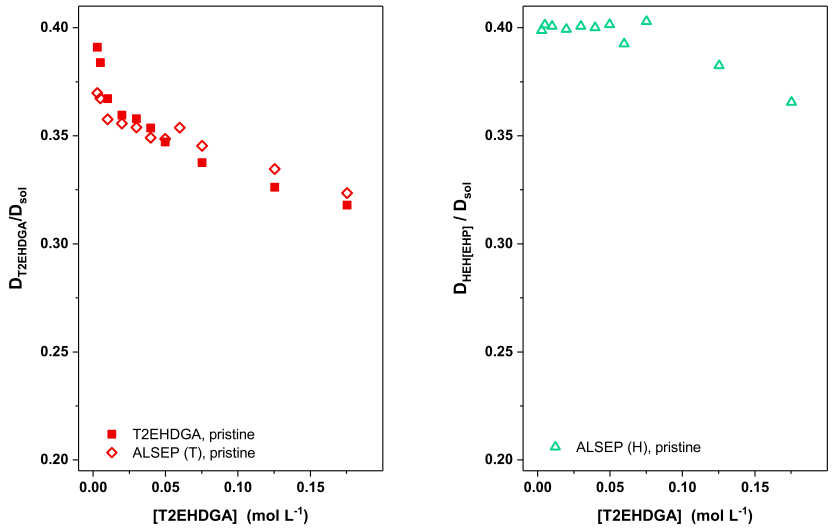

Figure 7.5: Left: D_{obs}/D_{sol} of T2EHDGA in solutions of pristine T2EHDGA (filled squares) and upon addition of 10 mM HEH[EHP] (ALSEP solution, 10 mM HEH[EHP] + variable T2EHDGA, open diamonds). Right: Change in D_{obs}/D_{sol} of HEH[EHP] in solution of ALSEP (10 mM HEH[EHP] + variable T2EHDGA, open triangles).

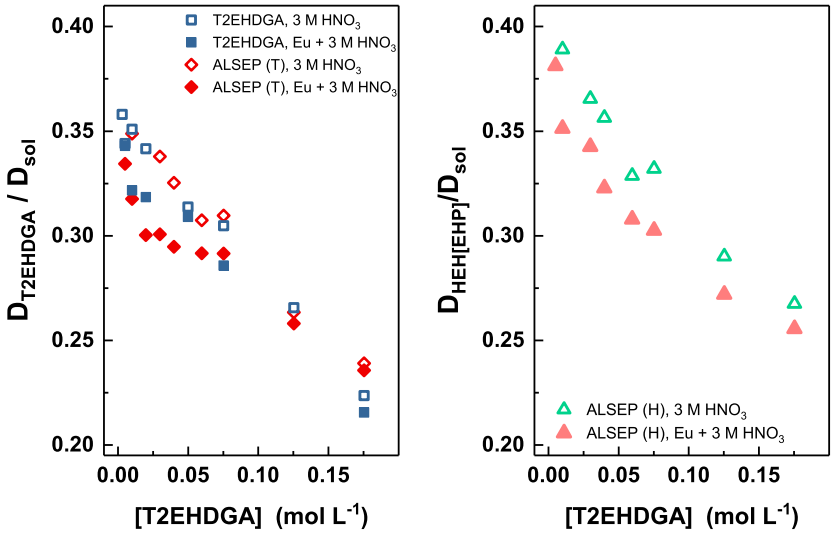

Figure 7.6: Left: $D_{\mathrm{T2EHDGA}}/D_{\mathrm{sol}}$ of T2EHDGA in solutions of independent T2EHDGA (blue squares) or ALSEP solvent (red diamonds) after equilibration with 3 M HNO_3 (open) or 2 mM Eu(III) / 3 M HNO_3 (filled). Right: $D_{\mathrm{HEH[EHP]}}/D_{\mathrm{sol}}$ of HEH[EHP] in ALSEP solvent after equilibration with 3 M HNO_3 (green open triangles) or 2 mM Eu(III) / 3 M HNO_3 (pink filled triangles).

of high ligand concentration and low organic phase metal concentration, the concentration of the T2EHDGA$_m$·(HNO$_3$)$_n$ species is expected to greatly exceed the concentration of the tris-T2EHDGA metal species, M·(T2EHDGA)$_3$(NO$_3$)$_3$. This will drive the value of $D_{\text{T2EHDGA}}/D_{\text{sol}}$ toward that of the T2EHDGA$_m$·(HNO$_3$)$_n$ species (Equation 7.4). This is consistent with the observed convergence of $D_{\text{T2EHDGA}}/D_{\text{sol}}$ between acid- and Eu(III)/acid- equilibrated solutions at high T2EHDGA concentrations.

At lower concentrations of T2EHDGA, there are greater differences between the ALSEP and the independent T2EHDGA ligand solutions. The decrease of $D_{\text{T2EHDGA}}/D_{\text{sol}}$ in the ALSEP solvent equilibrated with Eu(III)/3 M HNO$_3$ at low T2EHDGA concentrations may indicate the inclusion of HEH[EHP] in the extracted metal complex (Figure 7.6). Comparison of $D_{\text{T2EHDGA}}/D_{\text{sol}}$ of T2EHDGA in the ALSEP solvent after equilibration with 3 M HNO$_3$ or with Eu (III) /3 M HNO$_3$ (Figure 7.6) shows a decrease of $D_{\text{T2EHDGA}}/D_{\text{sol}}$ upon metal extraction. This is consistent with the addition of HEH[EHP] to the metal complex. However, the observed decrease in $D_{\text{T2EHDGA}}/D_{\text{sol}}$ under these conditions could also be consistent with the inclusion of additional Eu(III) and HNO$_3$ in the complex. This would require a significant deviation from the established coordination chemistry of the DGA.[112,114] Thus, inclusion of HEH[EHP] in the complex is more feasbile, and is also consistent with results of other portions of this dissertation.

Focusing now on the HEH[EHP] ligand, a drastic decrease in $D_{\text{HEH[EHP]}}/D_{\text{sol}}$ is observed upon equilibration of the ALSEP solvent with 3 M HNO$_3$ (Figure 7.6). This indicates the rapid growth of the HEH[EHP] aggregate. HEH[EHP] may join the T2EHDGA$_m$·(HNO$_3$)$_n$ adduct, forming a ternary complex, or may even displace HNO$_3$ to form the T2EHDGA$_m$·HEH[EHP]$_j$ adduct under these conditions. Because of the mass difference between HEH[EHP] (FW = 306 g/mol) and a T2EHDGA aggregate, the change in $D_{\text{HEH[EHP]}}/D_{\text{sol}}$ can be observed with more sensitivity *via* the HEH[EHP] resonance than *via* the T2EHDGA resonance.

After equilibration with Eu(III) /3 M HNO$_3$, the decrease in $D_{\text{HEH[EHP]}}/D_{\text{sol}}$ is larger still, suggesting a greater mole fraction of HEH[EHP] is associated with the T2EHDGA

species after metal extraction than after only acid equilibration, or that a larger aggregate is formed. This is consistent with one interpretation of the T2EHDGA/ALSEP data, and is also consistent with the spectroscopic and distribution data.

7.3.4 Determination of the Adduct Association Constant

The approach used to model the chemical shift analysis data was applied to the diffusion data to obtain the association constant between T2EHDGA and HEH[EHP]. Non-linear least squares was used to fit Equation 6.6 to the diffusion data (pristine ALSEP, T2EHDGA resonance) to obtain parameter estimates for the association constant, K_{11}, and the diffusion coefficients of the free and bound species, D_f and D_b. Fitting the T2EHDGA resonance of the pristine ALSEP solutions yielded results (Table 7.1) that are in good agreement with the value found by line width analysis of the titration of T2EHDGA by HEH[EHP]. The satisfactory fit of the 1:1 model again suggests the presence of the T2EHDGA·HEH[EHP] adduct. It is noted that the value obtained for K_{11}, 111, has relatively large associated standard error (34). Some of this results from the limited degrees of freedom (df = 7) of the model fit. A more accurate result might be obtained by taking into account other species likely to exist in the solution, namely, the dimers of each ligand. Including these additional species in the model quickly adds many additional parameters, and can easily lead to over-fitting. Given the degrees of freedom in the current data set, such models were not explored in this work. The stability constant between HDEHP, the stronger, phosphoric acid analog of HEH[EHP], with CMPO (octyl(phenyl)-N,N-diisobutylcarbamoylmethylphosphine oxide), has been reported as $\log \beta = 3.4$.[160] The CMPO·HDEHP adduct constant is over one log unit larger than that obtained for T2EHDGA·HEH[EHP]. However, it is expected that the T2EHDGA·HEH[EHP] adduct would be much weaker than the CMPO·HDEHP adduct, which is reported to form *via* hydrogen bonding between the phosphoryl of CMPO and the P-O-H of HDEHP. In the T2EHDGA·HEH[EHP], the available binding site is between the carbonyl and P-O-H.

Table 7.1: Stability constants of the 1:1 adduct, T2EHDGA·HEH[EHP] in *n*-dodecane, determined by NLS fitting (Eq. 6.6) of DOSY data.

Resonance	K_{11} $(\pm\sigma)$	D_{bound}/D_{sol} $(\pm\sigma)$	D_{free}/D_{sol} $(\pm\sigma)$
T2EHDGA in ALSEP	111 (34)	0.343 (0.002)	0.379 (0.003)

7.4 Conclusions

The DOSY method very clearly provides evidence for the dimerization (or possibly n-merization) of the pristine ligands, T2EHDGA and HEH[EHP], in independent solutions. Evidence consistent with the formation of larger aggregates after acid equilibration is consistent with existing literature reports of the reverse micelle tetramers observed with other DGAs.[43] In the modified ALSEP system explored for this study, data indicates that HEH[EHP] becomes part of a larger aggregate upon acid and metal extraction, presumably resulting in a ternary species containing both ligands and metal. The association constant for the T2EHDGA·HEH[EHP] adduct is obtained by DOSY, and is in agreement with the value found by one method of chemical shift analysis.

7.5 Contribution of Authors

Ying Chen assisted in set up of DOSY pulse sequence, in collection of some spectra, and in processing of DOSY data.

8 Conclusions

The object of this investigation has been to gain insight into the organic phase metal speciation and metal complexation in the ALSEP concept, which is currently under study as a method for MA/Ln separation from UNF as part of advanced reprocessing goals.

The effect of impurities in one of the commercially-available ligands used in ALSEP, HEH[EHP], was assessed. The major P- bearing and non-P impurities were identified *via* GC/MS, ^{31}P NMR, and ESI-MS. A new method for purification was developed, combining the literature copper salt precipitation with column chromatography, and was found to remove significantly more impurities than the literature methods in routine use. The effect of the various common HEH[EHP] impurities on the ALSEP process was examined, by testing the Am strip stage of ALSEP using solvent prepared with purified and unpurified HEH[EHP], and with solvent deliberately spiked with impurities. The most problematic impurities toward the ALSEP process were determined to be the acidic impurities EHPA and HDEHP.

A variety of techniques have been applied to study the complex equilibria that occur in the ALSEP concept. The results of radiotracer distribution studies (via slope analysis method) indicated the formation of a ternary species in the extraction step of ALSEP. This method also revealed the synergistic behavior of the ALSEP solvent toward Eu(III) and Am(III). Synergism observed in the ALSEP solvent was found to depend on the aqueous phase extraction conditions, with maximal synergism occurring on extraction from 1 M HNO_3. The existence of synergism, together with the results of slope analysis, are consistent with the formation of a ternary species involving HEH[EHP] in the ALSEP extraction step.

A spectroscopic investigation of the system, using IR, UV-vis, and NMR, provided further evidence for the ternary complex. IR spectroscopy of the ligands shows significant changes to the P=O and C=O groups after acid equilibration and after metal equilibration, both in the independent ligands and in the mixed ALSEP system. Decrease in

the intensity of the P-O-H stretch is consistent with dissociation of HEH[EHP] dimers after equilibration with HNO_3 and metal solutions, both in HEH[EHP] and ALSEP solvents. A scoping study using ^{13}C and ^{31}P NMR spectroscopy showed evidence for the formation of an adduct between T2EHDGA and HEH[EHP], which appeared to be stable toward water and HNO_3 extraction.

Electronic spectroscopy revealed significant changes in the spectra of Am(III) extracted into the ALSEP solvent, which were the result of changing aqueous phase acidity (extraction conditions). As concentration of nitric acid in the aqueous phase is increased, extraction into the ALSEP solvent appears to result in the formation metal complexes with lower symmetry. These spectra are distinctly different from the pure component spectra (extraction by T2EHDGA or by HEH[EHP]), again consistent with the formation of a ternary species, but furthermore, that the speciation is directly affected, if not determined, by aqueous phase extraction conditions.

An extensive NMR study was performed in order to obtain the dimerization and association constants of T2EHDGA and HEH[EHP], independently and in the ALSEP solvent. This was accomplished using both chemical shift analysis and by DOSY, a pulsed field gradient method. The dimerization constant of T2EHDGA in *n*-dodecane was found to be 4.3 ($\log K_2 = 0.63$), which is previously unreported in the literature. While many of the results of both NMR studies were inconclusive from the point of view of obtaining equilibrium constants with the lowest possible error, they are both valuable studies within the framework of ALSEP. Both studies show the existence of a T2EHDGA·HEH[EHP] adduct, which, beyond the potential process and modeling implications for ALSEP, may help to explain the true cause of the synergism observed in ALSEP. The adduct may provide favorable metal coordination sites (relative to either ligand, acting independently), thus enhancing phase transfer in the moderate acid regime. And, importantly, the DOSY method provides evidence consistent with participation of HEH[EHP] in the T2EHDGA complex, under metal extraction from 3 M HNO_3. This result is consistent with the distribution studies and all previous spectroscopic data.

Bibliography

[1] Salvatores, M.; Palmiotti, G. *Progress in Particle and Nuclear Physics* **2011**, *66*, 144–166.

[2] Gelis, A. V.; Lumetta, G. J. *Industrial & Engineering Chemistry Research* **2014**, *53*, 1624–1631.

[3] Todd, T. A. *Reprocessing and Recycling of Spent Nuclear Fuel*; Elsevier Ltd., 2015; pp 523–530.

[4] Di Nucci, M. R.; Brunnengraber, A. *European Policy Analysis* **2017**, *3*, 295–323.

[5] Conca, J. *Geological Repository Systems for Safe Disposal of Spent Nuclear Fuels and Radioactive Waste*; Elsevier Ltd, 2017; pp 667–709.

[6] Alonso, J. I. G.; Thoby-Schultzendorff, D.; Giovanonne, B.; Glatz, J. P.; Pagliosa, G.; Koch, L. *Journal of Analytical Atomic Spectrometry* **1994**, *9*, 1209–1215.

[7] Loveland, W.; Morrissey, D. J.; Seaborg, G. T. *Modern Nuclear Chemistry*, 1st ed.; John Wiley and Sons: Hoboken, NJ, 2006; p 671.

[8] Choppin, G. R. *Separation Science and Technology* **2006**, *41*, 1955–1963.

[9] Bunn, M.; Holdren, J. P.; Fetter, S.; van der Zwaan, B.; Holdren, J. P.; van der Zwaan, B. *Nuclear Technology* **2004**, *150*, 209–230.

[10] Schneider, E. A.; Deinert, M. R.; Cady, K. B. *Energy Economics* **2009**, *31*, 627–634.

[11] Poinssot, C.; Boullis, B.; Bourg, S. *Reprocessing and Recycling of Spent Nuclear Fuel*; Elsevier Ltd., 2015; pp 27–48.

[12] Poinssot, C.; Bourg, S.; Ouvrier, N.; Combernoux, N.; Rostaing, C.; Vargas-Gonzalez, M.; Bruno, J. *Energy* **2014**, *69*, 199–211.

[13] Choppin, G. R.; Liljenzin, J.-O.; Rydberg, J. *Radiochemistry and Nuclear Chemistry*, 3rd ed.; Butterworth Heinemann: Oxford, UK, 2001.

[14] Salvatores, M. *Nuclear Engineering and Design* **2005**, *235*, 805–816.

[15] Todd, T. A. In *Nuclear Energy and the Environment*; Wai, C., Ed.; American Chemical Society: Washington DC, 2010; Chapter 2, pp 13–18.

[16] Nash, K. L.; Braley, J. C. In *ACS Symposium Series*; Wai, C., Ed.; American Chemical Society: Washington DC, 2010; Vol. 1046; pp 19–38.

[17] Glatz, J. P.; Souček, P.; Malmbeck, R. In *Reprocessing and Recycling of Spent Nuclear Fuel*, 1st ed.; Taylor, R., Ed.; Woodhead Publishing, 2015; Chapter 3, pp 49–62.

[18] Runde, W. H.; Mincher, B. J. *Chemical Reviews* **2011**, *111*, 5723–41.

[19] Grimes, T. S.; Horne, G. P.; Dares, C. J.; Pimblott, S. M.; Mezyk, S. P.; Mincher, B. J. *Inorganic Chemistry* **2017**, *56*, 8295–8301.

[20] Weaver, B.; Kappelmann, F. *TALSPEAK: A new method of separating americium and curium from the lanthanides by extraction from an aqueous solution of an aminopolyacetic acid complex with a monoacidic organophosphate or phosphonate*; 1964; p 61.

[21] Lumetta, G. J.; Gelis, A. V.; Vandegrift, G. F. *Solvent Extraction and Ion Exchange* **2010**, *28*, 287–312.

[22] Cotton, S. *Lanthanide and Actinide Chemistry*, 1st ed.; John Wiley & Sons, Ltd, 2006; pp 1–263.

[23] Clark, D. L. *Los Alamos Science* **2000**, 364–381.

[24] Rhodes, R. *The Making of the Atomic Bomb*.

[25] Seaborg, G. T.; Thompson, S. G. Bismuth phosphate process for the separation of plutonium from aqueous solution. 1957.

[26] Serne, R.; Lindberg, M. J.; Jones, T. E.; Schaef, H. T.; Krupka, K. M. *Laboratory-Scale Bismuth Phosphate Extraction Process Simulation to Track Fate of Fission Products*; 2007; p 126.

[27] Anderson, H. H.; Asprey, L. B. Solvent Extraction Process for Plutonium. 1960.

[28] Lanham, W. B.; Runion, T. C. *PUREX Process for Plutonium and Uranium Recovery*; 1949; Vol. ORNL-479; p 12.

[29] Nash, K. L.; Nilsson, M. *Reprocessing and Recycling of Spent Nuclear Fuel*; Elsevier Ltd., 2015; pp 3–25.

[30] Coleman, C. F.; Leuze, R. E. *Journal of the Tennessee Acadamy of Science* **1978**, *53*, 102–106.

[31] Moore, F. L. *Analytical Chemistry* **1961**, *33*, 748–751.

[32] Maier, J. L. *Solvent Extraction Properties of Monooctyl Phosphate and Dioctyl Phosphate on Elements of Interest to the Atomic Energy Commission*; 1952.

[33] Peppard, D. F.; Mason, G.; Maier, J.; Driscoll, W. *Journal of Inorganic and Nuclear Chemistry* **1957**, *4*, 334–343.

[34] Svantesson, I.; Hagström, I.; Persson, G.; Liljenzin, J. O. *Journal of Inorganic and Nuclear Chemistry* **1979**, *41*, 383–389.

[35] Kolarik, Z. *Solvent Extraction and Ion Exchange* **2010**, *28*, 707–763.

[36] Jensen, M. P.; Chiarizia, R.; Urban, V.; Nash, K. L. Aggregation of the neodymium complexes of HDEHP, Cyanex 272, Cyanex 302, and Cyanex 301 in toluene. Proceedings of the International Symposium NUCEF (2002). 2001.

[37] Nash, K. L. *Solvent Extraction and Ion Exchange* **2015**, *33*, 1–55.

[38] Braley, J. C.; Grimes, T. S.; Nash, K. L. *Industrial & Engineering Chemistry Research* **2012**, *51*, 629–638.

[39] Lumetta, G. J.; Casella, A. J.; Rapko, B. M.; Levitskaia, T. G.; Pence, N. K.; Carter, J. C.; Niver, C. M.; Smoot, M. R. *Solvent Extraction and Ion Exchange* **2015**, *33*, 211–223.

[40] Lapka, J. L.; Nash, K. L. *Solvent Extraction and Ion Exchange* **2015**, *33*, 346–361.

[41] Lumetta, G. J.; Levitskaia, T. G.; Wilden, A.; Casella, A. J.; Hall, G. B.; Lin, L.; Sinkov, S. I.; Law, J. D.; Modolo, G. *Solvent Extraction and Ion Exchange* **2017**, *35*, 377–395.

[42] Wilden, A.; Lumetta, G. J.; Sadowski, F.; Schmidt, H.; Schneider, D.; Gerdes, M.; Law, J. D.; Geist, A.; Bosbach, D.; Modolo, G. *Solvent Extraction and Ion Exchange* **2017**, *35*, 396–407.

[43] Jensen, M. P.; Yaita, T.; Chiarizia, R. *Langmuir* **2007**, *23*, 4765–74.

[44] Nilsson, M.; Zalupski, P. R.; Antonio, M. R. In *Ion Exchange and Solvent Extraction*, 1st ed.; Moyer, B., Ed.; CRC Press: Boca Raton, 2013; Chapter 6, pp 197–268.

[45] Osseo-Asare, K. Microemulsions and Thrid Phase Formation. Proceedings of the International Solvent Extraction Conference, ISEC 2002. Cape Town, South Africa, 2002; pp 118–123.

[46] Steytler, D. C.; Jenta, T. R.; Robinson, B. H.; Eastoe, J.; Heenan, R. K. *Langmuir* **1996**, *12*, 1483–1489.

[47] Ibrahim, T. H.; Neuman, R. D. *Langmuir* **2004**, *20*, 3114–3122.

[48] McDowell, W.; Coleman, C. *Journal of Inorganic and Nuclear Chemistry* **1965**, *27*, 1117–1139.

[49] Ellis, R. J.; Demars, T.; Liu, G.; Niklas, J.; Poluektov, O. G.; Shkrob, I. A. *The Journal of Physical Chemistry B* **2015**, *119*, 11910–11927.

[50] Jensen, M. P.; Bond, A. H. *Radiochimica Acta* **2002**, *90*, 205–209.

[51] Yaita, T.; Herlinger, A. W.; Thiyagarajan, P.; Jensen, M. P. *Solvent Extraction and Ion Exchange* **2004**, *22*, 553–571.

[52] Nave, S.; Modolo, G.; Madic, C.; Testard, F. *Solvent Extraction and Ion Exchange* **2004**, *22*, 527–551.

[53] Ansari, S.; Pathak, P. N.; Manchanda, V. K.; Husain, M.; Prasad, a. K.; Parmar, V. S. *Solvent Extraction and Ion Exchange* **2005**, *23*, 463–479.

[54] Chiarizia, R.; Jensen, M. P.; Borkowski, M.; Ferraro, J. R.; Thiyagarajan, P.; Littrell, K. C. *Solvent Extraction and Ion Exchange* **2003**, *21*, 1–27.

[55] Chiarizia, R.; Briand, A. *Solvent Extraction and Ion Exchange* **2007**, *25*, 351–371.

[56] Ravi, J.; Prathibha, T.; Venkatesan, K.; Antony, M.; Srinivasan, T. G.; Vasudeva Rao, P. *Separation and Purification Technology* **2012**, *85*, 96–100.

[57] Plaue, J.; Gelis, A. V.; Czerwinski, K. *Separation Science and Technology* **2006**, *41*, 2065–2074.

[58] Sasaki, Y.; Sugo, Y.; Suzuki, S.; Tachimori, S. *Solvent Extraction and Ion Exchange* **2001**, *19*, 91–103.

[59] Modolo, G.; Asp, H.; Schreinemachers, C.; Vijgen, H. *Solvent Extraction and Ion Exchange* **2007**, *25*, 703–721.

[60] Bell, K.; Geist, A.; McLachlan, F.; Modolo, G.; Taylor, R.; Wilden, A. *Procedia Chemistry* **2012**, *7*, 152–159.

[61] Deepika, P.; Sabharwal, K.; Srinivasan, T. G.; Vasudeva Rao, P. R. P. *Solvent Extraction and Ion Exchange* **2010**, *28*, 184–201.

[62] Campbell, E. L.; Holfeltz, V. E.; Hall, G. B.; Levitskaia, T. G.; Nash, K. L.; Lumetta, G. J. *Solvent Extraction and Ion Exchange* **2017**, *35*, 586–603.

[63] Gullekson, B. J.; Breshears, A. T.; Brown, M. A.; Essner, J. B.; Baker, G. A.; Walensky, J. R.; Paulenova, A.; Gelis, A. V. *Inorganic Chemistry* **2016**, *55*, 12675–12685.

[64] Braley, J. C.; Grimes, T. S.; Nash, K. L. *Industrial & Engineering Chemistry Research* **2012**, *51*, 629–638.

[65] Vandegrift, G. F. In *Science and Technology of Tributyl Phosphate*; Schulz, W. W., Navratil, J. D., Eds.; CRC Press: Boca Raton, Chapter 4, pp 69–136.

[66] Horwitz, E. P.; Chiarizia, R.; Gatrone, R. *Solvent Extraction and Ion Exchange* **1988**, *6*, 93–110.

[67] Delmau, L. H.; Bonnesen, P. V.; Moyer, B. A. *Hydrometallurgy* **2004**, *72*, 9–19.

[68] Schulz, W. W. *Effects of some synergistic and antasynergistic agents on HDEHP extraction of strontium*; 1968; Vol. BNWL-759; p 27.

[69] Lumetta, G. J.; Gelis, A. V.; Carter, J. C.; Niver, C. M.; Smoot, M. R. *Solvent Extraction and Ion Exchange* **2014**, *32*, 333–347.

[70] Partridge, J.; Jensen, R. *Journal of Inorganic and Nuclear Chemistry* **1969**, *31*, 2587–2589.

[71] Zhengshui, H.; Ying, P.; Wanwu, M.; Xun, F. *Solvent Extraction and Ion Exchange* **1995**, *13*, 965–976.

[72] McDowell, W.; Perdue, P.; Case, G. *Journal of Inorganic and Nuclear Chemistry* **1976**, *38*, 2127–2129.

[73] Sainz-Diaz, C. I.; Klocker, H.; Marr, R.; Bart, H. J. *Hydrometallurgy* **1996**, *42*, 1–11.

[74] Schmitt, J.; Blake, C. *Purification of di(2-ethylhexyl)-phosphoric acid*; 1964; Vol. ORNL-3548; p 11.

[75] Stewart, D.; Crandall, H. *Journal of the American Chemical Society* **1951**, *73*, 1377–1378.

[76] Gatrone, R. C.; Kaplan, L.; Horwitz, E. P. *Solvent Extraction and Ion Exchange* **1987**, *5*, 1075–1116.

[77] Honaker, C. B.; Schulz, W. W. *Journal of Inorganic and Nuclear Chemistry* **1977**, *39*, 1703–1704.

[78] Schulz, W. W. United States Patent 3,793,408. 1974.

[79] Pretsch, E.; Buhlmann, P.; Badertscher, M. *Structure Determination of Organic Compounds*, 4th ed.; Springer, 2009; p 433.

[80] Kuhl, O. *Phosphoros-31 NMR Spectroscopy: A concise introduction for the synthetic organic and organometallic chemist*, 1st ed.; Springer-Verlag: Berlin, 2008; p 131.

[81] Brahmmananda Rao, C. V. S.; Srinivasan, T. G.; Vasudeva Rao, P. R. *Solvent Extraction and Ion Exchange* **2007**, *25*, 771–789.

[82] Mayer, U.; Gutmann, V.; Gerger, W. *Monatshefte fur Chemie* **1975**, *106*, 1235–1257.

[83] Yankov, D.; Molinier, J.; Albet, J.; Malmary, G.; Kyuchoukov, G. *Biochemical Engineering Journal* **2004**, *21*, 63–71.

[84] Poposka, F. A.; Nikolovski, K.; Tomovska, R. *Chemical Engineering Science* **1998**, *53*, 3227–3237.

[85] Wang, M.; Qin, W.; Dai, Y. *Separation Science and Technology* **2004**, *39*, 185–198.

[86] Matsumoto, M.; Takahashi, T.; Fukushima, K. *Separation and Purification Technology* **2003**, *33*, 89–93.

[87] Peppard, D. F.; Ferraro, J. R.; Mason, G. *Journal of Inorganic and Nuclear Chemistry* **1959**, *12*, 1–6.

[88] Pecheur, O.; Guillaumont, D.; Dourdain, S.; Berthon, L.; Turgis, R.; Fillaux, C.; Arrachart, G.; Testard, F. *Solvent Extraction and Ion Exchange* **2016**, *34*, 260–273.

[89] Mason, J., Ed. *Multinuclear NMR*, 1st ed.; Plenum Press: New York, 1987; p 639.

[90] Claridge, T. D. *High-Resolution NMR Techniques*, 3rd ed.; Elsevier: Amsterdam, 2016; p 541.

[91] Pauli, G. F.; Jaki, B. U.; Lankin, D. C. *Journal of Natural Products* **2007**, *70*, 589–595.

[92] Saito, T.; Nakaie, S.; Kinoshita, M.; Ihara, T.; Kinugasa, S.; Nomura, A.; Maeda, T. *Metrologia* **2004**, *41*, 213–218.

[93] Uetake, N. *Analyst* **1987**, *112*, 445–448.

[94] Gorenstein, D. G., Ed. *Phosphorus-31 NMR: Principles and Applications*, first ed. ed.; Academic Press, Inc.: Orlando, 1984; p 604.

[95] Gorenstein, D. G.; Goldfield, E. M.; Chen, R.; Kovar, K.; Luxon, B. A. *Biochemistry* **1981**, *20*, 2141–2150.

[96] Barrans, R.; McAlister, D. R.; Herlinger, A. W.; Chiarizia, R.; Ferraro, J. R. *Solvent Extraction and Ion Exchange* **1999**, *17*, 1195–1217.

[97] Grimes, T. S.; Tian, G.; Rao, L.; Nash, K. L. *Inorganic Chemistry* **2012**, *51*, 6299–307.

[98] Peppard, D. F.; Mason, G.; Hucher, I. *Journal of Inorganic and Nuclear Chemistry* **1961**, *18*, 245–258.

[99] Peppard, D. F.; Mason, G. W.; Hucher, I. R.; Brandao, F. A. J. A. *Journal of Inorganic and Nuclear Chemistry* **1962**, *24*, 1387–1397.

[100] Otu, E. O.; Westland, A. D. *Solvent Extraction and Ion Exchange* **1990**, *8*, 759–781.

[101] Komasawa, I.; Otake, T.; Hattori, I. *Journal of Chemical Engineering of Japan* **1982**, *16*, 210–217.

[102] Miralles, N.; Sastre, A.; Martinez, M.; Aguilar, M. *Analytical Sciences* **1992**, *8*, 773–777.

[103] Kumar, V.; Kumar, A.; Mondal, S.; Sharma, J.; Hubli, R.; Wattal, P.; Suri, A. *Separation and Purification Technology* **2012**, *98*, 118–122.

[104] Campbell, E. L.; Holfeltz, V. E.; Hall, G. B.; Nash, K. L.; Lumetta, G. J.; Levitskaia, T. G. *Solvent Extraction and Ion Exchange* Accepted.

[105] Holfeltz, V. E.; Campbell, E. L.; Peterman, D. R.; Standaert, R. F.; Paulenova, A.; Lumetta, G. J.; Levitskaia, T. G. *Solvent Extraction and Ion Exchange* **2018**, *36*, 22–40.

[106] Gullekson, B. J.; Brown, M. A.; Paulenova, A.; Gelis, A. V. *Industrial & Engineering Chemistry Research* **2017**, *56*, 12174–12183.

[107] Rydberg, J.; Cox, M.; Musikas, C.; Choppin, G. R. *Solvent Extraction Principles and Practice*, 2nd ed.; Marcel Dekker, Inc.: New York, 2004; p 750.

[108] Johnson, A. T.; Nash, K. L. *Solvent Extraction and Ion Exchange* **2015**, *6299*, 1–14.

[109] Kawasaki, T.; Okumura, S.; Sasaki, Y.; Ikeda, Y. *Bull. Chem. Soc. Jpn.* **2014**, *87*, 294–300.

[110] Kannan, S.; Moody, M. A.; Barnes, C. L.; Duval, P. B. *Inorganic Chemistry* **2008**, *47*, 4691–5.

[111] Reilly, S. D.; Gaunt, A. J.; Scott, B. L.; Modolo, G.; Iqbal, M.; Verboom, W.; Sarsfield, M. J. *Chemical Communications* **2012**, *48*, 9732–4.

[112] Antonio, M. R.; McAlister, D. R.; Horwitz, E. P. *Dalton Transactions* **2015**, *44*, 515–521.

[113] Narbutt, J.; Wodyński, A.; Pecul, M. *Dalton Transactions* **2015**, *44*, 2657–2666.

[114] Brigham, D. M.; Ivanov, A. S.; Moyer, B. A.; Delmau, L. H.; Bryantsev, V. S.; Ellis, R. J. *Journal of the American Chemical Society* **2017**, *139*, 17350–17358.

[115] Jensen, M. P.; Chiarizia, R.; Ulicki, J. S.; Spindler, B. D.; Murphy, D. J.; Hossain, M. M.; Roca-Sabio, A.; de Blas, A.; Rodríguez-Blas, T. *Solvent Extraction and Ion Exchange* **2015**, *33*, 329–345.

[116] Jensen, M. P.; Bond, A. H.; Rickert, P. G.; Nash, K. L. *Journal of Nuclear Science and Technology* **2002**, *Suppl. 3*, 255–258.

[117] Gray, M. F.; Zalupski, P. R.; Nilsson, M. *Solvent Extraction and Ion Exchange* **2013**, *31*, 550–563.

[118] Cocalia, V. a.; Jensen, M. P.; Holbrey, J. D.; Spear, S. K.; Stepinski, D. C.; Rogers, R. D. *Dalton Transactions* **2005**, 1966–71.

[119] Brown, M. A.; Wardle, K. E.; Lumetta, G. J.; Gelis, A. V. *Procedia Chemistry* **2016**, *21*, 167–173.

[120] Lumetta, G. J.; Sinkov, S. I.; Krause, J. A.; Sweet, L. E. *Inorganic Chemistry* **2016**, *55*, 1633–1641.

[121] Moyer, B. A.; Lumetta, G. J.; Mincher, B. J. *Reprocessing and Recycling of Spent Nuclear Fuel*; Elsevier Ltd., 2015; pp 289–312.

[122] Danesi, P. R.; Cianetti, C. *Separation Science and Technology* **1982**, *17*, 969–984.

[123] Sasaki, Y.; Rapold, P.; Arisaka, M.; Hirata, M.; Kimura, T.; Hill, C.; Cote, G. *Solvent Extraction and Ion Exchange* **2007**, *25*, 187–204.

[124] Reilly, S. D.; Gaunt, A. J.; Scott, B. L.; Modolo, G.; Iqbal, M.; Verboom, W.; Sarsfield, M. J. *Chemical Communications* **2012**, *48*, 9732.

[125] Lumetta, G. J.; Braley, J. C.; Sinkov, S. I. *Separating the Minor Actinides Through Advances in Selective Coordination Chemistry*; 2012; p 19.

[126] Liu, Y.; Lee, M. S. *Solvent Extraction and Ion Exchange* **2016**, *34*, 74–85.

[127] Ferraro, J. R. *Journal of Inorganic and Nuclear Chemistry* **1959**, *10*, 319–322.

[128] Peppard, D. F.; Ferraro, J. R. *Journal of Inorganic and Nuclear Chemistry* **1960**, *15*, 365–370.

[129] Mills, A.; Logan, W. *Journal of Inorganic and Nuclear Chemistry* **1964**, *26*, 2191–2193.

[130] Johnson, A. T.; Alvarez, J.; Nash, K. L. *Solvent Extraction and Ion Exchange* **2017**, *35*, 35–48.

[131] Rama Swami, K.; Kumaresan, R.; Venkatesan, K. A.; Antony, M. P. *Journal of Molecular Liquids* **2017**, *232*, 507–515.

[132] Zalupski, P. R.; Grimes, T. S.; Heathman, C. R.; Peterman, D. R. *Applied Spectroscopy* **2017**, *71*, 2608–2615.

[133] Tian, G.; Shuh, D. K. *Dalton Transactions* **2014**, *43*, 14565–14569.

[134] Reichardt, C. *Solvents and Solvent Effects in Organic Chemistry*, 3rd ed.; Wiley-VCH, 2003; p 629.

[135] Letcher, J. H.; Van Wazer, J. R. *The Journal of Chemical Physics* **1966**, *44*, 815–829.

[136] Gorenstein, D. G. *Journal of the American Chemical Society* **1975**, *97*, 898–900.

[137] Masiker, M. C.; Mayne, C. L.; Eyring, E. M. *Magnetic Resonance in Chemistry* **2006**, *44*, 220–229.

[138] Fielding, L. *Tetrahedron* **2000**, *56*, 6151–6170.

[139] Pastor, A.; Martínez-Viviente, E. *Coordination Chemistry Reviews* **2008**, *252*, 2314–2345.

[140] Connors, K. A. *Binding Constants: The Measurement of Molecular Complex Stability*, 1st ed.; John Wiley & Sons, Ltd: New York, 1987; p 411.

[141] Williamson, M. P. *Progress in Nuclear Magnetic Resonance Spectroscopy* **2013**, *73*, 1–16.

[142] Victor, M.; Van Wazer, J. R. *The Journal of Organic Chemistry* **1967**, *32*, 1187–1189.

[143] Deranleau, D. A. *Journal of the American Chemical Society* **1969**, *91*, 4044–4049.

[144] Person, W. B. *Journal of the American Chemical Society* **1965**, *87*, 167–170.

[145] Frassineti, C.; Ghelli, S.; Gans, P.; Sabatini, A.; Moruzzi, M. S.; Vacca, A. *Analytical Biochemistry* **1995**, *231*, 374–82.

[146] Hynes, M. J. *J. Chem. Soc., Dalton Transactions* **1993**, *0*, 311–312.

[147] R Core Team, R: A language and environment for statistical computing. R Foundation for Statistical Computing. 2017.

[148] Orfi, L.; Lin, M.; Larive, C. K. *Analytical Chemistry* **1998**, *70*, 1339–45.

[149] Berthon, C. *Etude par RMN de la conformation des extractants a fonction amide en phase organique*; 1993; p 209.

[150] Fu, N.; Tanaka, M. *Materials Transactions* **2006**, *47*, 136–142.

[151] Danesi, P. R.; Vandegrift, G. F. *Inorganic and Nuclear Chemistry Letters* **1981**, *17*, 109–115.

[152] Kavallieratos, K.; Bertao, C. M.; Crabtree, R. H. *Journal of Organic Chemistry* **1999**, *64*, 1675–1683.

[153] Van Wazer, J. R.; Callis, C. F.; Shoolery, J. N.; Jones, R. C. *Nuclear Magnetic Resonance of Phosphorus Compounds* **1956**, *78*, 5715–5726.

[154] Prado, F. R.; Giessner-Prettre, C.; Pullman, B.; Daudey, J. P. *Journal of the American Chemical Society* **1979**, *101*, 1737–1742.

[155] Olivier, C.; Grote, Z.; Solari, E.; Scopelliti, R.; Severin, K. *Chemical Communications* **2007**, 4000–4002.

[156] Sudmeier, J.; Evelhoch, J.; Jonsson, N.-H. *Journal of Magnetic Resonance* **1980**, *40*, 377–390.

[157] Craven, C. J.; Whitehead, B.; Jones, S. K. A.; Thulin, E.; Blackburn, G. M.; Waltho, J. P. *Biochemistry* **1996**, *35*, 10287–10299.

[158] London, R. *Journal of Magnetic Resonance* **1993**, *104*, 190–196.

[159] Kovrigin, E. L. *Journal of Biomolecular NMR* **2012**, *53*, 257–270.

[160] Tkac, P.; Vandegrift, G. F.; Lumetta, G. J.; Gelis, A. V. *Industrial & Engineering Chemistry Research* **2012**, *51*, 10433–10444.

[161] Byriel, K. A.; Gasperov, V.; Gloe, K.; Kennard, C. H. L.; Leong, A. J.; Lindoy, L. F.; Mahinay, M. S.; Pham, H. T.; Tasker, P. A.; Thorp, D.; Turner, P. *Dalton Transactions* **2003**, 3034–3040.

[162] Muller, J. M.; Berthon, C.; Couston, L.; Zorz, N.; Simonin, J. P.; Berthon, L. *Solvent Extraction and Ion Exchange* **2016**, *34*, 141–160.

[163] Adam, K.; Atkinson, I. *Pure and Applied Chemistry* **1998**, *70*, 2345–2350.

[164] Lumetta, G. J.; Rapko, B. M.; Garza, P. A.; Hay, B. P.; Gilbertson, R. D.; Weakley, T. J.; Hutchison, J. E. *Journal of the American Chemical Society* **2002**, *124*, 5644–5645.

[165] Parks, B. W.; Gilbertson, R. D.; Hutchison, J. E.; Healey, E. R.; Weakley, T. J.;

Rapko, B. M.; Hay, B. P.; Sinkov, S. I.; Broker, G. A.; Rogers, R. D. *Inorganic Chemistry* **2006**, *45*, 1498–1507.

[166] Jansone-Popova, S.; Ivanov, A. S.; Bryantsev, V. S.; Sloop, F. V.; Custelcean, R.; Popovs, I.; Dekarske, M. M.; Moyer, B. A. *Inorganic Chemistry* **2017**, *56*, 5911–5917.

[167] Sengupta, A.; Bhattacharyya, A.; Verboom, W.; Ali, S. M.; Mohapatra, P. K. *Journal of Physical Chemistry B* **2017**, *121*, 2640–2649.

[168] Ellis, R. J.; Brigham, D. M.; Delmau, L. H.; Ivanov, A. S.; Williams, N. J.; Vo, M. N.; Reinhart, B.; Moyer, B. A.; Bryantsev, V. S. *Inorganic Chemistry* **2017**, *56*, 1152–1160.

[169] Sella, C.; Bauer, D. *Solvent Extraction and Ion Exchange* **1988**, *6*, 819–833.

[170] Johnson Jr., C. S. *Progress in Nuclear Magnetic Resonance Spectroscopy* **1999**, *34*, 203–256.

[171] Stejskal, E. O.; Tanner, J. E. *The Journal of Chemical Physics* **1965**, *42*, 288–292.

[172] Basilio, N.; García-Río, L.; Martín-Pastor, M. *The Journal of Physical Chemistry B* **2010**, *114*, 4816–4820.

[173] Brand, T.; Cabrita, E. J.; Berger, S. *Progress in Nuclear Magnetic Resonance Spectroscopy* **2005**, *46*, 159–196.

[174] Pianet, I.; André, Y.; Ducasse, M.-A.; Tarascou, I.; Lartigue, J.-C.; Pinaud, N.; Fouquet, E.; Dufourc, E. J.; Laguerre, M. *Langmuir* **2008**, *24*, 11027–11035.

[175] Perez, A.; de Saa, D.; Ballesteros, A.; Serrano, J. L.; Sierra, T.; Romero, P. *Chemistry* **2013**, *19*, 10271–10279.

[176] Jang, H. B.; Rho, H. S.; Oh, J. S.; Nam, E. H.; Park, S. E.; Bae, H. Y.; Song, C. E. *Organic & Biomolecular Chemistry* **2010**, *8*, 3918.

[177] Cohen, Y.; Avram, L.; Evan-Salem, T.; Frish, L. *Analytical Methods in Supramolecular Chemistry*; 2007; pp 163–219.

[178] Cameron, K. S.; Fielding, L. *The Journal of Organic Chemistry* **2001**, *66*, 6891–6895.

[179] Simova, S.; Berger, S. *Journal Of Inclusion Phenomena And Macrocyclic Chemistry* **2005**, *53*, 163–170.

[180] Patil, S. M.; Keire, D. A.; Chen, K. *The AAPS Journal* **2017**, *19*, 1760–1766.

[181] Pregosin, P. S.; Kumar, P. G. A.; Ferna, I. *Chemical Reviews* **2005**, *105*, 2977–2998.

[182] Cabrita, E. J.; Berger, S. *Magnetic Resonance in Chemistry* **2001**, *39*, S142–S148.

[183] Simpson, A. J. *Magnetic Resonance in Chemistry* **2002**, *40*, 72–82.

[184] Molinier, V.; Fenet, B.; Fitremann, J.; Bouchu, A.; Queneau, Y. *Journal of Colloid and Interface Science* **2005**, *286*, 360–368.